A PETROLOGICAL, GEOCHEMICAL AND ISOTOPIC INVESTIGATION OF GRANITOIDS FROM THE OLARY PROVINCE OF SOUTH AUSTRALIA - IMPLICATIONS FOR PROTEROZOIC CRUSTAL GROWTH

By

Rachel Yvette Benton B.Sc.

This thesis is submitted as partial fulfillment for the Honours degree of Bachelor of Science

Department of Geology and Geophysics
University of Adelaide
November 1994

National Grid Reference (SI 54-2) 1:250 000

TABLE OF CONTENTS

TABLES, PLATES and FIGURES

KEY TO ABBREVIATIONS

Al-Index	aluminium index = molar $Al_2O_3/(CaO + Na_2O + K_2O)$
bt	biotite
CHUR	Chondritic Uniform Reservoir
DM	depleted mantle
fld	feldspar
Ga	Giga-anna = billions of years before present
gt	garnet
haem	haematite
hb	hornblende
HREE	Heavy Rare Earth Elements
kb	kilobar
K-fld	potassium feldspar
ky	kyanite
LREE	Light Rare Earth Elements
Ma	Mega-anna = millions of years before present
MORB	Mid Ocean Ridge Basalt
mu	muscovite
Na-plag	sodium plagioclase
Nd-Sm	neodymium-samarium isotopic system
ORG	ocean ridge granites
plag	plagioclase
px	pyroxene
qtz	quartz
Rb-Sr	rubidium-strontium isotopic system
REE	Rare Earth Elements
sill	sillimanite
syn-COLG	syn-collisional granites
tour	tourmaline
VAG	volcanic arc granites
WPG	within plate granites
wt%	weight percent

ABSTRACT

Analysis of granitoids from the Olary Block of South Australia, gave rise to the identification of three genetically different granitoids. The Bimbowrie Granite, characterised by high Al_2O_3, CaO, K_2O, P_2O_5, Rb, Sr, Pb, Zn and low Na_2O, Nb, Zr, Ga and Y is an S-type granite, considered to be largely a product of partial anatexis and melt segregation from adjacent and underlying migmatitic metasediments during a high grade metamorphic event. The Basso Granodiorite with high SiO_2, Zr, Nb, Y and LREE and low CaO, Al_2O_3, MgO, V, Ba and Sr is a typical A-type granite that is, it formed from remelting of crust from which earlier granites had been extracted, or alternatively from fractionation of basaltic magma. It intrudes the host metasediments and is subsequently intruded by the Bimbowrie Granite. Thirdly, the Antro Tonalite exhibits I-type characteristics with high Fe_2O_3, Na_2O, CaO and TiO_2 levels and low LREE and K_2O.

Rb-Sr dating produced an isochron age of 1642 ± 5 Ma for the Basso Granodiorite and metasedimentary units. The Rb-Sr isotope system is easily reset, and generally registers significantly younger ages. Hence, 1642 ± 5 Ma may reflect the timing of a metamorphic/ deformational event.

Sm-Nd isotope investigations into the Olary Block, revealed a clustering of model ages. The Bimbowrie Granite has DM model ages of 2.6 - 2.67 Ga, recording the age of extraction from the mantle. One sample did however produce an age of 3.28 Ga, reflecting the granites source. That is, it may be sampling metasediment derived from older crust, present either as a basal sequence upon which the current stratigraphy is deposited or alternatively it may be sourcing a metasedimentary pile with a greater crustal residence time than the exposed metasediments. DM model age for the metasediment of 2.55 Ga further supports the notion that the Bimbowrie Granite formed as a result of *in situ* melting of the metasedimentary sequence.

2.12 - 2.13 Ga DM model ages were determined for the Basso Granodiorite. One sample did however have a TDM similar to the S-type granites of 2.61 Ga; this clearly indicates crustal contamination of this sample during emplacement, whereas the other samples reflect true mantle separation ages.

Regardless of the exact rates of crustal growth, it is clear that large volumes of continental crust were formed during the Palaeo- Mesoproterozoic. Identification of crustal production peaks for the Australian continent at ~3600 Ma, ~2600 Ma, ~2200 Ma and ~1800 Ma by McCulloch (1987), are reinforced by the data obtained herein. Two peaks were established, one at ~2600 Ma for the Bimbowrie Granite and the other at ~2200 for the Basso Granodiorite. Controversy still remains over whether these periods are discrete growth episodes or simply reflect a variation in the rate of recycling of continental crust into the mantle.

CHAPTER 1 - INTRODUCTION

1.1 The Problem

A geoscientist is constantly faced with the problem of interpreting what they observe and applying their observations to an understanding of how the Earth works. Proterozoic terrains present many such problems, including how and why did orogeny occur, has the volume of continental crust grown, and if so how and when, and what were the tectonic environments responsible for the unique geochemical nature of melts during this period.

Australia abounds in Proterozoic terrains that potentially offer fundamental insights into these and many other problems. The task of a geoscientist is to document observations and expand the total amount of information available in order to be able to address such problems. Possibly the most useful indicators are igneous rocks, and in particular granites. Granites act as probes of their source regions, and therefore contain inherent information about the processes responsible for their formation.

The Olary Block, in South Australia provides an excellent opportunity to address these and other problems due to types and number of rocks exposed.

By establishing geochemically and isotopically the nature of the granitoids in the Olary Block, and comparing these with other terrains of similar age, it is hoped that insights into problems involving Proterozoic crustal growth and tectonism may be obtained.

1.2 Aims Of This Study

It is beyond the scope of this thesis to tackle all the problems mentioned above. However, by the use of mapping, petrology, geochemistry and geochronology, the poorly exposed area of the Olary Block under investigation has been detailed in such a manner as to be useful for further interpretation following the completion of this thesis. With a view to looking further abroad (ie., at the Gawler Craton, Lachlan Fold Belt and Mount Painter Inlier) it is hoped this thesis may provide important insights into crust-mantle evolution during the Proterozoic.

The following is a list of aims proposed for this project:

1) To produce a 70km^2, 1:10 000 geological map of the Outalpa-Bimbowrie-Antro area, Olary, South Australia.
2) To formulate nomenclature for the granitoids petrologically.
3) To classify the granite suites geochemically.

4) To establish a systematic geochronologic framework for the local region by the use of Rb-Sr and Sm-Nd isotopes.

5) To delineate the provenance of the sediments and granitoids by the use of Sm-Nd isotopes and geochemistry.

6) To integrate geochemical and isotopic features and thus elucidate Proterozoic crustal evolution.

7) To synthesise data available from selected Australian Proterozoic terrains eg., Gawler Craton, Lachlan Fold Belt, Broken Hill Block and the Mount Painter and Babbage Inliers, in order to establish temporal and/or spatial relationships between such terrains and thus address the larger scale problem of crustal evolution during the Palaeo-Mesoproterozoic for the Australian continent.

CHAPTER 2 - REGIONAL GEOLOGY

2.1 Geological Setting

The Olary Province of the western Willyama Block, a promontory of the Gawler Province of the Precambrian shield of Australia (Flint and Webb, 1980), has been the focus of long-standing geological attention due to its proximity and tectonic relationships with the silver-lead-zinc deposits of Broken Hill.

Palaeoproterozoic rocks in the Willyama Inlier form a series of semi-isolated, partly exposed blocks which characteristically have faulted western margins and are unconformably overlain by Adelaidean metasediments along their eastern margins (Flint and Parker, 1993). A major sinistral north-northeast trending fault (Mundi-Mundi fault) separates the basement of the Willyama Inlier in South Australia (Olary Block) from that in New South Wales (Broken Hill Block) (fig. 2.1.1). Correlations have been made between the two blocks, however due to the lack of substantive data, they are at best tentative.

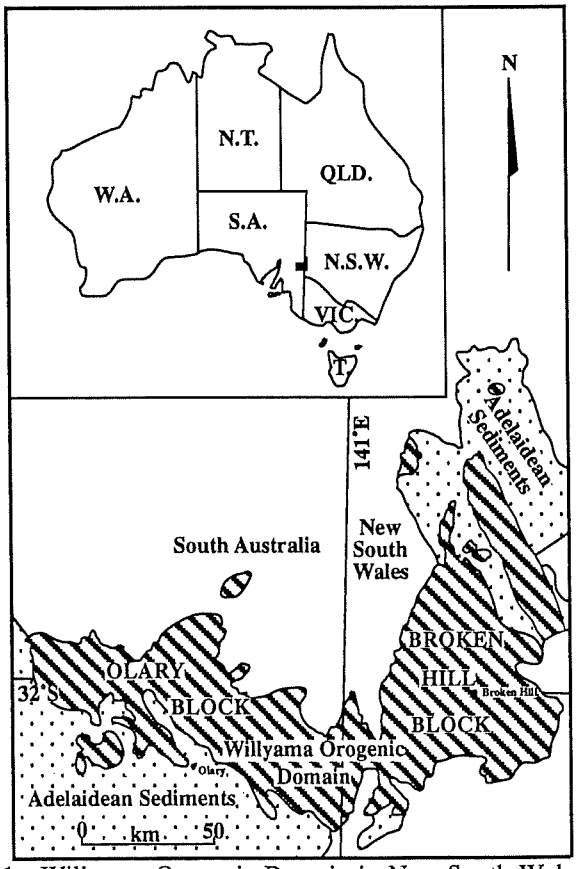

Figure 2.1.1 - Willyama Orogenic Domain in New South Wales and South Ausralia

The Olary Block contains medium to high grade regionally metamorphosed and generally strongly deformed sedimentary and minor volcanic rocks, intruded by extensive

volumes of granitoids and scattered occurrences of mafic dykes. The oldest rocks in the Willyama Inlier comprises mixed clastic and chemical sedimentary sequences referred to as the Willyama Supergroup. The Olary Block portion of the Willyama Supergroup is suggested to represent a rift margin and although detailed palaeoenvironmental syntheses are scarce, it is recognised that the sequence may be consistent with deposition in a predominantly shallow marine environment interspersed with non-marine playa lakes, deepening upward (ie., shelf or intracratonic basin; Rutland, 1976; Cook and Ashley, 1992). Flint and Parker (1993) have suggested that deposition took place in an ensialic rift zone characterised by immature terrigenous and volcanic derived clastics and bi-modal volcanism. Such deposition is suggested to have taken place prior to ~1700 Ma. Dating by Page and Laing (1992) in the Broken Hill Block of the Willyama Supergroup recorded a maximum age of sedimentation defined by the minimum age of detrital zircons of 1690 ± 5 Ma.

Rifting, extrusion of tholeiitic magma and development of a slightly deeper trough in which carbonaceous silty turbidites accumulated soon followed.

Deformation and metamorphism of these sediments to amphibolite grade occured during the Olarian Orogeny, accompanied by intrusion of felsic granitoids around ~1700-1550 Ma which caused local migmatisation and melting of host rocks as well as concentration of some economic minerals (eg., uranium and beryllium) (app. B, plate 4A).

Adelaidean rifting and deposition began at ~900 Ma, following uplift and erosion of the Palaeo- to Mesoproterozoic rocks. Sand sedimentation and possibly some volcanism (Boucant Volcanics) took place at this time in the partially fault controlled basin. Continental to marine deposition continued through the Adelaidean and included shallow-water, possibly fluvial, hematitic arkose and magnesitic, and silty sedimentation. Deep water sedimentation of laminated silt and carbonate units followed Sturtian glaciation.

The Cambro-Ordovician Delamerian Orogeny left Adelaidean rocks folded, metamorphosed and intruded (by the Anabama Granite and associated dykes). This deformation gave rise to N-S trending folds and a second phase produced NE-SW folds. Gold, copper and molybdenum concentration took place at this time (Clarke *et al.*, 1987).

Tertiary instability led to downwarping and downfaulting, allowing deposition of continental sand and shallow marine to estuarine clay and limestone. Much of the current topography and plain sedimentation may be traced back to Pleistocene uplift, erosion and deposition.

Geological mapping and related investigations in the Olary Block (Flint, 1981) have been modest in comparison with the extensive and very detailed structural and stratigraphic investigations undertaken around Broken Hill (eg. Stevens and Stroud, 1983). Thus the need for an investigation involving detailed field observations and regional geological synthesis is apparent. A geological framework for the study area has been established (as below) in order to fully understand subsequent isotopic and geochemical investigations.

2.2 Previous Investigations

Mawson (1912) first described the petrology and structure of the crystalline basement, which he called the Willyama Complex, and the overlying Adelaidean sedimentary sequence. Later, Campana and King (1958) divided the Willyama Complex within the Olary Block into four broad sedimentary units; the Weekeroo schist, Ethiudna Calcsilicate Group, Outalpa quartzites and the migmatite and granite gneisses, of inferred Archaean age 'granitised' during the Proterozoic to produce large granitic terrains within the metasediments. Talbot (1967) inverted the stratigraphy of Campana and King (1958) and placed the granitic terrains at the base of the stratigraphy. He described five stratigraphic units in an antiform within the Willyama Complex and recognised at least two phases of pre-Adelaidean deformation.

Parker (1972) and Flint and Flint (1975) divided the sequence into units directly correlatable with the stratigraphy used herein. Modest mapping of the Willyama Complex within the Olary Block by the South Australian Deptartment of Mines and Energy (Pitt, 1977; Forbes and Pitt, 1980) and structural work of a fragmentary nature with limited regional context (Berry *et al.*, 1978; Grady *et al.*, 1984) comprises most of the work undertaken in more recent years.

Detailed mapping and analysis by mineral exploration companies has enabled an incomplete database of small yet widely distributed sequences, and a summary of the local mineralisation (reviewed in King, 1958; Blissett, 1975; Pitt, 1978) to be outlined.

More recent studies by Flint and Parker (1993) have provided an excellent overview of the geology of the Olary Block.

2.3 Stratigraphy of the Olary Block

The Palaeoproterozoic Willyama Supergroup and Mesoproterozoic granitoids form a series of inliers, generally surrounded by stratigraphically younger sediments of the Adelaide Geosyncline. The establishment of a stratigraphic compendium for the Olary region is difficult due to the absence of continuous exposure.

Most stratigraphic studies of the Willyama Inliers have recognised a broad subdivision of gneissic and migmatitic units at the base, structurally overlain by schistose and fine grained metasediments (Flint and Parker, 1993). Due to intense deformation and metamorphism, sedimentary structures are rare and stratigraphic sequences have been considerably disturbed. Furthermore because of the variable metamorphic grade and lack of regional tectonic syntheses, it has been difficult to distinguish metamorphic units from primary stratigraphic units.

Clarke *et al.*, (1986) proposed five broad lithological suites for the Olary Block;

- Composite Gneiss Suite
- Quartzofeldspathic Suite

- Calcsilicate Suite
- Bimba Suite
- Carbonaceous Pelite Suite

Each of these are detailed below and summarised in figure 2.3.1. No evidence for unconformities in this sequence has been observed in the Olary Block.

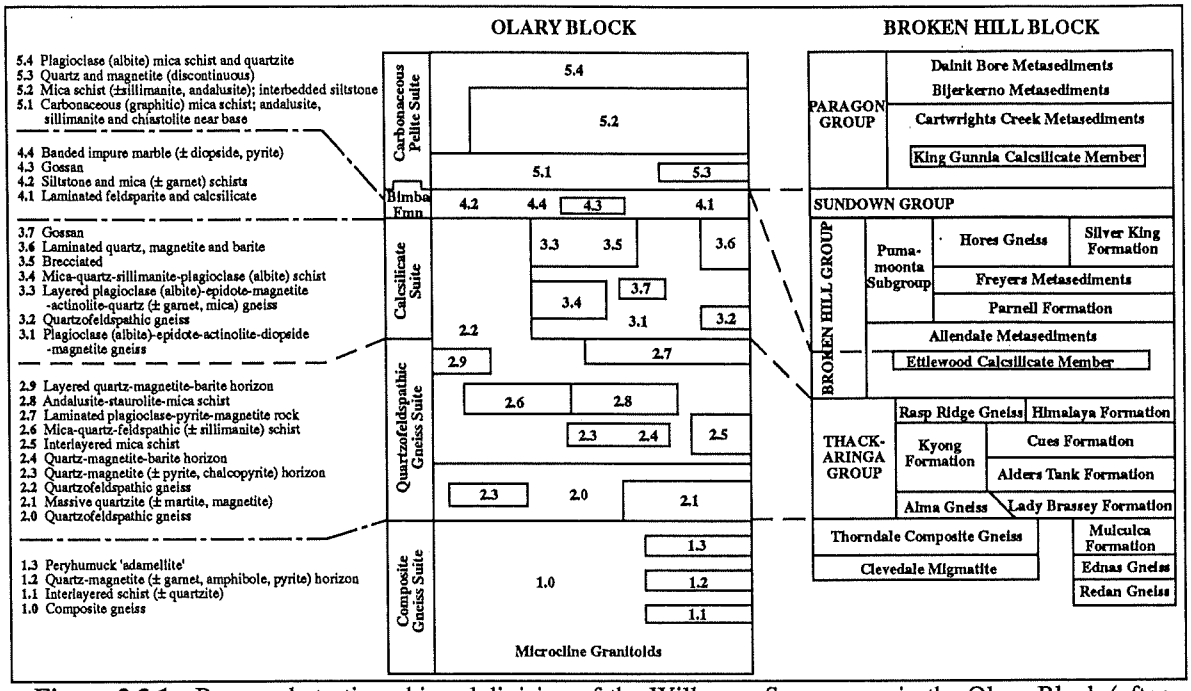

Figure 2.3.1 - Proposed stratigraphic subdivision of the Willyama Supergroup in the Olary Block (after Clarke *et al.*, 1986) and tentative correlation with equivalents in the Broken Hill Block (after Stevens *et al.*, 1990) (Flint and Parker, 1993)

Composite Gneiss Suite

The Composite Gneiss Suite is interpreted as the basal unit in the Olary Block. The sediments are generally coarse grained, migmatitic, qtz-fld-bt ± sill ± gt gneisses. Gradations exist into psammopelitic and pelitic schists and quartzofeldspathic units.

These gneisses are probably metasedimentary, derived from anatectic melting of the enclosing psammopelitic sediments (Flint and Parker, 1993), but there are zones in which there is complete conversion via *in situ* migmatites into banded, migmatitic and locally massive leucocratic granitoids. Although intrusive relationships are locally preserved, the granitoids commonly contain rafts and xenoliths of layered gneiss and have nebulitic textures often grading into typical *in situ* migmatites. This suite should not be strictly viewed as a distinct stratigraphic unit; its field relations imply that there has been large scale doming and mobilisation about some of the larger granitoid bodies and therefore it could be partly intrusive.

Quartzofeldspathic Suite

This extensive suite is characterised by massive to layered qtz-plag-bt ± K-fld gneiss, commonly with disseminated grains and/or thin laminae of magnetite (± haem) and pyrite. The quartzofeldspathic rocks comprise the informally termed 'Lower Albite' unit of massive to thickly layered albite - qtz (± K-fld ± bt ± mu ± magnetite ± pyrite) rocks, the 'Upper Albite' unit of commonly well laminated albite - qtz (± K-fld ± bt ± magnetite ± calcsilicates) and the intervening 'Middle Schist' unit of psammopelitic and pelitic schist and composite gneiss (Ashley *et al.*, 1994).

Lithological layering varies from a few millimetres to tens of metres in thickness, and sedimentary structures have been recorded, including graded bedding, ripple marks and cross laminations.

The presence of laminated iron formations and pelitic schistose horizons in addition to sedimentary structures, indicates a sedimentary origin. Flint and Parker (1993) suggest the origin of this suite to be derived from felsic volcanoclastic sediments containing saline rich fluids.

Calcsilicate Suite

The calcsilicate suite is characterised by massive, banded and finely laminated calcsilicate and feldspathic rocks. It is typically fine grained and includes scattered stratabound occurrences of calcsilicate matrix breccia. Their mineralogy typically comprises amphibole (actinolite, hornblende), clinopyroxene (diopside - hedenbergite) and epidote with minor garnet (grossular - andradite) and accessory sphene, zircon, tourmaline, pyrite and magnetite.

The calcsilicate suite is thought to gradationally overlie the quartzofeldspathic suite. Flint and Parker (1993) have suggested that the upper portions of the quartzofeldspathic suite and most of the calcsilicate suite may in fact be correlated laterally.

Cook and Ashley (1992) suggest a clastic sedimentation (of felsic provenance) and interaction with evaporative brines, together with chemical sedimentation of evaporites and local hot spring exhalites for the calcsilicates. Depositional conditions being an oxidising, lacustrine/playa and possibly sabkha environment, with local hot spring activity.

Bimba Suite

This unit is up to 50m thick, laterally continuous, finely laminated and host to predominantly pyritic sulphides. It is characterised by qtz-bt-albite ± mu ± sill metasiltstone interlayered with marble, albitic chert and calcsilicate gneiss. The mineralogy of the calcsilicate gneiss has many similarities with the calcsilicate suite with the addition of calcite, vesuvianite and fluorite, and traces of scheelite and magnetite.

The Bimba Formation is interpreted to represent a shallow water, mixed carbonate - pelite unit transitional between the underlying evaporitic and overlying deeper water marine

sediments; with the metal-rich sulphide accumulations a result of episodic hot spring exhalations (Flint and Parker, 1993).

Carbonaceous Pelite Suite

This suite is dominated by pelitic and psammopelitic schist (bt + mu + qtz ± Al silicates ± gt ± tour), locally grading into thin psammites higher in the sequence. The base of the pelite is marked by a graphitic facies commonly accompanied by chiastolite porphyroblasts or andalusite/sillimanite. Thin stratiform pegmatoid-tourmaline horizons, rare garnet-rich calcsilicates and stratabound pegmatites also occur within the lower part of the suite.

A regionally distinctive and sharp contact exists between this unit and the underlying Bimba Suite, hence creating a useful stratigraphic marker.

The pelite suite is interpreted as having been deposited as mud and silt, possibly turbiditic in part, in a deepening marine basin.

2.4 Lithological Descriptions of the Mapped Sequences - Field and Petrological

The development of a detailed understanding of the origin of the granitic rocks that comprise a significant portion of the exposed area of the Olary Block has been hampered by a lack of relative and absolute geochronology, geochemistry and regional mapping of both the intrusive rocks themselves and surrounding lithologies.

The mapped area enabled three granitoids to be identified; the Antro Tonalite, Bimbowrie Granite and the Basso Granodiorite (new names). Detailed below are field observations combined with petrological descriptions of these three granitoids and the host, a metasedimentary sequence.

2.4.1 Metasediments

The focus of the field assignment was primarily to investigate the igneous rocks, however a complete tectonic understanding of the map area required not only investigation of the igneous suites but also of the metasedimentary sequences in which they 'intrude'.

Typically the metasediments consisted of a series of finely laminated to thickly bedded, medium to fine grained pelitic and psammitic schists (plate 1A), with thin calc-silicate bands and albitised layers at certain localities.

The pelitic schists, usually more finely laminated, are Al-rich (as evident by the presence of garnet) and consist of quartz (~45%) biotite (~25%) muscovite (~20%) K-feldspar (~10%) with minor amounts of pyroxene, opaques (?magnetite) and ± garnet, varying with initial bulk composition (plate 1B, 1C). Under thin section a strong fabric was observed, most

PLATE 1

A Metasediment showing compositional variation from quartz rich to biotite rich. Field of view = 7.6 mm (sample number 1027-011).

B Garnet porphyroblasts in a pelitic schist with phyllosilicates (bt and mu) wrapping around. Field of view = 6.2 mm (sample number 1027-098).

C Pelitic schist, with the growth of garnet crystals, during metamorphism.

D A calcsilicate band rich in epidote, actinolite and diopside, within the quartzofeldspathic unit.

E Brecciated calcsilicate containing dominantly epidote, sphene, diopside, quartz and plagioclase. Field of view = 6.7 mm (sample number 1027-006).

F Brecciated calcsilicate in hand specimen, note the distinctive green colour of epidote and diopside (sample number 1027-006).

G Retrograded ?andalusite porphyroblast (now muscovite) within a psammite. Note the wrapping of the finer grained muscovite rich matrix around the porphyroblast. Field of view = 10.9 mm (sample number 1027-010).

H Hand Specimen of retrograded ?andalusite porphyroblasts in a psammitic rock (sample number 1027-010).

A

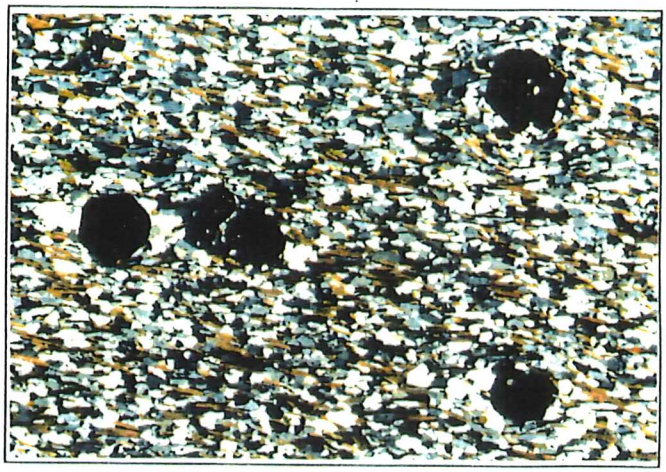

B

C

D

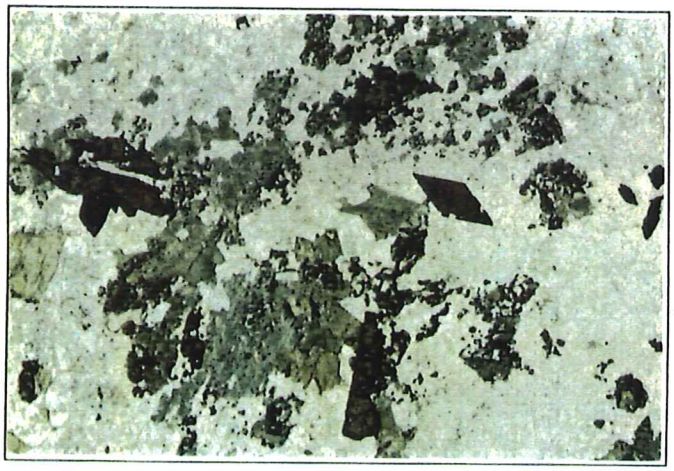

E

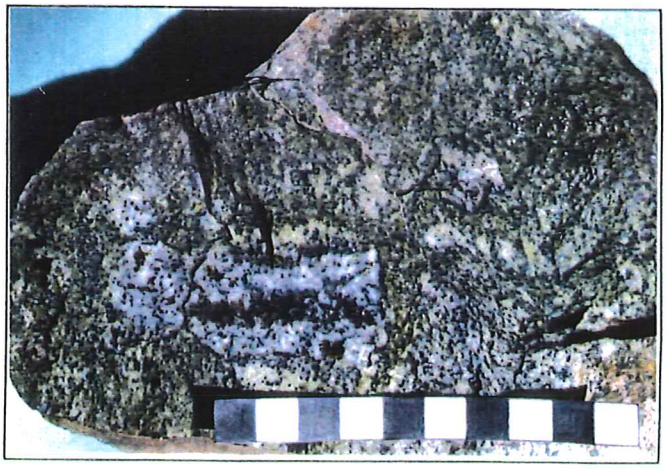

F

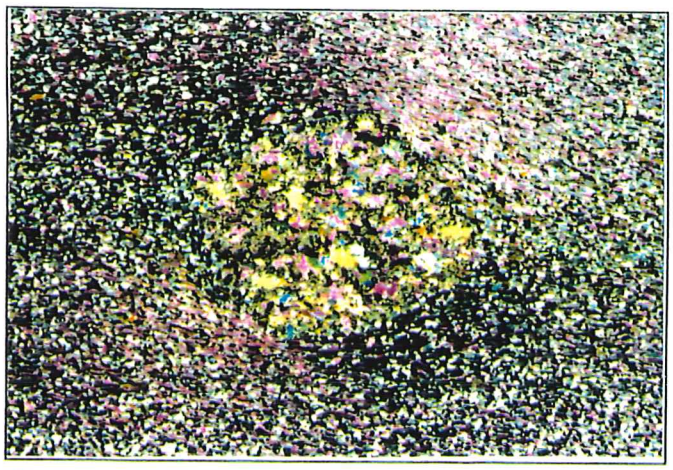

G

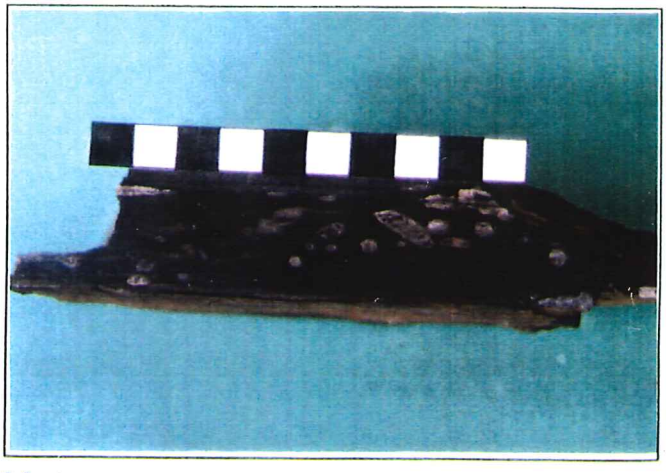

H

likely a result of deformation, illustrated by the wrapping of phyllosilicates (bt and mu) around garnet porphyroblasts.

Thin calcsilicate bands of epidote, actinolite and diopside were found on numerous occasions amongst the more psammitic, quartzofeldspathic rocks (plate 1D). Such bands are useful marker beds due to their regional extent. Diopside is the most abundant mineral (~25%) followed by quartz (~20%) which shows strong undulose extinction. Distinctive green epidote is present in significant amounts (~15%), together with plagioclase (10%). Actinolite (~10%), chlorite (~5%), muscovite (~5%), minor opaques and euhedral, diamond shaped sphene are important minor phases (plate 1E). A brecciated calc-silicate outcrop can be seen 1-2 kilometres east of Antro Woolshed (appendix H) (plate 1F).

Retrograde ?andalusite porphyroblasts (now muscovite) preferentially growing along bedding planes exist within some of the more psammitic sequences (plate 1G, 1H; app. B plate 4B). The most likely explanation for their confined extent is due to variation in initial bulk composition (app. B plate 4C). Regionally pervasive albitite interbeds up to 0.5 metres thick form continuous bands useful for determining bedding orientation (plate 2A). Cross-bedding was found within a few of these distinctive sequences, allowing determination of younging direction.

In addition to the above, the metasediments also include finer grained, pale brown schist, coarser haematitic schist and crenulated biotite schist. Ripple laminations were preserved at a few localities.

Numerous cross-cutting pegmatites, both pre and late-syn deformational were identified in the field (app. B plate 4D, 4E).

2.4.2 Antro Tonalite

This tonalite of locally minimal extent consists of plagioclase (~55%), quartz (~25%), clinopyroxene (~15%) and K-feldspar (< 5%), with minor phases of sphene, subhedral to euhedral lozenge shaped apatite, and secondary minerals including muscovite and chlorite (plate 2B). Opaques (?magnetite or ilmenite, commonly cubic shaped) are present in a significant amount (~20%). This rock is relatively mafic and based on its mineralogy (ie., being quartz undersaturated, and containing sphene) it initially appears to have an I-type nature.

One - two kilometres northeast of Antro Woolshed (refer appendix H) exists a poorly exposed and highly weathered outcrop of this granite, the only one within the mapped area. It is extensively recrystallised and variably deformed hence measurement of exact foliation and lineation is unable to be determined. It appears to be intrusive into a sequence of phyllitic metasediments however no contact between the two lithologies was exposed.

Based on the classification scheme of Streckeisen (1973), this granitoid is a tonalite (fig. 2.4.2.1).

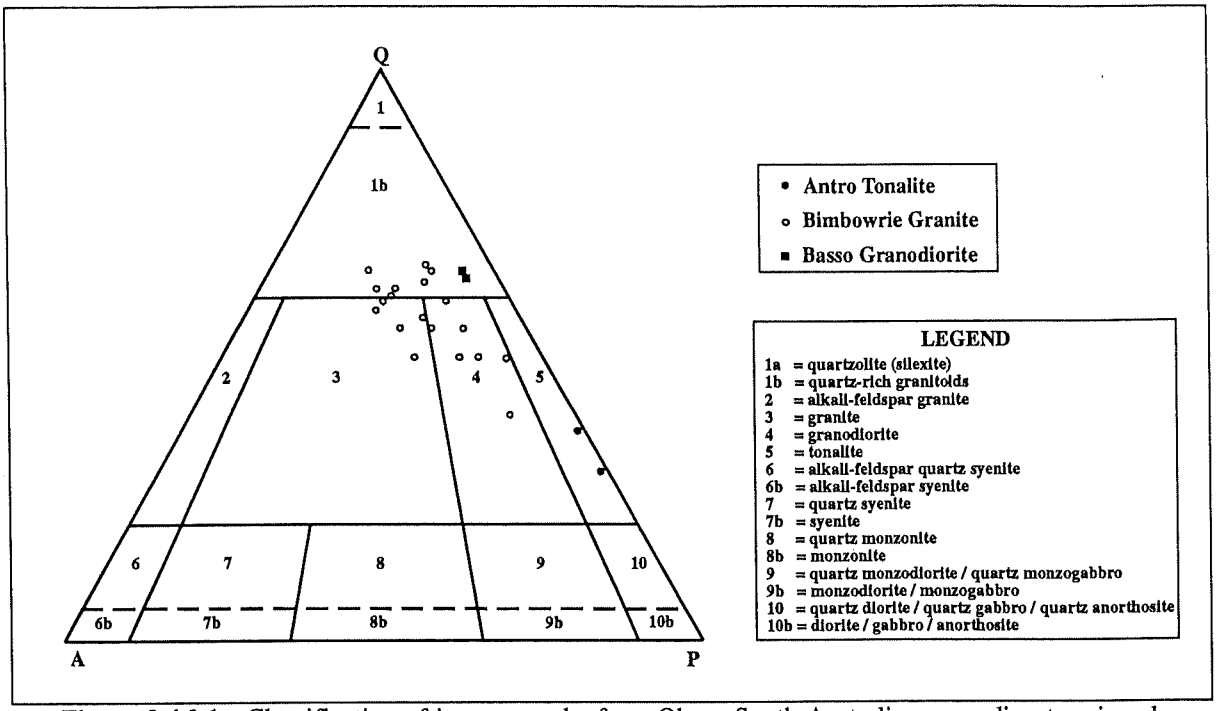

Figure 2.4.2.1 - Classification of igneous rocks from Olary, South Australia - according to mineral composition (after Streckisen, 1973)

2.4.3 Basso Granodiorite

The Basso Granodiorite is located near Basso Mine, Tommie Wattie Bore, Ameroo Hill, Boundary Deposit and Doughboy Well Mine. It is a quartz-feldspar-biotite rock, exhibiting a strong foliation, delineated by the planar arrangement of micaceous aggregates (plate 2C). The granitoid is composed of quartz (~50%), plagioclase (~25%), biotite (~20%), K-feldspar (<10%) with minor muscovite, apatite and opaques(?magnetite) (plate 2D).

In view of the classification scheme outlined in chapter 3, the informally-termed Ameroo Granite of previous workers (eg., Ashley *et al.*, 1994), falls into the category of the Basso Granodiorite (app. B plate 4F).

Anhedral quartz grains with undulose extinction exist, with the larger grains annealed to form aggregates of smaller quartz subgrains. Anhedral to subhedral multiple twinned plagioclase grains containing minor poikilitic inclusions of quartz, biotite and muscovite; together with K-feldspar commonly in the form of microcline makes up the majority of this rock. However subhedral, pleochroic dark-brown-green to straw coloured biotite grains, strongly aligned and intergrown within the quartz and feldspar framework are a major constituent. Within these, included zircons are highlighted by black alteration haloes. Less commonly, smaller aggregates of brown-brown-orange biotite overprints the textural features. Opaque oxides (?magnetite or ilmenite) may comprise up to 10% of the rock (plate 2E).

The Basso Granodiorite, intimately associated with, yet intruded by the Bimbowrie Granite, is both petrologically and in outcrop significantly different (plate 2F). The Basso Granodiorite intrudes the host metasediments, and at a later date both lithologies are intruded by

PLATE 2

A Hand specimen of a typical albitite.

B Antro Tonalite, showing dominantly plagioclase. Note the fine grain size and degree of recrystallisation, Field of view = 13.0 mm (sample number 1027-001).

C Basso Granodiorite in outcrop. A strong fabric can be seen, delineated by the planar arrangement of micaceous aggregates.

D Basso Granodiorite in hand specimen, note the abundance of biotite (sample number 1027-017).

E Basso Granodiorite in thin section, composed of quartz, plagioclase, biotite, K-feldspar, muscovite and apatite + opaques. Field of view = 13.4 mm (sample number 1027-017).

F Contact between the Basso Granodiorite (bottom) and the intruding Bimbowrie Granite (top). Note the pull away clast from the Basso Granodiorite.

G Xenolith of the Basso Granodiorite in the Bimbowrie Granite.

H Metasediment xenolith within the Bimbowrie Granite (sample number 1027-114).

A

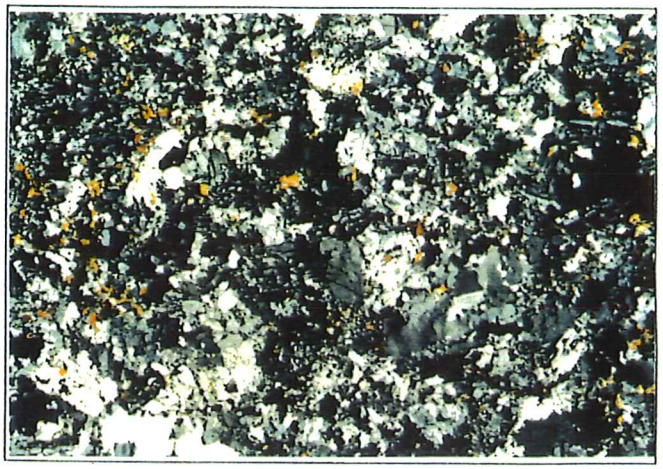

B

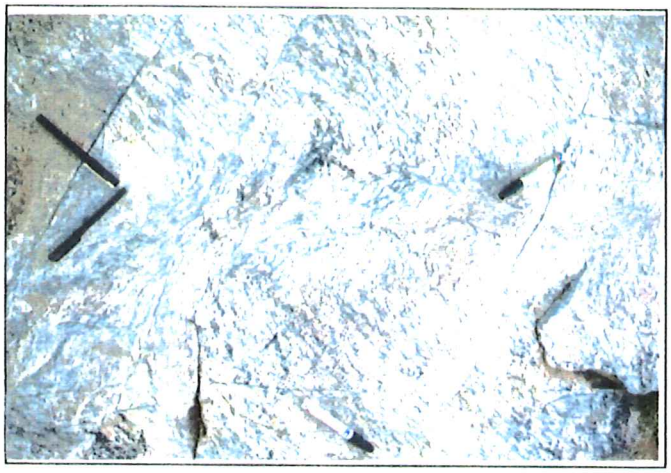

C

D

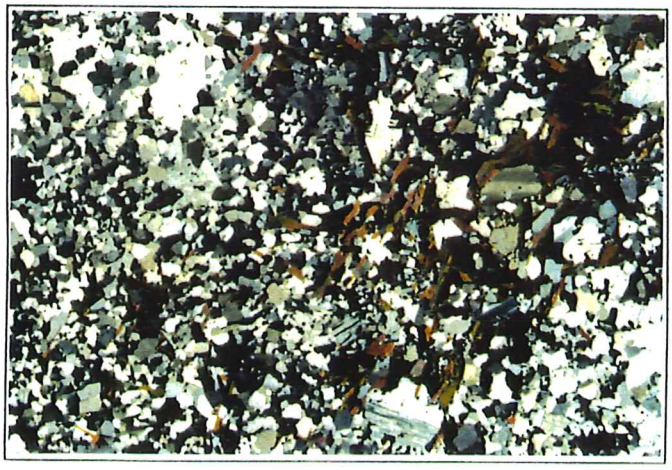

E

F

G

H

PLATE 3

A Contact in thin section between a fine grained metasediment xenolith and the much coarser Bimbowrie Granite. Field of view = 8.2 mm (sample number 1027-036b).

B Hand specimen of the Bimbowrie Granite with the diagnostic very coarse grained feldspar phenocrysts (sample number 1027-005).

C Bimbowrie Granite with a fine grained matrix, and a few diagnostic feldspar phenocrysts (sample number 1027-046).

D Bimbowrie Granite in thin section, note the very large feldspar phenocrysts diagnostic of this granitoid. Field of view = 21.7 mm (sample number 1027-005).

E Migmatite in hand specimen (sample number 1027-008).

F Migmatites, formed by *in situ* anatexis of local sediments, with only minimal melt migration.

G Metasediment xenolith with original bedding still evident, contained within the Bimbowrie Granite.

H The Bimbowrie Granite containing an abundance of metasedimentary xenoliths at contact margins, declining in frequency towards the centre of the granitoid.

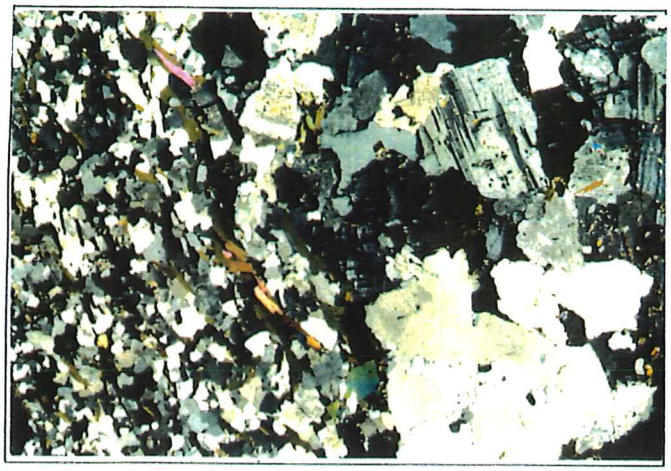

A

B

C

D

E

F

G

H

the Bimbowrie Granite, as evident by the presence of Basso Granodiorite and metasedimentary xenoliths within this granite (plate 2G, 2H, 3A). Clear contact margins may be seen within the field (two such localities are near Boundary Deposit and Basso Mine); and as illustrated in plate 2F, an injection direction of the Bimbowrie Granite may be established.

This medium grained essentially equigranular biotite-rich granitoid is classified as a qtz-rich granitoid however a granodiorite (qtz-rich) gneiss would perhaps be more applicable (fig. 2.4.2.1).

2.4.4 Bimbowrie Granite

The Bimbowrie Granite is medium to coarse grained, relatively leucocratic, pink to buff in colour, and composed of qtz-mu-bt-K-fld (microcline) and plag (plate 3B, 3C). Quartz the most abundant mineral (~40 %) has strong undulose extinction. Plagioclase, defined by its distinctive multiple twinning contains inclusions of muscovite and quartz and together with microcline, makes up the majority of the rock (~30% and ~20% respectively). Muscovite is present in all of the rocks examined but textural relationships suggest that it is possibly a primary mineral in only a few cases (plate 3D). In thin section, muscovite appears as flakes interleaved with biotite, that appear to be recrystallised aggregates. This implies that the muscovite may be a subsolidus phase.

With reference to the 1:10 000 geological map produced for the area (appendix H), the Bimbowrie granite outcrops near Antro Woolshed, Tommie Wattie Bore, Basso Mine, Boundary Deposit, Doughboy Well Mine and Brady Mine. These intrusions are large, relatively homogeneous and show weak NW-trending (042) fabrics defined by the alignment of very coarse grained feldspar phenocrysts (app. B plate 4G).

Their field relations imply that they are largely the product of variable segregation of migmatite leucosomes, exhibiting a complete range of contact phenomena ranging from sharply intrusive (with the Basso Granodiorite) to gradational into migmatites. Thus it is considered that they are largely the products of partial anatexis and melt segregation from adjacent and underlying migmatitic rocks, formed during a high grade metamorphic event (plate 3E, 3F).

This granite has strong S-type characteristics, supporting the notion that it is derived by *in situ* anatexis of local sediments, with only minimal melt migration. In support of this is the presence in thin section of ubiquitous red-brown biotite which invariably contains zircon crystals with black circular alteration haloes. Geochemical based reasoning gives confirmation to this notion, discussed in chapter three.

The Bimbowrie Granite contains significant quantities of metasedimentary xenoliths, in greatest abundance at the margins in contact with the metasediments; declining in frequency at a distance from this zone (plate 3G, 3H). From this observation, it may be said that assimilation of the metasediments is taking place.

Based on the classification scheme of Streckeisen (1973) these granites may be classed as qtz-rich granitoids, granites or granodiorites (fig. 2.4.2.1).

2.5 Structural and Metamorphic History

Throughout the Olary Block, the Willyama Supergroup has been extensively deformed and metamorphosed. The Palaeoproterozoic Olarian Orogeny and the Cambro-Ordovician Delamerian Orogeny are two major periods of deformation widely recognised (Thomson, 1969ab; Glen *et al.*, 1977; Berry *et al.*, 1978). Five deformational phases ranging from the Palaeo- or Mesoproterozoic to Ordovician have been recognised within the Willyama Supergroup. D_1 to D_3 are ascribed to the Olarian Orogeny and D_4 and D_5 are manifestations of the Delamerian Orogeny.

Olarian Orogeny

Within the Palaeoproterozoic basement, the Olarian Orogeny was by far the more pervasive, of higher metamorphic grade and formed the majority of meso- and macroscopic structures. The earliest deformation (D_1) is represented by a schistosity (S_1) with layer parallel sillimanite, biotite and/or muscovite. At this time, amphibolite facies metamorphism, with estimated temperature and pressure conditions of 650-720°C and 2-4kb (Berry *et al.* 1978) gave rise to the growth of sillimanite, andalusite, kyanite and garnet within the Palaeoproterozoic metasediments. Also during this deformational period impure carbonaceous sediments grew diopside, vesuvianite, garnet, wollastonite and piedmontite metamorphic assemblages (Parker, 1986).

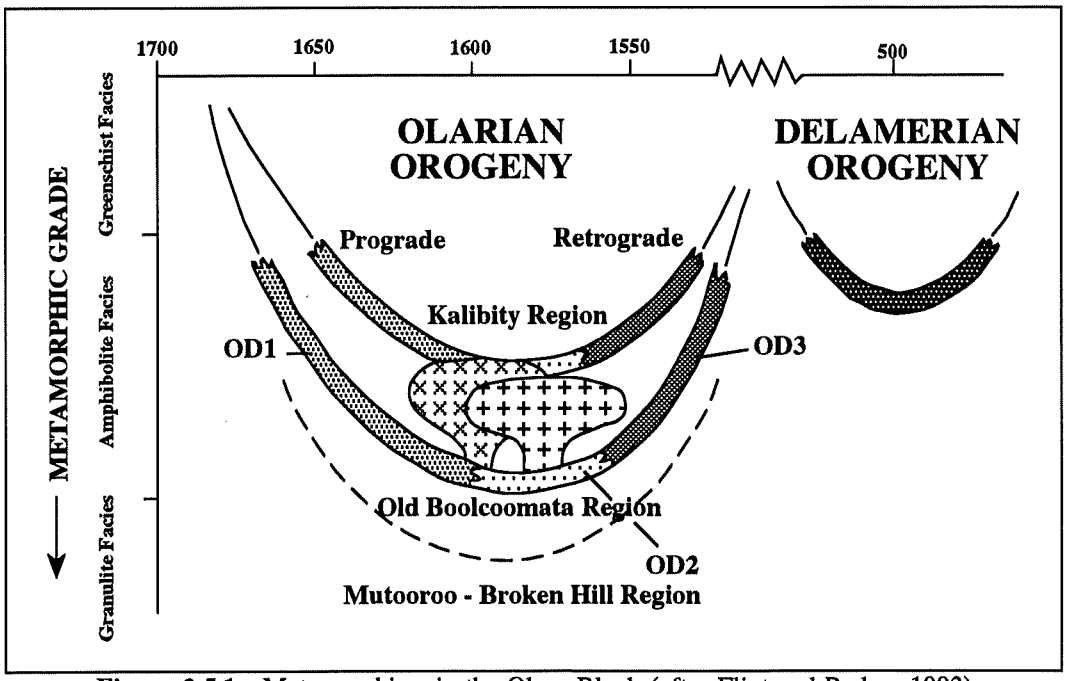

Figure 2.5.1 - Metamorphism in the Olary Block (after Flint and Parker, 1993)

The north to south increase in metamorphic grade evident in the Broken Hill Block (Phillips, 1980) is broadly present in the Olary Block. Significant local perturbations of grade proximal to some granitoids (eg., Plumbago area and near Cathedral Rock) does however occur.

Clarke *et al.* (1987) recognised four metamorphic zones (I, IIa, IIb and III) which have been spatially partially modified in more recent years, by Flint and Parker (1993). A more detailed account of these metamorphic zones is set out below.

Zone I

Zone I contains andalusite porphyroblasts, enveloped by a pervasive S_2 mineral fabric defined by muscovite and chlorite, with less garnet and biotite or fibrolitic sillimanite. In the carbonaceous rocks, andalusite commonly occurs as chiastolite.

Zone IIa

Zone IIa metapelites are typically chloritoid bearing schists with associated muscovite, chlorite and garnet. In garnet absent metapelitic rocks, andalusite porphyroblasts are surrounded by abundant fibrolitic sillimanite (as in zone I).

Zone IIb

Zone IIb contains similar assemblages to those of zone IIa with the addition of rare staurolite. Close to the syntectonic granitoids, the sequences have been known to contain all three aluminosilicate polymorphs (Clarke *et al.*, 1987).

Zone III

Zone III is largely restricted to a region of poor outcrop in the south-east of the Olary Block. This pelitic zone contains assemblages of either kyanite and sillimanite or garnet.

The timing relationships of the aluminosilicate polymorphs, together with the peak metamorphic and overprinting paragenesis, imply an anticlockwise P-T path for the Olarian Orogeny, pressure increasing with cooling from the metamorphic peak (Clarke *et al.*, 1987).

The presently exposed variation in metamorphic grade is best explained by regional block tilting as documented for example in the Himalayas (Le Fort, 1975) and the Alps (Zingg, 1980), and not by a variation in heat flow.

Within the lower Proterozoic metasediments, the stratigraphy is principally controlled by NE-E trending upright, open to tight D_2 folds, refolding an earlier D_1 recumbent terrain. The F_1 folds are not often seen yet are inferred to be recumbent, giving rise to downward facings (Clarke *et al.*, 1987). F_2 folds exhibit a steeply NW dipping axial plane schistosity (S_2) defined by sillimanite and biotite (Glen *et al.*, 1977). The S_2 axial plane is commonly defined by moderate to strong crenulation of the S_1 fabric producing a widespread intersection and crenulation lineation, L_2. The sub-parallelism of the F_1 and F_2 axial traces causes interference patterns on a mesoscopic scale to be rare. In summary, is seems simplest to consider the D_1 and D_2 events as having developed progressively during the same continuum of orogenic event, which suggests that the time span between them is likely to be small.

D_3 is represented throughout the Olary Block by east striking retrograde shear zones disecting the sequence, overprinting D_1 and D_2 folds. Recrystallisation of mineral fabrics to lower amphibolite - greenschist metamorphic facies occurs, with extensive hydration of previous assemblages. Clarke *et al.*, (1986) recognised that the retrograde shear zones cross-cut unfoliated (post-tectonic) granitoids. Steeply plunging elongation and mineral lineations present within the east striking retrograde shear zone preserve evidence for a reverse sense of movement (S over N) whilst zones oblique to the approximate N-S compression axis preserve a considerable transcurrent component of movement.

Sedimentation of the Willyama Supergroup sequences is required to have taken place prior to 1700Ma., as this is the approximate age for the D_1 event, estimated by Flint and Webb (1980), based on the Rb-Sr isotopic system. Intrusion of felsic granitoids occurred over the period of ~1700 - 1550 Ma. and caused local migmatisation and melting of host rocks. An imprecise Rb-Sr age of 1503 ± 223 Ma. (Flint and Webb, 1980) has been obtained for the intrusion of granitoids during D_3, the final phase of the Olarian Orogeny.

Delamerian Orogeny

Adelaidean and Willyama Supergroup rocks were both affected by deformations D_4 (northerly trending axes) and D_5 (easterly trending axes).

The Cambro-Ordovician Delamerian Orogeny left Adelaidean rocks folded, metamorphosed (to biotite grade) and intruded (by the Anabama Granite and associated dykes). This deformation gave rise to N-S trending folds and a second phase produced NE-SW folds.

North trending synclinal wedges of Adelaidean rocks between the crystalline inliers is an example of D_4 folding. Adjacent to basement inliers, D_5 is manifested by deformed pebbles within the basal Adelaidean, ie., pebbles are tectonically elongated in the direction of plunge of D_5 fold axes (Grady *et al.*, 1984). The D_5 folding has caused arching of the major D_4 fold axes.

Faults initiated during sedimentation along the western sides of inliers were propagated during D_4. Both D_4 and D_5 produced axial planar schistosity or cleavage. Adelaidean rocks display large broad D_5 folds which have steeply dipping axial planes striking E-NE, and are strongly affected by N-W directed faults (eg. MacDonald Fault) bounding the S-W edges of crystalline basement inliers.

Detailed analyses of the effects of the Cambrian 'Delamerian' Orogeny within the Olary Block are presented by Forbes and Pitt (1980) for the upper Proterozoic Adelaidean sequence, and in Berry *et al.* (1978) and Grady *et al.* (1984) for the Willyama Complex.

CHAPTER 3 - GEOCHEMISTRY

3.1 Granite Classification

The most widely used concept amongst igneous petrologists over the last few decades has been the I- and S-type genetic classification for igneous rocks of Chappell and White (1974). I-type stands for infracrustal (or igneous precursor), and S-type for supracrustal (or sedimentary precursor), both however are generated during tectonism (ie., are generally related to orogenesis) (Whalen *et al.*, 1987). To delineate this further, S-types are derived from the partial melting of metasedimentary source rocks or pre-existing S-type granites and I-types are produced either by partial melting or by fractional crystallisation of mantle derived source material, that have not experienced surface weathering processes (Chappell and White, 1992). Both however are regarded as essentially crustal melts of pre-existing igneous or sedimentary material. Unfortunately a large number of granite plutons are difficult to allocate convincingly to either S- or I-type. In part this arises because some S-type characteristics can be inherited through extensive hydrothermal interaction with sedimentary country rocks. Additionally, alteration of a granite's geochemical signature may be dependant upon the extent to which reworking has taken place.

The additional term M-type has been introduced (as a subset of I-type) for granites of limited crustal residence time, possibly of mantle or mantle-wedge derivation (Tarney and Jones, 1994).

To complicate matters further, a fourth granite type, A-type (A for anorogenic or alkaline) has been introduced, documented for example by Collins *et al.* (1982) in the Lachlan Fold Belt and Tuner *et al.* (1992a) from Padathway Ridge, South Australia. They are chemically and mineralogically distinct from the more common I- and S-types implying a different petrogenesis, the exact form of which is a subject of considerable controversy (Turner *et al.*, 1992a). Collins *et al.* (1982) suggest that such granites result from remelting of crust from which earlier granites had been extracted. Alternatively Turner *et al.* (1992a), suggests that fractionation of basaltic parental magma gives birth to such granites. A-types are generally siliceous, reduced, iron-rich, flourine-rich, often niobium-rich, and have consistently high levels of rare earth elements (REE) (Tarney and Jones, 1994). It is important to note that I-type granites require by definition a two-stage melting process (one mantle, one crustal) for generation, S-types also need an intervening sedimentary cycle, and A-types, depending on the model, are generated by either a three-stage melting cycle (mantle, crustal, crustal) or simply a single cycle directly from the mantle.

Hence, the differences between the groups are not the result of differences in the melt forming process but reflect differences in the nature of the source material.

Three distinct groups of granitoids can be recognised within the field area. In this chapter these granites are classified by virtue of their geochemistry and classified into tectonic and source regimes.

3.2 Objectives

Extensive X-ray fluorescence (XRF) whole rock analysis was carried out on metasediments, migmatites and amphibolites, in addition to the three granite types within the field area in order to:

(1) Support field evidence that three different granite types exist
(2) Categorise the granitoids into I, S or A type
(3) Note the geochemical affinities of the three granitoids
(4) Constrain source regions of the granitoids
(5) Put constraints on Proterozoic tectonics and crustal evolution in the Olary Block

Note: Refer to appendix C for information regarding analytical techniques, and appendix D for a complete list of data obtained.

3.3 Geochemical Affinities

Previous geochemical investigations in the Olary Block are restricted to various honours students and a few workers (eg., Ashley, 1984). Problems with correlating such data with that of this study lie in inconsistent lithological descriptions, inadequate sample localities and simply the scarcity of geochemical data.

The multi-element variation patterns obtained for Proterozoic granites are relatively uncomplicated when normalised against mantle compositions. There are usually negative Ba, Nb (Ta), Sr (Eu), P and Ti anomalies, that reflect fractionation by mineral phases containing these elements at some time during the history of the source, or of the magma (Tarney and Jones, 1994). A progressive enrichment from the more compatible to the most incompatible element is notable. These distinctive features may be seen in the three granitoid types studied (see following sections).

Fifty-two samples were analysed by XRF from the field area; this database forming the basis for classification and subdivision of the granites, allowing scope for identification and comparison of distinctive features on a local scale.

Figure 3.3.1.1a - Trace element discrimination diagram for the Bimbowrie Granite

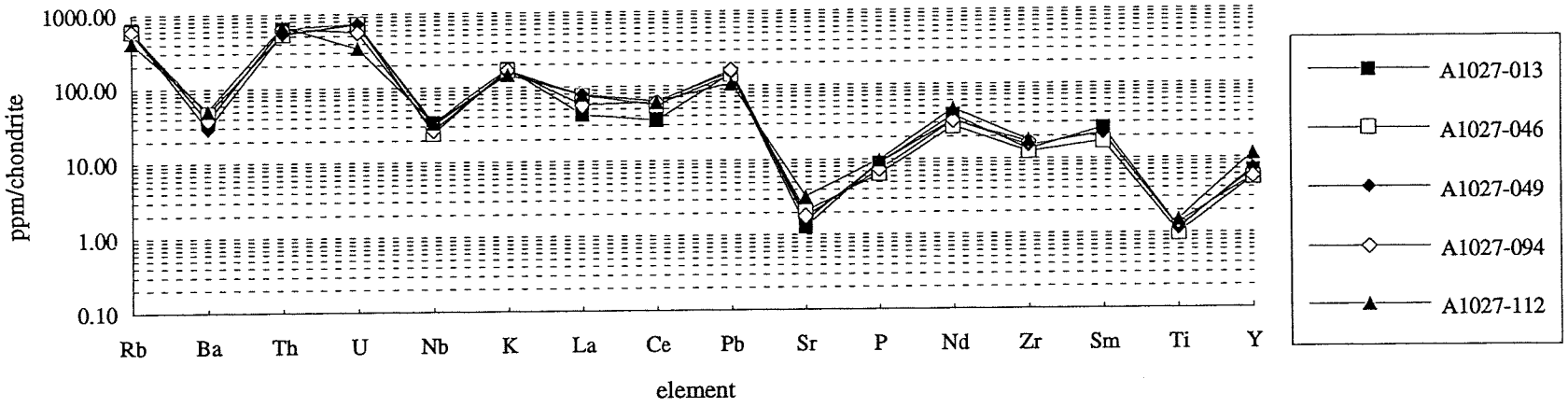

Figure 3.3.1.1b - Trace element discrimination diagram for the Bimbowrie Granite

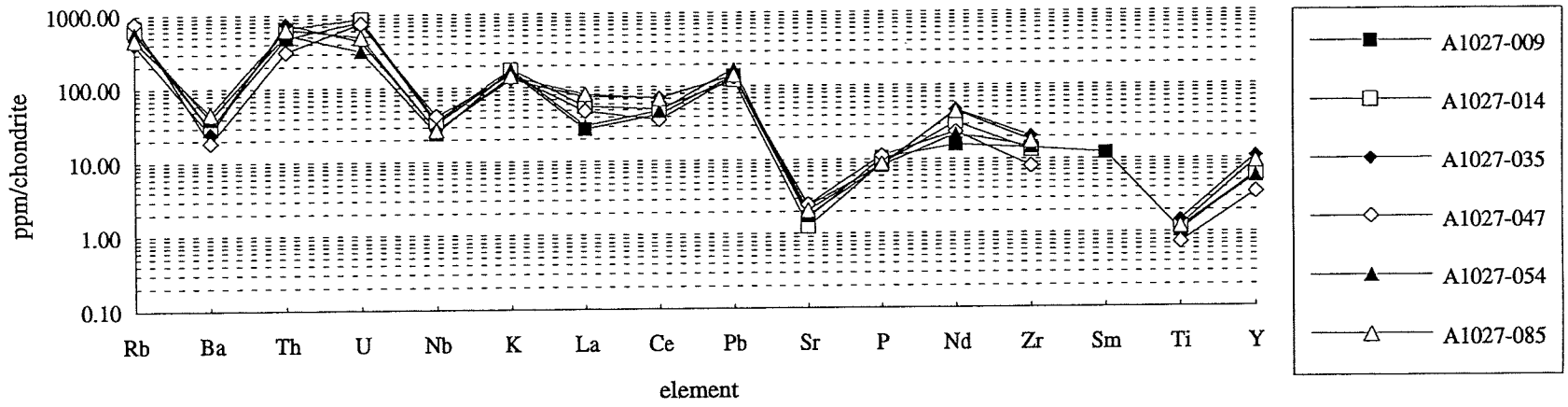

3.3.1 Bimbowrie Granite

As a suite, the Bimbowrie granitoids range in composition from quartz rich granites to granodiorites (fig. 2.4.2.1). They exhibit a limited SiO_2 range, from 71-76%; significantly less than the Basso Granodiorite. They are substantially higher in Al_2O_3, CaO and K_2O, lower in Na_2O and an excellent discriminant exists in P_2O_5 where much higher levels are detected.

The Bimbowrie Granite are typically enriched in Rb, Sr, Pb and Zn, depleted in Nb, Zr, Ga and Y (fig. 3.3.1.1a, b; table 3.3.1.1) with an Al index (molar $Al_2O_3/(CaO + Na_2O + K_2O)$) in most cases greater than 1.1 (fig. 3.3.1.2), indicative of S-type granitoids (Chappell and White, 1974).

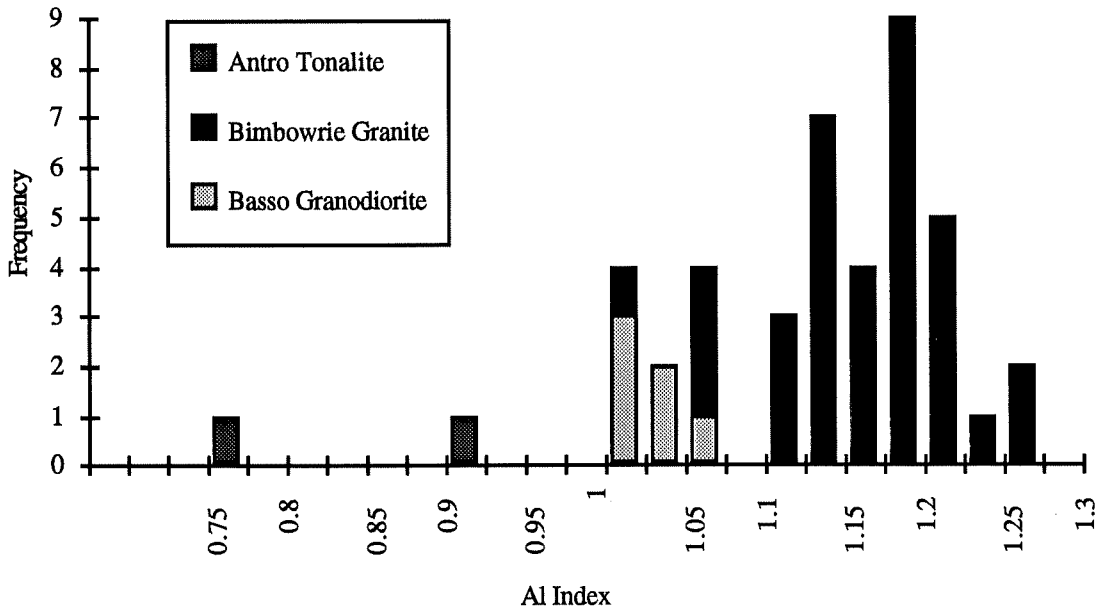

Figure 3.3.1.2 - Histogram showing the frequency of Al Index for granitoids of the Olary Block

The Na_2O-K_2O plot (fig. 3.3.1.3) shows the most fundamental chemical difference between the three granitoids in the map area. The more potassium rich S-types are lower in sodium and the separation of the three groups is unambiguous. Differences of this type are a useful criterion in recognising I- and S-type granitoids and were an important factor in determining that the overall I- and S-type characteristics were reflections of fundamentally different sources (Chappell and White, 1974). Field evidence and petrological information suggests this granite has S-type affinities, geochemistry allows for confirmation and precise discrimination of this lithology.

Numerous workers (eg., Hine *et al.*, 1978; Turekian and Wedepohl, 1961; Kolbe and Taylor, 1966) consider that aluminium is enriched relative to Na and Ca in the production of shales by chemical weathering, since Ca is concentrated in limestones and Na is removed into seawater and evaporites. Thus pelitic rocks relative to Na and Ca have high K contents,

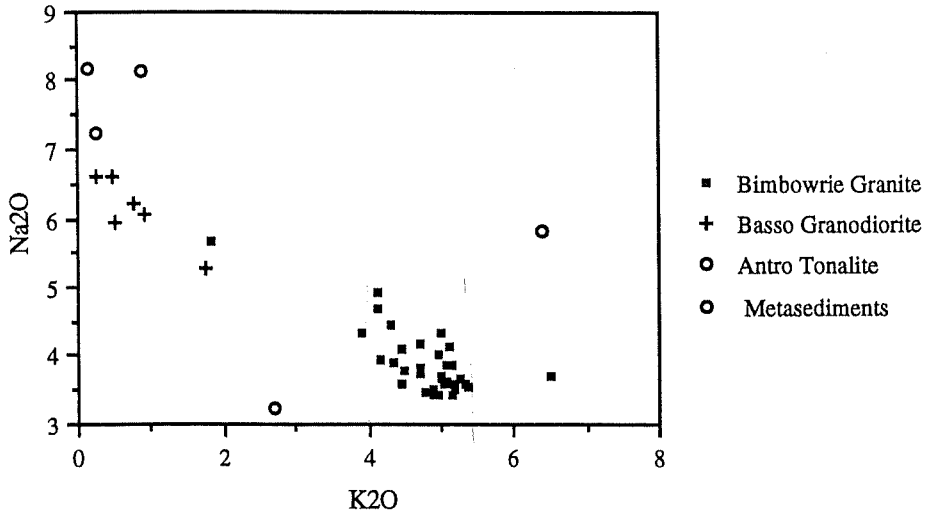

Figure 3.3.1.3 - Na_2O vs K_2O discrimination diagram

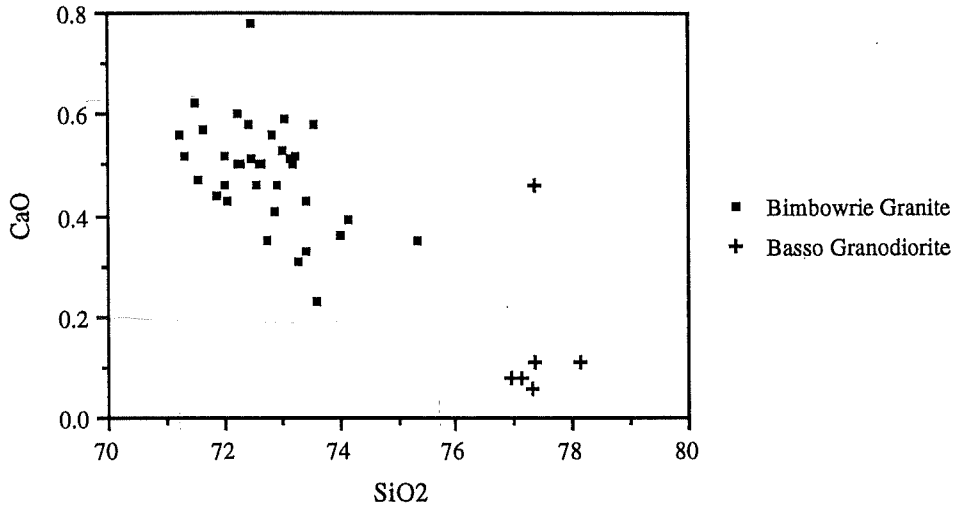

Figure 3.3.1.4 - SiO_2 vs CaO discrimination diagram

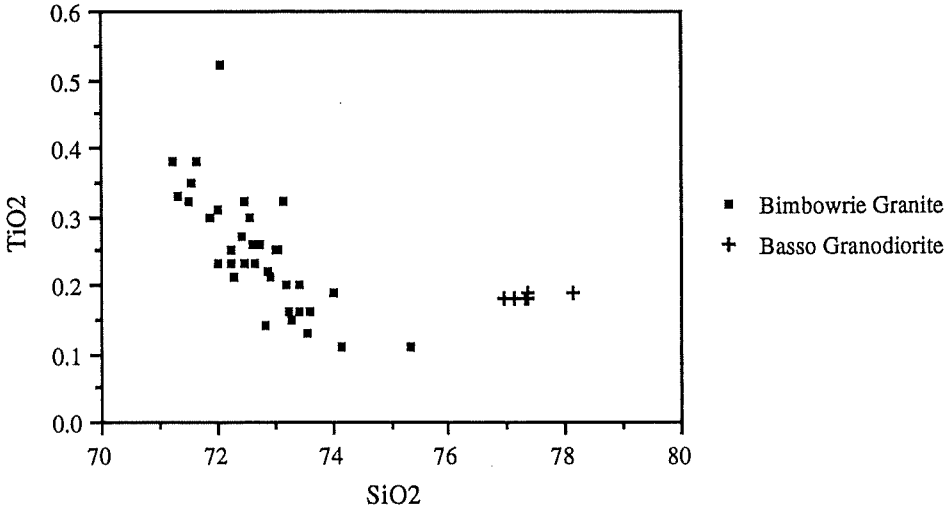

Figure 3.3.1.5 - SiO_2 vs TiO_2 discrimination diagram

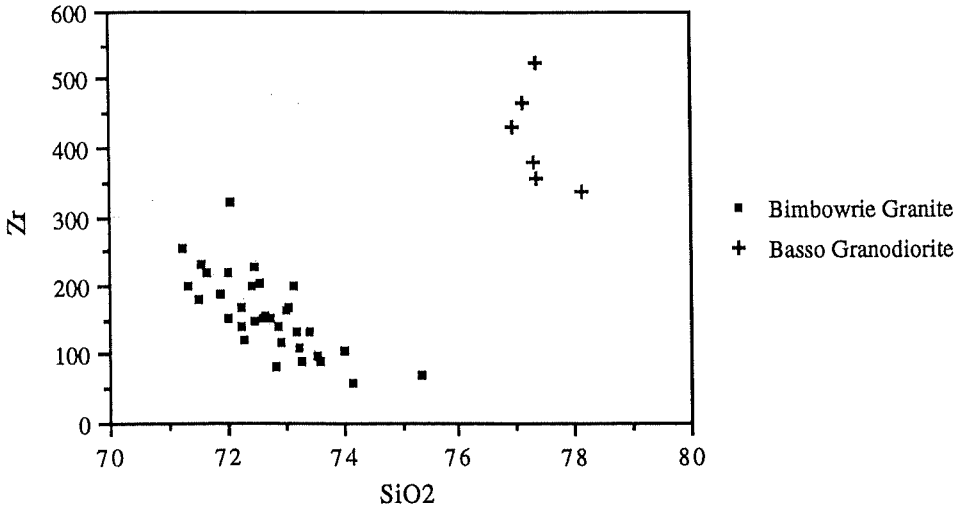

Figure 3.3.1.6 - SiO_2 vs Zr discrimination diagram

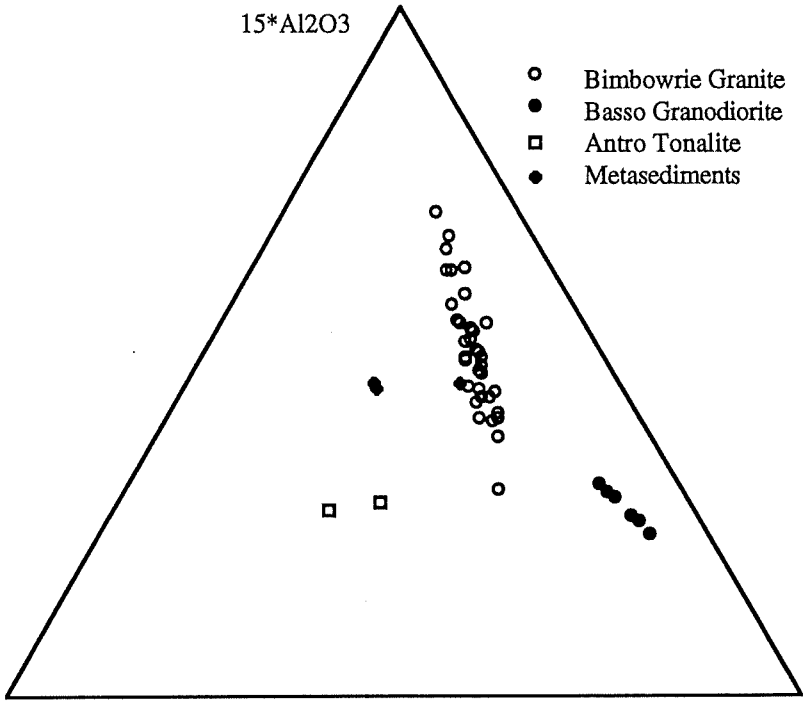

Figure 3.3.1.6 - Ternary plot of Al_2O_3, Zr and TiO_2

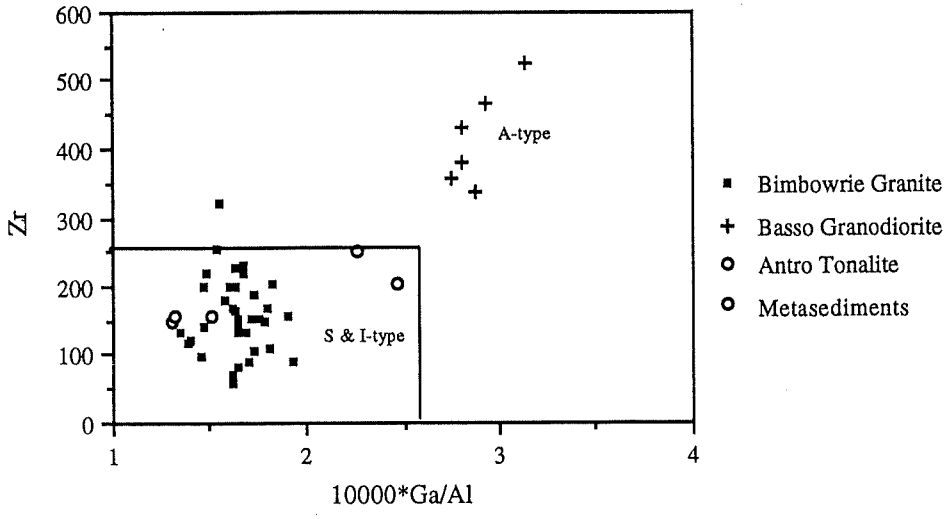

Figure 3.3.1.8a - Ga/Al vs Zr discrimination diagram

reflected in high K/Na ratios of S-type granitoids (fig. 3.3.1.3) and relatively low Ca contents (fig. 3.3.1.4). Such characteristics are directly reflected in the Al index factor where S-type granitoids are greater than 1.1.

TiO_2 contents are similar for the Bimbowrie and Basso granitoids however no systematic variation of TiO_2 with SiO_2 is identified within the Basso suite (fig. 3.3.1.5), implying that it is derived from fractionated igneous rocks (Hine *et al.*, 1978). Similarly, the plot of Al, Zr and Ti shows an excellent discrimination. The Bimbowrie Granite is spread over the ternary plot and possibly indicates the movement from a restite phase to a melt phase, as indicated by high Al values (Garcia *et al.*, 1994).

The S-type Bimbowrie suite characteristically contain elevated levels of Rb and Sr, in addition to P, Pb and Zn. Zirconium exhibits a strong negative correlation with SiO_2 despite it being appreciably more abundant within the Basso group (fig. 3.3.1.7). Ga is appreciably lower, as represented in the Ga/Al plots (figs. 3.3.1.8a,b,c,d).

Figure 3.3.1.1a, b demonstrates the uniformity of the Bimbowrie granite despite regionally extensive outcrop sampling. The compositional (trace) element variation for the three granite types and a metasediment, illustrating the differences and similarities between each lithology is detailed in figure 3.3.3.2.

An excellent positive correlation exists between TiO_2 and Zr in the Bimbowrie group, comparitively the TiO_2 content of the Basso suite remains constant (fig. 3.3.1.9).

3.3.2 Basso Granodiorite

Discrimination classifications based on trace element geochemistry for the Basso granite produces a well-defined group corresponding to A-type affinities. The informally termed Ameroo granite of previous workers (eg., Ashley *et al.*, 1994) has a U-Pb zircon age of 1703 ± 6 and is geochemically indistinguishable from the Basso, it is therefore included with the Basso Granodiorite for the remainder of this paper.

A-type granites exhibit chemical analyses characterised by high SiO_2, $Na_2O + K_2O$, Fe/Mg, F, Zr, Nb, Ga, Sn, Y and REE (except Eu) contents and low CaO, Al, Mg, V, Ba and Sr (Loiselle and Wones, 1979; Collins *et al.*, 1982; White and Chappell, 1983). Mineralogically these granites contain annite-rich biotite and/or alkali amphiboles and commonly sodic pyroxene. High Ga/Al values appear to be particularly diagnostic of A-type granites (fig. 3.3.1.8a,b,c,d). Isotopically, high ε_{Nd} and low $^{87}Sr/^{86}Sr$ ratios are measured, supporting the notion that A-type suites are of direct mantle origin, and arguing against a major crustal component in their genesis (Turner *et al.*, 1992).

Whalen *et al.* (1987) rely heavily on utilising plots of Ga/Al versus certain trace and major elements, with the fields indicated for M-, I-, A- and S-type granites. These fields have been used for discrimination of the A-type Basso granite, relative to the Bimbowrie and Antro granites, with S- and I-type characteristics respectively. Additionally, plots of Zr + Nb + Ce +

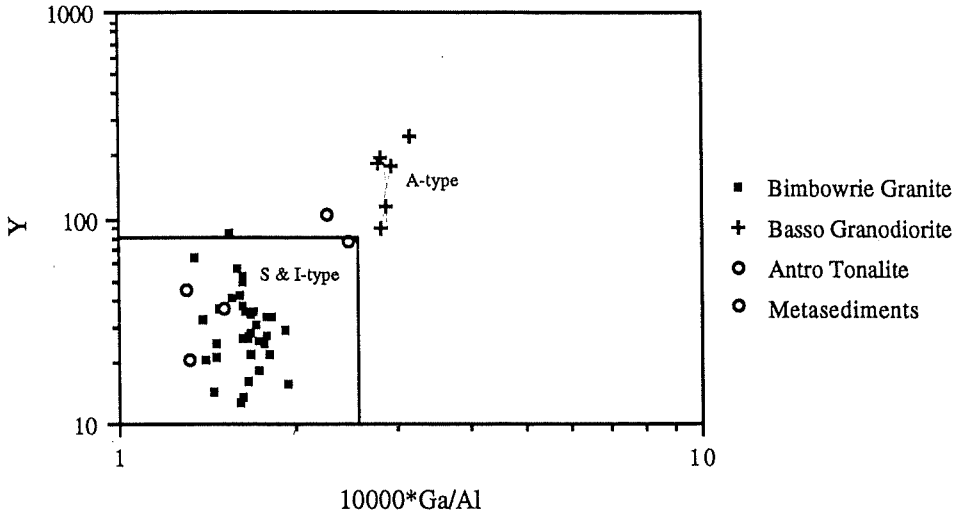

Figure 3.3.1.8b - Ga/Al vs Y discrimination diagram

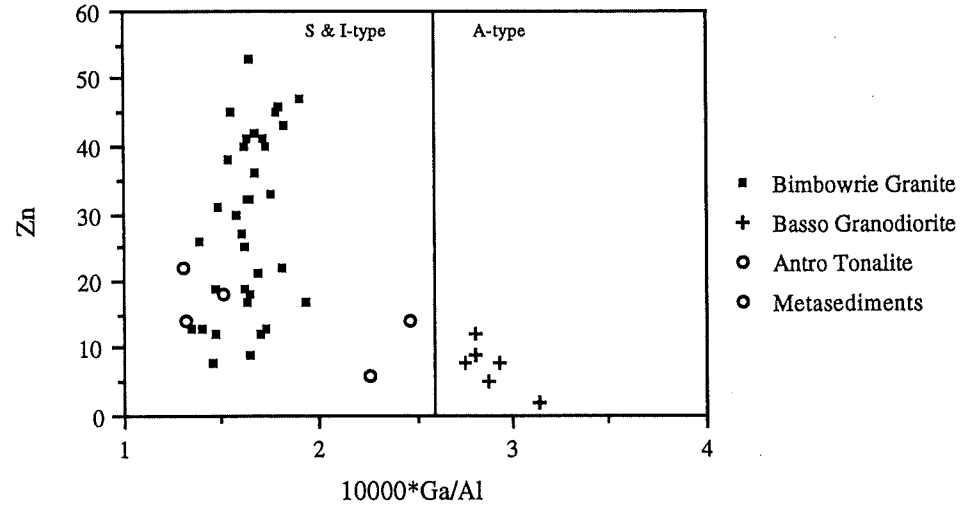

Figure 3.3.1.8c - Ga/Al vs Zn discrimination diagram

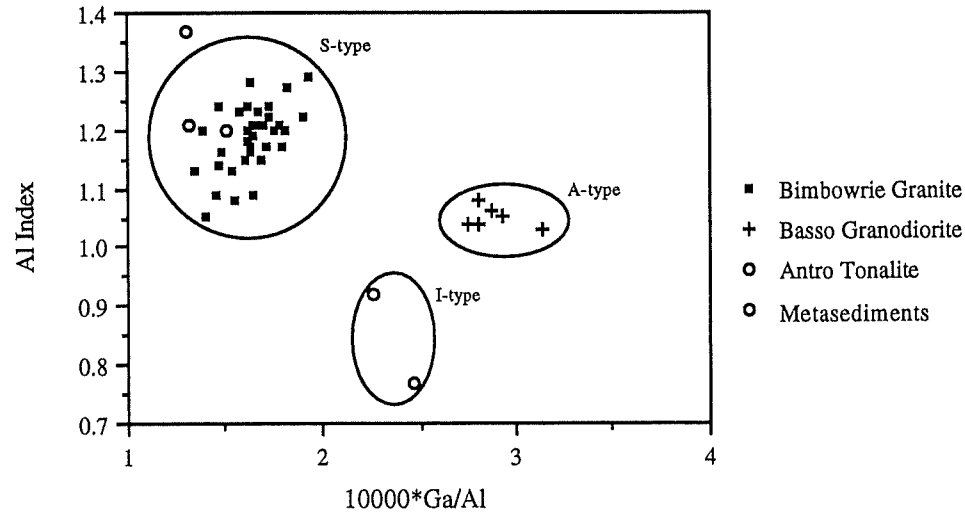

Figure 3.3.1.8d - Ga/Al vs Al Index discrimination diagram

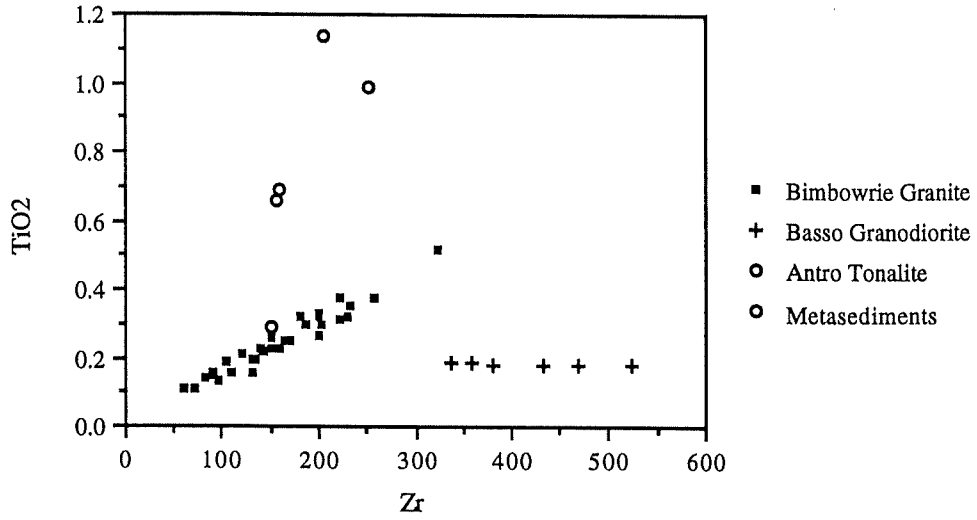

Figure 3.3.1.9 - Zr vs TiO_2 discrimination diagram

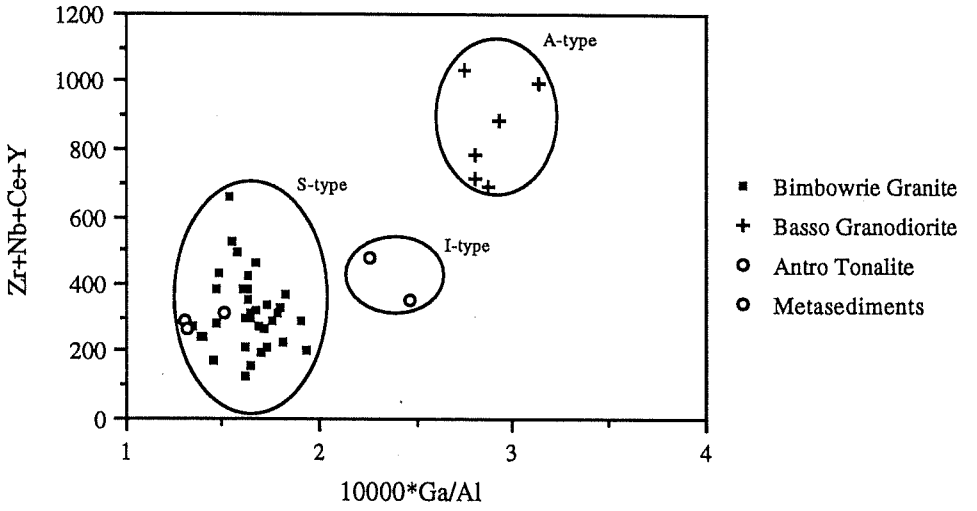

Figure 3.3.2.1 - Ga/Al vs Zr+Nb+Ce+Y discrimination diagram

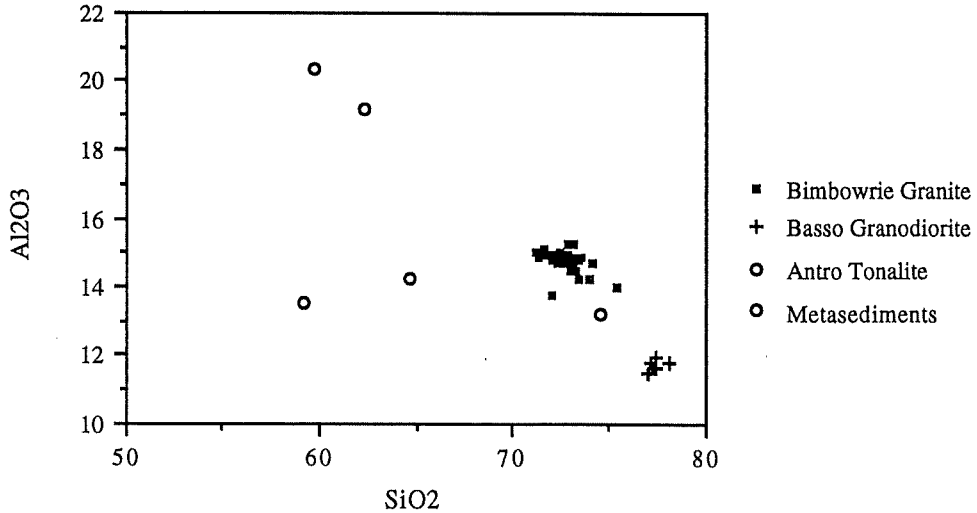

Figure 3.3.2.2 - SiO_2 vs Al_2O_3 discrimination diagram

Y versus major element ratios, are equally effective in identification of A-type granitoids (fig. 3.3.2.1).

The elements employed in most of these diagrams (Al, Fe, Mg, Ga, Zr, Nb, Ce and Y) have been found to be relatively insensitive to low to moderate degrees of alteration (Pearce and Cann, 1973) hence they should be equally effective for both fresh and altered granitic rocks. As the Basso granitoid shows strong foliation this may potentially be a problem, which is avoided by the use of these elements.

The Basso granitoid satifies all criteria set by Whalen *et al.* (1987), regarding A-type granites. SiO_2 is higher, in the range 77-79%, Al_2O_3 is lower than for S-type (Bimbowrie) granites (fig.3.3.2.2) and they have an Al-index <1.1 (fig. 3.3.1.2). Zr, Nb, Ga and Y are significantly higher, and Ca, Mg, Ba, V and Sr are significantly depleted (fig. 3.3.2.3; table 3.3.1.1). The Basso Granodiorite falls into the A-type category for both Ga/Al and Zr + Nb + Ce + Y plots of Whalen *et al.* (1987).

There are four lines of evidence for the A-type nature of the Basso, namely:

- high LREE
- high SiO_2
- high Zr, Nb, Y
- low Ca, Rb, Ba, V

It therefore seems apparent that the Basso granitoid displays A-type affinities and will thus be regarded as of this nature for the remainder of this thesis.

3.3.3 Antro Tonalite

Due to the weathered outcrop and recrystallised nature of the Antro Tonalite, definitive geochemistry was difficult to obtain. It is clear however, that several distinctive geochemical signatures allow discrimination from the other granite types in the study area. The initial feature is an Al Index < 0.95, the only granitoid in the area to show this (fig. 3.3.1.2). The criteria for distinction between I- and S-type granites is based on the Al Index, with a numerical separation between the two groups at 1.1 (I-type = <1.1, S-type = >1.1). Thus at first look, this tonalite can be classified as I-type.

High Fe_2O_3 levels, 12.29 wt% average and low LREE values (fig. 3.3.3.1 compared with the very elevated levels of the A-type Basso Granodiorite, is diagnostic of this granitoid, in addition to low levels of SiO_2 (table 3.3.1.1). Na_2O, CaO and TiO_2 are high and K_2O is comparitively much lower. All of these features, are consistent with the characteristics of an intermediate magma, with distinctly I-type affinities. This granite is high in copper, on average ~95 ppm, consistent with the abundance of opaques seen in thin section.

Figure 3.3.2.2 - Trace element plot discrimination diagram for the Basso Granodiorite

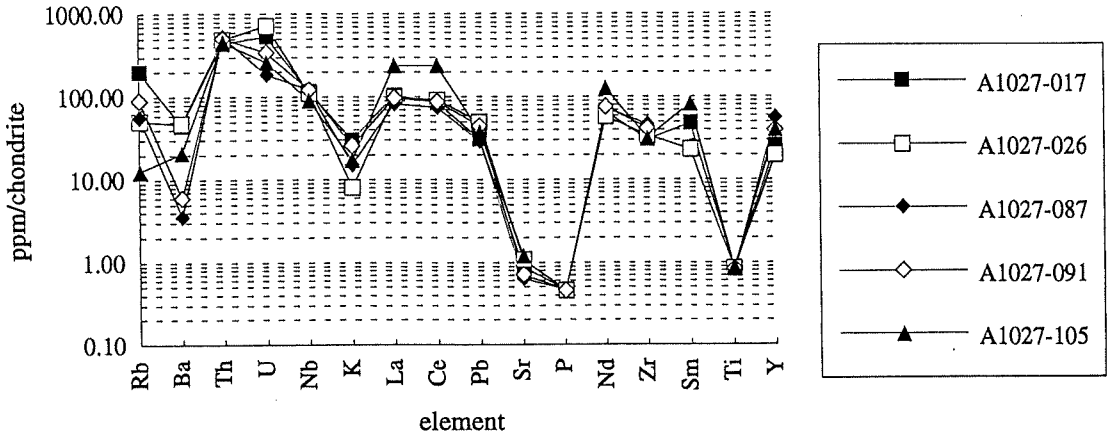

Figure 3.3.3.1 - Trace element discrimination diagram for the Antro Tonalite

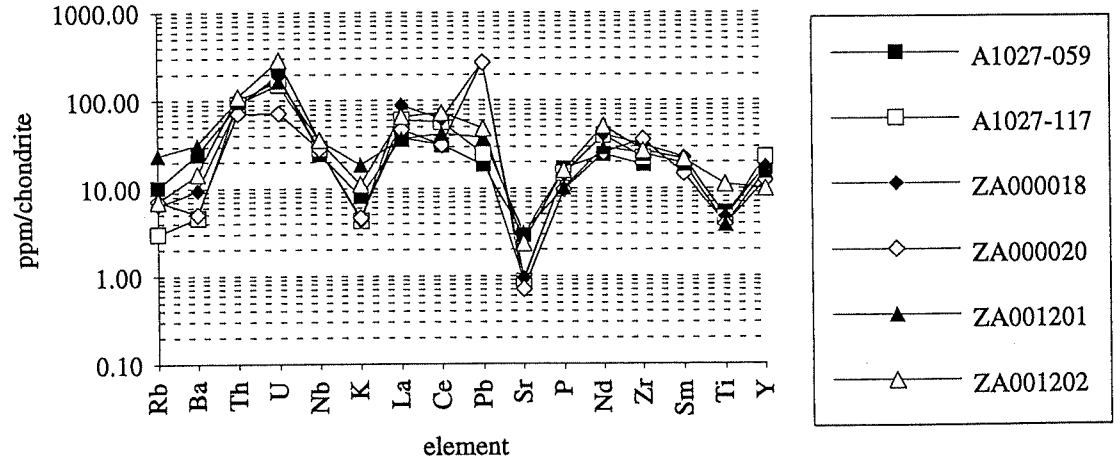

Figure 3.3.4.1 - Comparative trace element diagram of units in map area

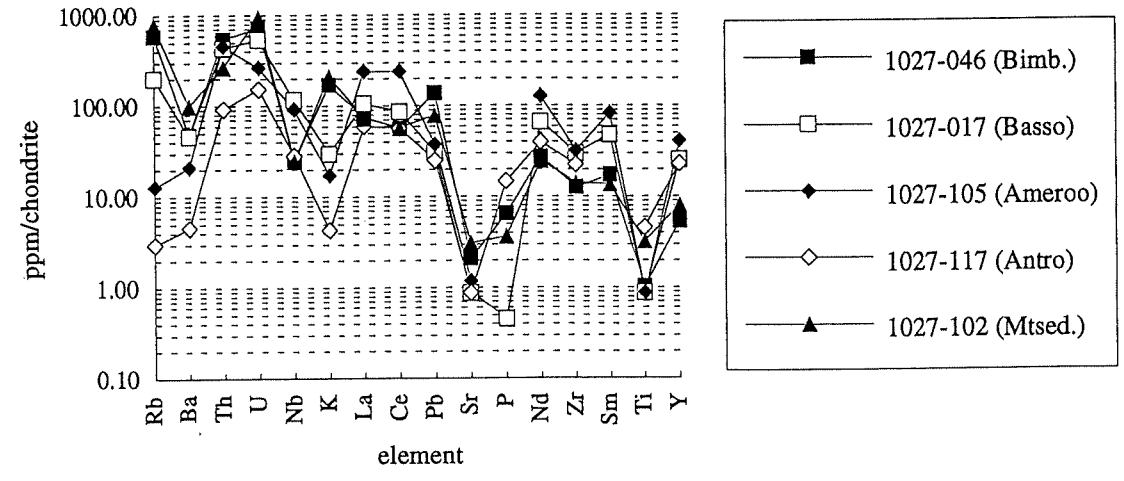

3.3.4 Metasediments

Analysis was carried out on several metasediment samples (psammitic to pelitic in composition) in order to establish any geochemical affinities with the S-type Bimbowrie Granite, and to help elucidate potential provenance regions.

The metasediments showed signatures typical of psammo-pelitic rocks, with moderately high Al levels, very high Al index values and low LREE values (fig. 3.3.3.1). Such patterns are mirrored in the S-type Bimbowrie Granite, reinforcing the genetic link suggested earlier. Figure 3.3.4.1 demonstrates the similarities and differences between all lithologies.

LITHOLOGY	Bimbowrie Granite	Basso Granodiorite	Antro Tonalite	Metasediment Psammite
No. of Samples	n=38	n=7	n=6	n=3
ELEMENT Major (Wt %)				
SiO2	72.71	77.37	61.86	65.51
Al2O3	14.75	11.73	13.20	17.58
Fe2O3	1.67	2.47	11.50	3.39
MnO	0.01	0.01	0.05	0.03
MgO	0.46	0.90	1.16	2.17
CaO	0.48	0.15	2.65	0.62
Na2O	3.88	6.11	7.37	5.74
K2O	4.79	0.77	0.25	3.32
TiO2	0.25	0.18	1.20	0.55
P2O5	0.20	0.01	0.30	0.08
SO3	0.00	0.00	-	0.00
LOI	0.75	0.23	0.26	1.17
Total	99.96	99.92	33.43	100.15
Al Index	1.19	1.05	0.78	1.26
Trace (ppm)				
Rb	359.46	71.84	6.05	268.55
Ba	240.00	150.67	103.67	456.00
Th	47.73	40.73	7.77	22.53
U	10.62	8.95	3.73	10.40
Nb	22.31	82.55	21.28	15.73
K	39747.52	6419.82	2103.04	27533.26
La	43.63	75.50	38.17	45.00
Ce	103.26	181.50	88.00	85.33
Pb	25.28	7.05	20.67	10.13
Sr	43.40	17.76	38.26	88.25
P	880.32	36.37	1287.44	363.68
Nd	49.50	95.45	47.67	34.45
Zr	158.27	416.67	297.73	154.77
Sm	8.50	22.80	5.75	6.05
Ti	1479.91	1099.08	7193.99	3277.26
Y	31.87	169.92	71.93	33.97
Sc	4.04	3.90	25.25	12.03
Cr	10.03	2.67	-	69.00
V	16.43	12.35	-	77.30
Co	69.31	59.30	42.67	42.67
Ga	20.35	28.55	25.40	20.53
Cu	7.46	3.83	94.67	7.33
Zn	28.74	7.33	-	18.00
Ni	2.23	2.67	-	21.00

Table 3.3.4.1 - Average Whole Rock XRF data for the Olary Block, South Australia

3.4 Tectonic Classification Based on Geochemistry

Pearce *et al.* (1984) and Brown *et al.* (1984) constructed a different type of granite classification based on statistical analysis of a large number of granitic chemical analyses from

well defined tectonic settings. Discrimination diagrams which can be utilised in identifying the tectonic setting of other granite suites developed as a result of this approach.

They proposed a tectonic classification of granites based on discrimination diagrams using Rb, Y, Nb, Yb and Ta trace element data, categorising granites as syn-collisional (syn-COLG), volcanic-arc (VAG), ocean ridge (ORG) and within plate type granites (WPG).

Plots of geochemical data from the map area, on these diagrams (figs. 3.4.1; 3.4.2) highlights a classification of syn-COL bordering on WP type granite for the Bimbowrie granitoids. The A-type Basso Granodiorites plot within the WP granite field. The metasediments are distributed amongst the Bimbowrie granites, consistent with the Bimbowrie being sourced from them. The Antro granites represents something significantly different, categorised as WP to OR type. The significant feature of both diagrams, is the complete separation of the syn-COL and WP granites (Bimbowrie and Basso respectively).

By the time granites are exposed, it is often difficult to obtain unambiguous geological evidence for the tectonic setting at the time of intrusion. This is a major difficulty faced when tectonic interpretation is to be undertaken. To confuse matters further, granites undergo a complicated petrogenetic history, thus interpretation of their chemical compositions becomes quite difficult.

Geochemical perturbations in granite magmas form as a result of variable elemental exchange between trace element rich minor phases, fluxing of volatiles, crystal accumulation and by contamination of pre-existing continental crust (Pearce *et al.*, 1984). Hence, the validity of the tectonic classification diagrams must be questioned.

In addition to the above, Precambrian rocks cannot automatically be applied to these diagrams which are based on analyses of Phanerozoic rocks. A study of the Precambrian results in a lack of evidence for the notion of uniformitarian principles, that is, that processes acting today existed in the past.

Emphasis must be made here that fields on the discriminant diagrams strictly reflect source regimes (and melting and crystallisation histories) rather than present tectonic regimes (Pearce *et al.*, 1984). This must be kept in mind when undertaking such analyses.

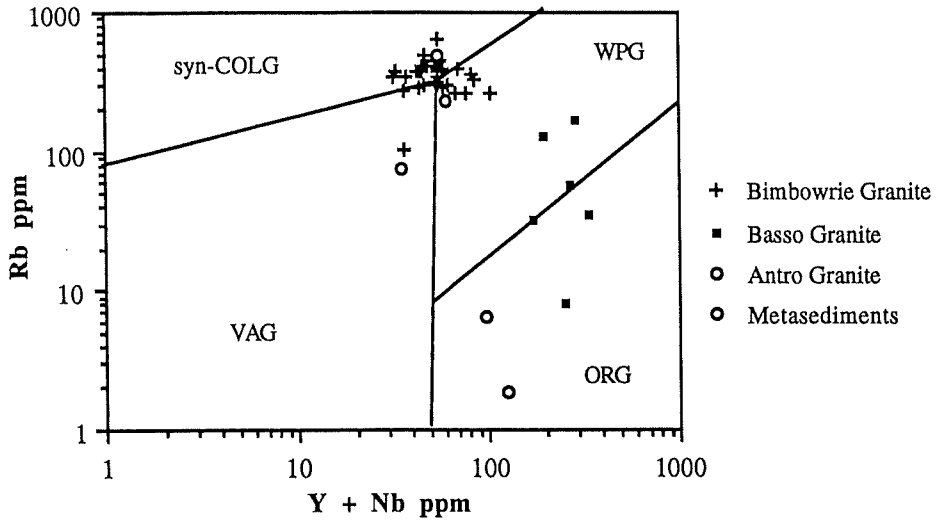

Figure 3.4.1 - Tectonic discrimination diagram (after Pearce *et al.*, 1984)

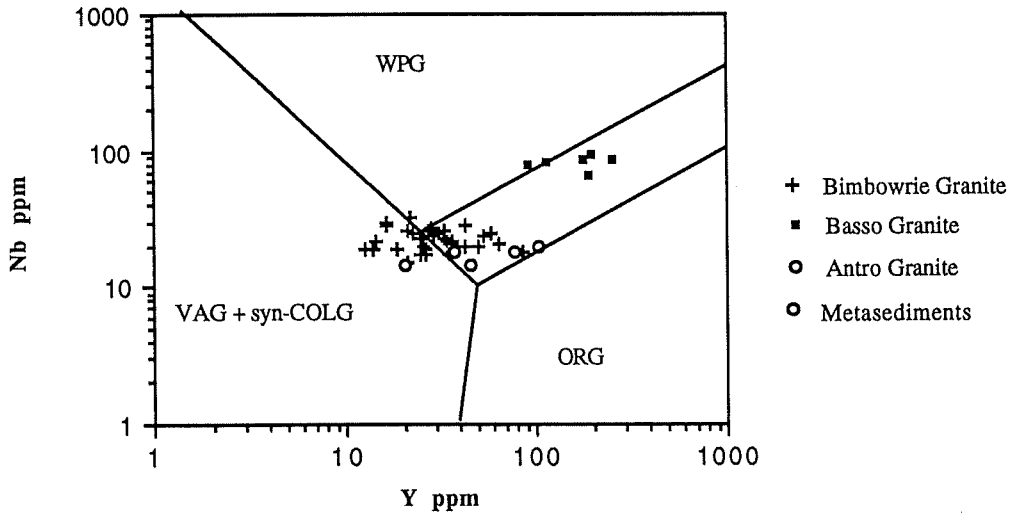

Figure 3.4.2 - Tectonic discrimination diagram (after Pearce *et al.*, 1984)

CHAPTER 4 - INTERREGIONAL CORRELATION

Whole rock geochemistry has enabled categorisation and investigation of the geological history of the Olary Block. An integral part of geochemistry is the ability to compare and contrast data with that obtained from terrains further abroad, offering insights into large scale tectonic and magmatic processes.

A generalised distribution of the major Australian Precambrian orogenic provinces, sedimentary basins and the major Phanerozoic Tasman Belt is shown in figure 4.0.1. Relationships have been demonstrated between Archaean sediments, and Palaeoproterozoic granites and the younger Mesoproterozoic Hiltaba Suite granites of the Gawler Craton. The Neoproterozoic - Early Cambrian sediments of the Adelaide Fold Belt and the early Palaeozoic granites of the Lachlan Fold Belt have also been compared.

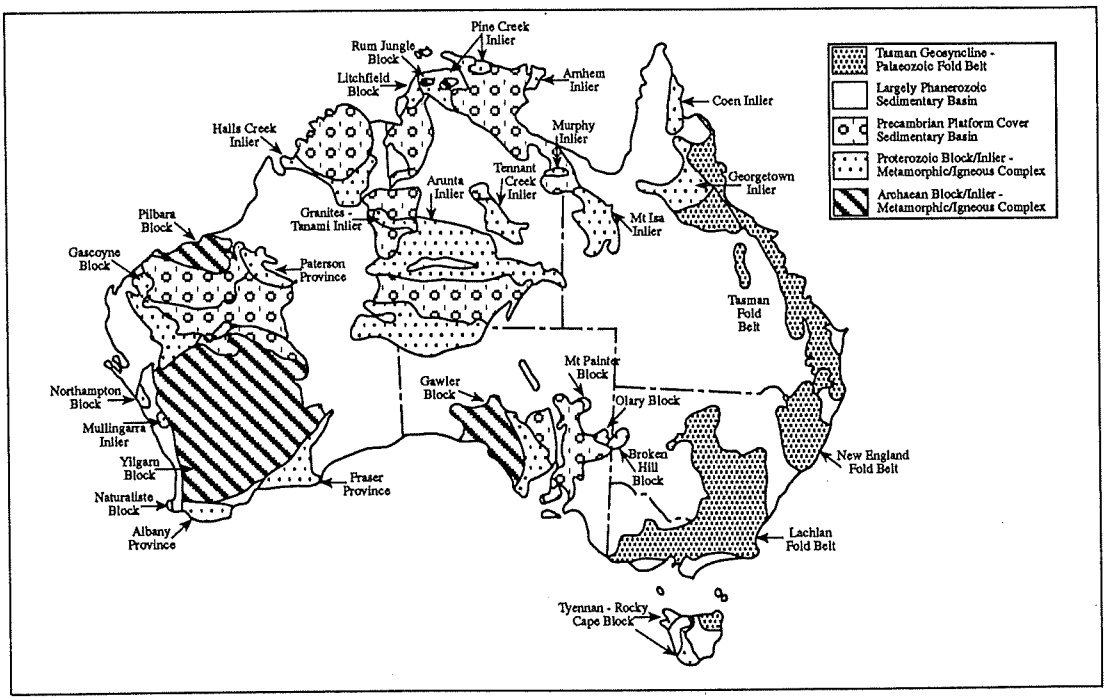

Figure 4.0.1 - Map showing the distribution of the major Australian Precambrian orogenic provinces, sedimentary basins and the Phanerozoic Tasman Belt (after McCulloch, 1987; Wyborn *et al.*, 1992)

4.1 Geochemistry

Figure 4.1.1 clearly illustrates a correlation between the Bimbowrie Granite (and the metasediments form which they were sourced) and the Archaean sediments from the Gawler Craton. All suites exhibit chemical analysis characterised by elevated Rb, Sr, Pb, Ba, K and P contents and low Nb, Zr, Ga and Y. On the basis of this geochemistry, it is proposed that the

Figure 4.1.1 - Comparative diagram of the Bimbowrie Granite and Archaean metasediments of the Gawler Craton

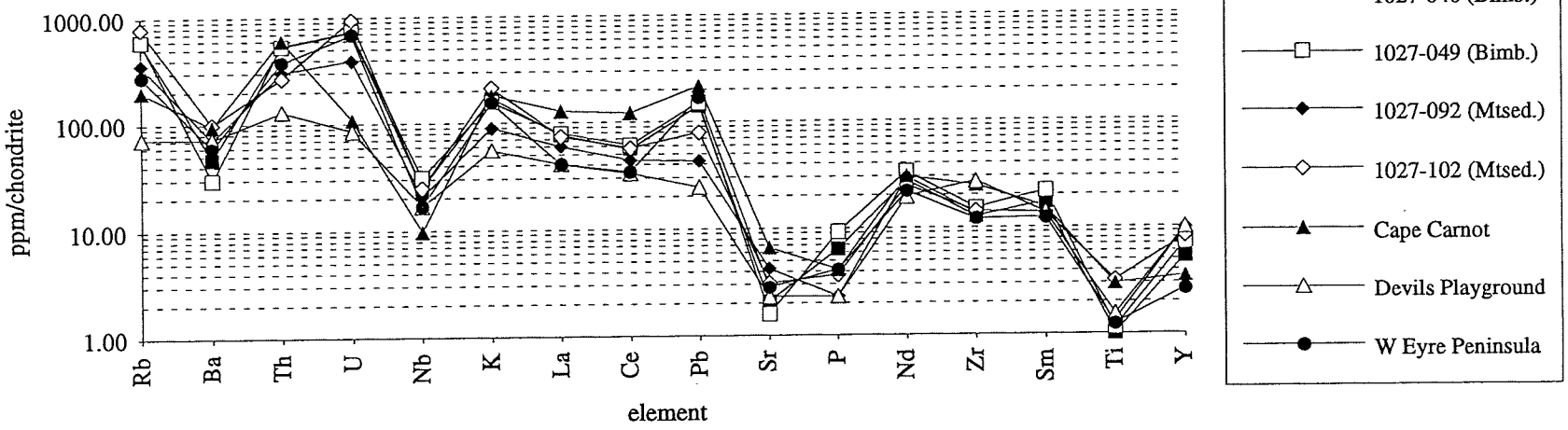

Figure 4.1.2 - Comparative diagram of the Basso Granodiorite and Hiltaba Suite Granitoids

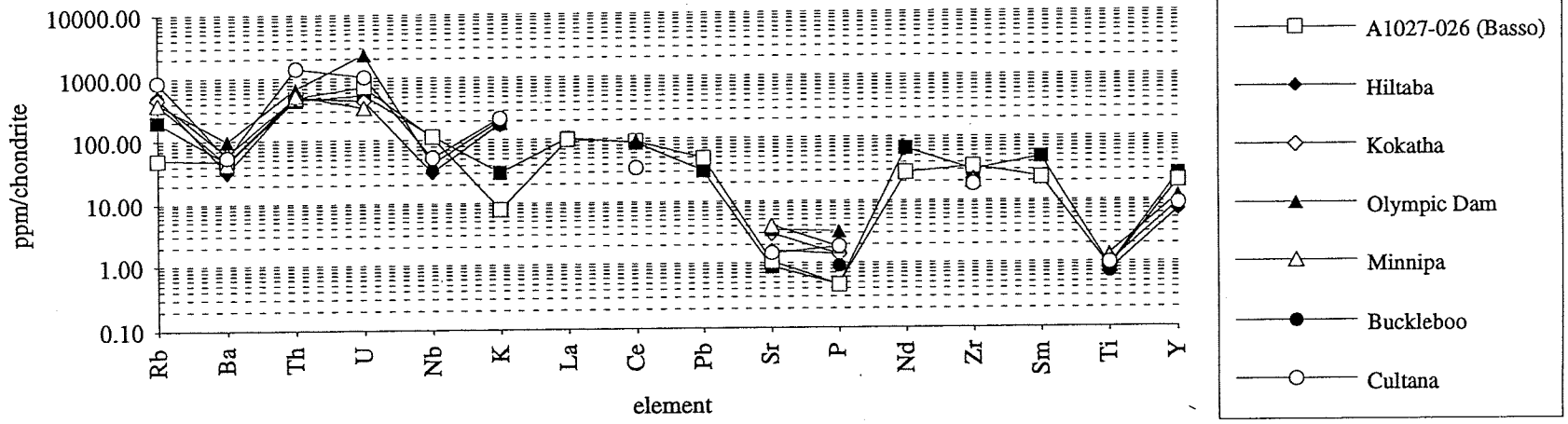

Gawler Craton Archaean metasediments are the source for the metasediments of the Olary Block, from which in turn the Bimbowrie granite has been derived.

Similarly, multi element variation diagrams display an excellent correlation between the Palaeo- Mesoproterozoic Basso Granodiorite and the contemporaneous Hiltaba Suite Granite (fig. 4.1.2). This comparison is highlighted by similar major element characteristics and distinctive elevated levels of Zr, Nb, Ga and Y. On these grounds it appears feasible to correlate the Basso Granodiorite with the Hiltaba Suite magmatism. Similar trends are also reflected in Delamerian I- and A-type granites and the Lachlan Fold Belt I-type (fig. 4.1.3), suggesting a genetic link between these magma types as opposed to representing a unique source.

Of interest is comparison of selected I-type Palaeoproterozoic granitoids of the Donington Suite, Gawler Craton, with the A-type Basso Granodiorite, no geochemical grounds for similarity exist. However, when the Donington Suite samples are plotted with the Bimbowrie Granite and the metasediments, from which they were derived, a distinct correlation may be made (fig. 4.1.4). Hence the notion that the metasediments may be derived from the Donington Suite Granitoids must be born in mind, however lies out of the scope of this investigation.

In summary, it is clear that the granitoids of the Olary Block display geochemical similarities with terrains of similar age. Whether those similarities are merely a reflection of magmatic processes in similar tectonic regimes or record a fundamental Proterozoic process is uncertain from the current database.

Comparison with Phanerozoic analogues results in ambiguous relationships between tectonism in the respective eras.

Figure 4.1.3 - Comparative trace element diagram of I- and A-type granites

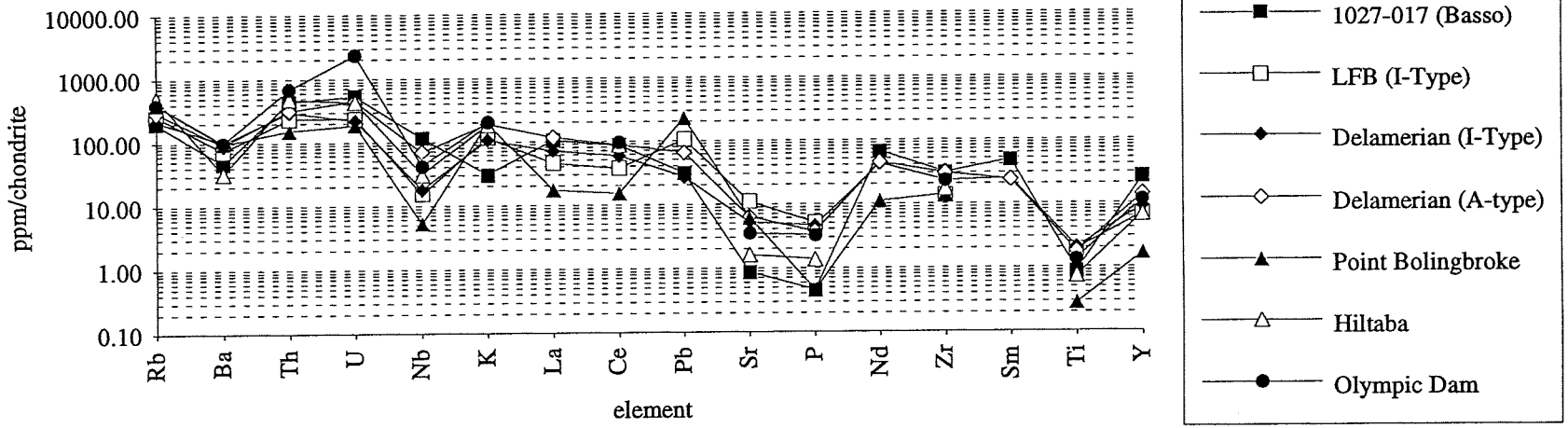

Figure 4.1.4 - Comparative trace element diagram for the Bimbowrie Granite and Lincoln Complex granites

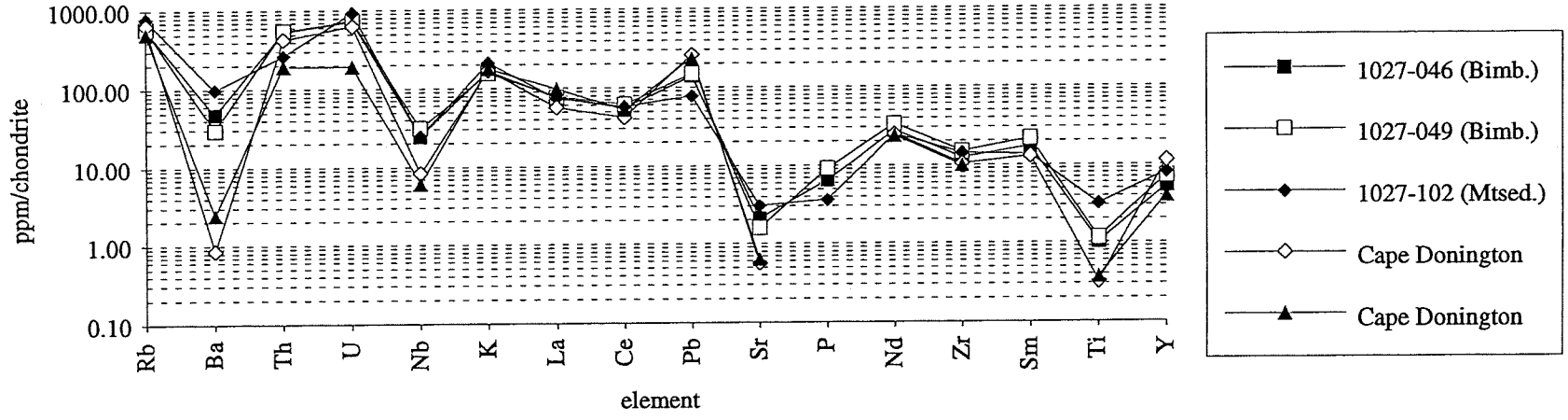

CHAPTER 5 - ISOTOPES

5.1 Isotope Systematics

The ability to determine the time of formation of new crustal segments is of fundamental importance in attempting to understand the growth and evolution of continental crust. The decay of radioactive isotopes provide a natural clock for the absolute measurement of geological time. The principle methods measure the ratio of radioactive parent isotopes and their daughter products, for example, rubidium and strontium (^{87}Rb and ^{86}Sr) and samarium and neodymium (^{147}Sm and ^{143}Nd), to record the time elapsed, with each having its own specific characteristics and suitability for determining the ages of various geological events.

Interpretation of isotopic data and ages is complex due to the effects of metamorphism and deformation. Figure 5.1.1 is a schematic illustration of the relationship between tectonic events and isotopic ages in rocks. In this ideal situation, the Sm-Nd system generally records the time at which a magma separated from the mantle and was emplaced in the crust. Additionally, identification of source areas (provenances) of sedimentary rocks is possible as the sediments retain information about the time of formation of the crustal segments that were their sources (McCulloch and Wasserburg, 1978).

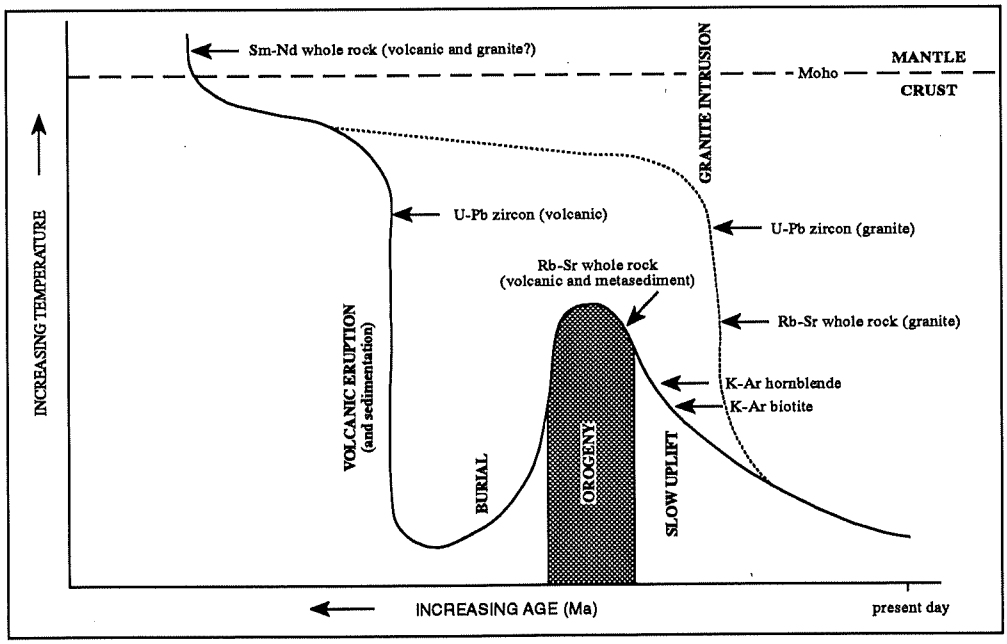

Figure 5.1.1 - Schematic illustration of the relationship between tectonic events and isotopic ages in rocks (after Drexel *et al.*, 1993)

The Rb-Sr isotopic system is a useful dating tool, however it is less reliable for rocks that have been thermally, tectonically or chemically perturbed as both Rb and Sr are particularly mobile in the metamorphic environment (McCulloch and Wasserburg, 1978; Goldstein, 1988).

As the Rb-Sr system is more easily reset, it generally registers significantly younger ages, reflecting various phases in the cooling and uplift history of these rocks after burial, deformation and metamorphism. Emplacement ages of granites may be recorded if they intruded after an orogenic event.

The recognition that most provinces (including Olary) contain a mixture of primary ages and thermal overprints has led to the more frequent use of the more 'robust' Sm-Nd isotopic system in place of the Rb-Sr system. The Sm-Nd system offers the advantage of a simple chemical fractionation step between continents and the mantle, which allows the original time of crust-mantle separation, as opposed to times of later thermal and orogenic reworking, to be obtained. The validity of this does however, depend on the degree of preservation of the Nd isotopic system within crustal rocks (DePaolo *et al.*, 1991); that is, it assumes that the system has remained closed since extraction from the mantle.

Samarium - neodymium isotope systematics provide a means of determining the age of the continental crust, where 'age' refers to the amount of time the crustal rock material has been isolated from the convecting mantle. This age is referred to as the Sm-Nd model age or the mantle separation age.

Sm-Nd model age studies enable the delineation of major periods of crustal growth. The application of this technique and thus the quantification of rates of crustal formation, first detailed by DePaolo and Wasserburg (1976), McCulloch and Wasserburg (1978) and Nelson and DePaolo (1985), is important for determining not only overall rates of continental growth and recycling, but also for constraining general models of continental crustal development.

Refinement of the initial application of Sm-Nd model ages, undertaken by DePaolo (1981) and McCulloch and Compston (1981), led to the recognition of a more complex depleted mantle (DM) evolution rather than a chrondritic Sm-Nd reservoir (Chondritic Uniform Reservoir - CHUR) as initially assumed. Under this model, the depleted mantle evolves to increasingly more positive ε_{Nd} values whereas CHUR corresponds to ε_{Nd} of 0. However in view of the obvious spatial and temporal heterogeneities in the mantle, it is clear that no single mantle evolutionary curve can be justified (McCulloch, 1987).

Precambrian crust evolves to increasingly negative ε_{Nd} values (as in fig. 5.1.2); and the complementary depleted mantle evolves to more positive ε_{Nd} values through time. The intersection of a sample evolution with the depleted mantle evolution gives the T_{Nd} model age.

It is important to remember that T_{Nd} model ages do not reflect crystallisation ages, but the crustal pre-history of a rock. Disparities between model ages and stratigraphic ages may be resolved in terms of, firstly, assimilation of older crustal material, resulting in a model age reflecting the contribution of both older and younger components (fig. 5.1.2), or alternatively, an extended protolith prehistory may account for the difference between T_{Nd} model ages and crystallisation ages. In the second case, derivation of continental crustal materials from the mantle requires multi-stage differentiation and partial melting processes. Thirdly, it is likely that the mantle source reservoir may have a different composition to that assumed by the bulk of the

Figure 5.2.1 - Eps Nd evolution of granitoids and a metasediment from the Olary Block, South Australia

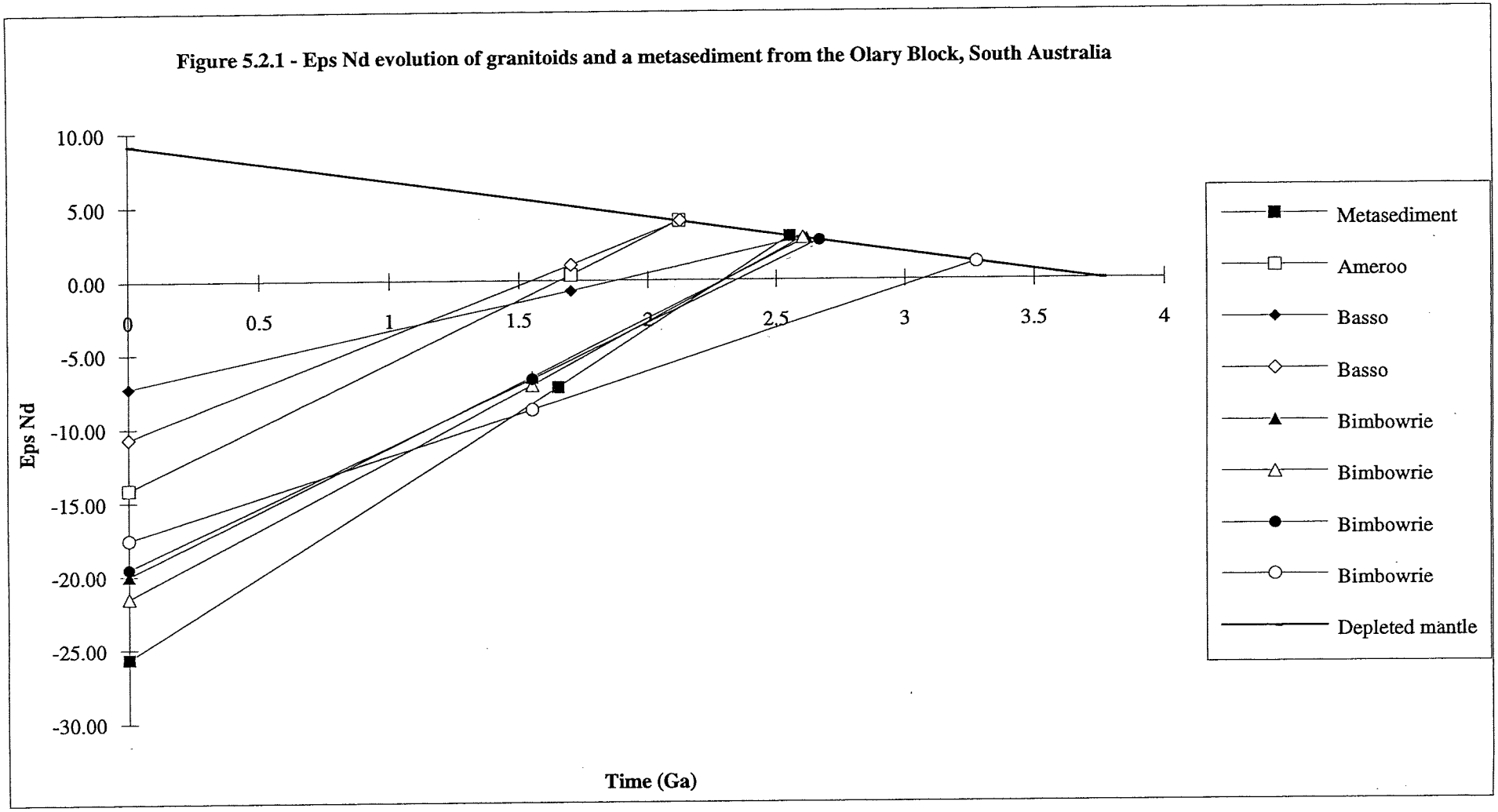

convecting upper mantle being progressively depleted due to extraction of continental crustal materials. Hence, model ages calculated for less depleted mantle sources will be erroneous.

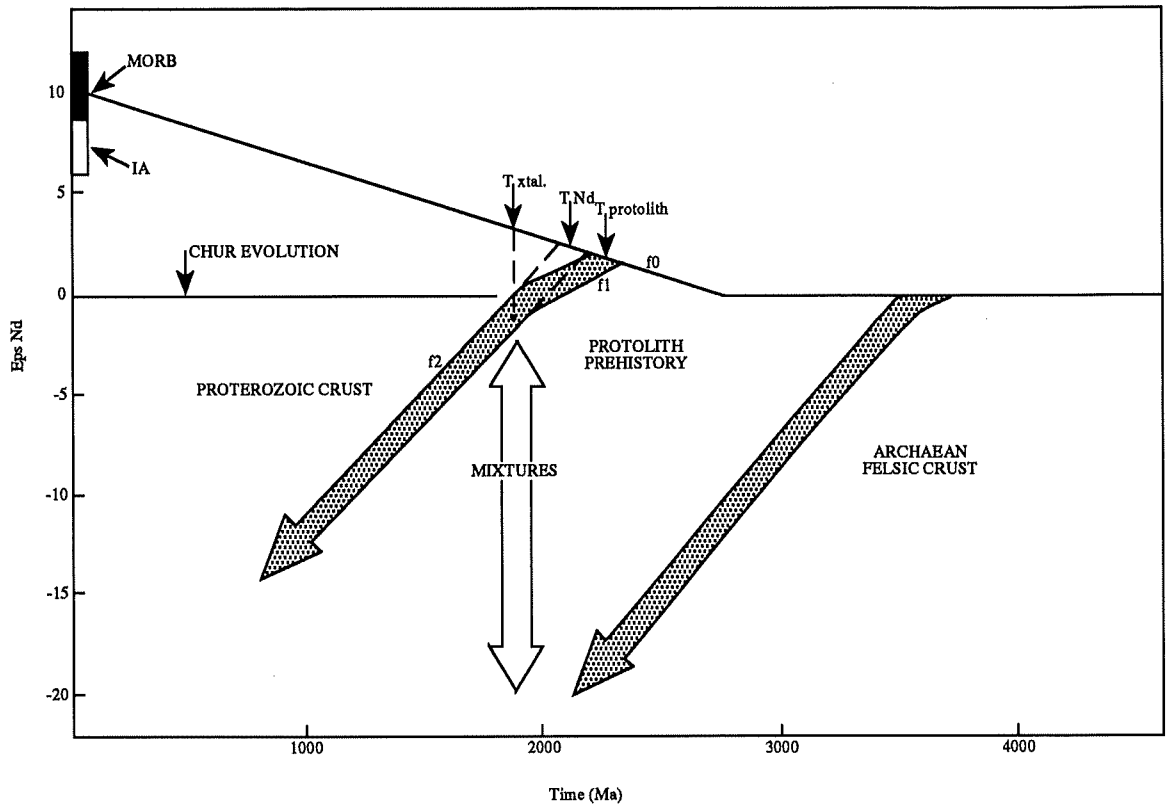

Figure 5.1.2 - Schematic diagram showing the evolution of ε_{Nd} with time, for Archaean and Proterozoic crust, relative to the depleted mantle (after McCulloch, 1987)

5.2 Olary Isotopic Data

Seven granite samples and an additional metasediment sample were collected from the Antro-Bimbowrie-Outalpa area for the purpose of Sm-Nd and Rb-Sr whole rock dating. Criteria for selection of samples is briefed in appendix C, however the selected samples were purposely spatially widespread. A summary of the results obtained is given in table 5.2.1.

Model Ages

The geochemical discriminations of granite types given in chapter three are supported by the isotopic characteristics. Criteria for distinction include the model ages determined, both depleted mantle and relative to CHUR, and initial ε_{Nd} values.

Model ages of 2.30 - 2.35 Ga relative to CHUR and 2.60 - 2.67 Ga depleted mantle (DM) were obtained for three of the four Bimbowrie granite samples analysed. The fourth produced a quite different value of 3.08 Ga and 3.28 Ga for CHUR and DM respectively (table

Sample Type	Number	Sample Location			Nd (ppm)	Sm (ppm)	147Sm/144Nd	143Nd/144Nd	TCHUR	TNd DM	ENd (0)	ENd (T)	Sr ppm	Rb ppm	87Rb/86Sr	87Sr/86Sr	87/86 (T)
	(A1027)	Locality	E	N					(Ma)	(Ma)							
Bimbowrie Granite	1027-009	Tommie Wattie	420871	6446818	21.60	5.44	0.1525	0.511738	3.08	3.28	-17.56	-8.80	35.07	444.31	39.7601	1.5741	0.68924
Bimbowrie Granite	1027-013	Brady Mine			51.90	11.34	0.1322	0.511638	2.35	2.67	-19.51	-6.71	27.64	410.04	47.4433	1.7830	0.72722
Bimbowrie Granite	1027-046	Antro			37.08	7.61	0.1242	0.511536	2.31	2.60	-21.50	-7.12	43.95	375.05	25.9372	1.2245	0.64729
Bimbowrie Granite	1027-049	NNE Tommie Wattie			44.90	9.59	0.1292	0.511613	2.30	2.62	-19.99	-6.60	33.27	379.17	35.5180	1.4955	0.70510
Basso Granodiorite	1027-017	Basso Mine	421517	6449801	90.07	21.29	0.1430	0.512090	1.55	2.13	-10.69	1.03	18.52	126.43	20.6780	1.1865	0.68125
Basso Granodiorite	1027-026	Doughboy Well Mine	416497	6450953	36.99	10.19	0.1667	0.512265	1.89	2.61	-7.28	-0.73	22.50	32.27	4.1920	0.8144	0.71194
Ameroo Granodio.	1027-105	Ameroo Hill	425140	6445328	171.62	36.92	0.1301	0.511912	1.66	2.12	-14.16	0.36	25.05	8.13	0.9412	0.7353	0.71231
Metasediment	1027-102	NE Tommie Wattie	422650	6447200	33.35	6.05	0.1097	0.511323	2.29	2.55	-25.64	-7.27	65.50	499.24	23.2527	1.2640	0.71279

Table 5.2.1 - Summary of the isotopic data obtained for the map area, Olary Block, South Australia. Details are in appendix D.

5.2.1, fig. 5.2.1). This significant difference may be reflecting the granites source region. That is, it may be sampling metasediment derived from older crust, present either as a basal sequence upon which the current stratigraphy is deposited, or alternatively it may be sourcing a metasedimentary pile with a greater crustal residence time than the exposed metasediments. In either case, the older crust it is sampling is not exposed, hence such interpretations must remain speculative.

The metasediment model age is, as expected, similar to the Bimbowrie granites, 2.29 Ga relative to CHUR and 2.55 Ga depleted mantle (table 5.2.1, fig. 5.2.1). This supports the notion that the Bimbowrie granites formed as a result of near *'in situ'* melting of the metasedimentary sequence. Therefore it is clear that the metasediment and three of four Bimbowrie granites reflect a similar source region, and have similar crustal residency times.

Examination of the A-type granites in the same manner reveals that one of the Basso group and the sample from Ameroo Hill have T_{DM} of 2.12 - 2.13 Ga and T_{CHUR} of 1.55 - 1.66 Ga, with the other Basso Granodiorite sample giving a T_{DM} similar to the S-types (2.61 Ga), but a T_{CHUR} closer to the other A-types (1.89 Ga) (table 5.2.1, fig. 5.2.1). This is clearly indicative of crustal contamination of this sample during emplacement, whereas the other samples appear to reflect true mantle separation ages.

Isochron Ages

Examination of the isotope data in the form of whole rock isochrons potentially allows interpretation of crystallisation and metamorphic events. Analysis of the data in this manner gave rise to the following observations (refer to appendix G for isochron diagrams).

The $^{143}Nd/^{144}Nd$ versus $^{147}Sm/^{144}Nd$ plot of the Bimbowrie data results in an isochron age of 1194 ± 221 Ma, considerably lower than expected. Removal of sample 1027-009 results in a three point isochron of 2323 ± 206 Ma, which is a similar age obtained for T_{CHUR} for these three samples and the metasediment. This suggests that the Sm-Nd isotopic system is so incredibly robust as to preserve the crystallisation age of the original protolith, despite having been through at least one crustal cycle.

Isochrons obtained using the Rb-Sr isotopic system, plotting $^{87}Sr/^{86}Sr$ against $^{87}Rb/^{86}Sr$ resulted in ambiguous ages. The older Basso Granodiorite with an established U-Pb zircon age of 1703 ± 6 Ma (Ashley *et al.*, 1994) produced a Rb-Sr isochron age of 1638 ± 6 Ma; and with the addition of the metasediment, an age of 1642 ± 5 Ma. I suggest that these values reflect a metamorphic/deformational event, responsible for resetting the Rb-Sr system and forming the pervasive tectonic fabric seen within this sequence.

Crystallisation of the Bimbowrie Granite took place following, or late within this tectonothermal event, thus the Rb-Sr isochron age (1809 ± 20 Ma) does not reflect this episode. However this isochron is most likely a result of perturbation of this granite during or after emplacement by either hydrothermal alteration or a subsequent later metamorphic event. This

uncertainty is consistent with the doubts expressed about the Rb-Sr dating system for determination of crystallisation age as detailed earlier.

5.3 Interpretations

From the preceeding discussion, it is clear that the isotopic data describes a geochronological framework incorporating the following elements. Firstly, the growth of continental crust at ~2.6 Ga, which subsequently acted as a source region for the metasediments and hence ultimately is preserved in the Bimbowrie Granite. An orogenic cycle at ~1640 Ma is recorded by Rb-Sr isochrons in the metasediments and the Basso Granodiorite. It is likely that the 1703 ± 6 Ma zircon age for Ameroo Hill (Ashley *et al.*, 1994) signals the onset of this event, the Olarian Orogeny, which was responsible for deformation and metamorphism of both the Basso Granodiorite and the metasediments. Coincident with this orogeny was the input of further mantle material into the crust, as observed in 2.13 Ga T_{DM} for the Basso Granodiorite.

The derivation and emplacement of the S-type Bimbowrie Granite occured immediately after tectonism ceased and contains disturbed Sr isotope signatures, but records the crustal growth episode of the metasediments. The actual age of emplacement of these magmas is unconstrained however the isotopes (model ages) are able to give an insight into the timing of crustal growth within the Olary Block.

CHAPTER 6 - PROTEROZOIC CRUSTAL EVOLUTION AND TECTONICS

6.1 Crustal Growth - An Overview

A great deal of uncertainty exists regarding Proterozoic tectonics and crustal evolution. Two schools of thought have dominated geoscience for some time. Workers including Rutland, 1976; Katz, 1985; and Etheridge *et al.,* 1987 adopt a nonuniformitarianistic approach, whereby it is suggested that reworking of the Archaean crust into Proterozoic environments is dominant; with mobile belts representing intracratonic features such as rift or collision zones and thus highlighting the reworking nature. Additionally vertical crustal growth due to underplating of mantle derived magmas is inferred to play a significant role.

Alternative models view Proterozoic crustal development in essentially contemporary plate tectonic terms, for example, Burke *et al.*, 1976; Hoffman, 1980; Windley, 1981, claiming that Proterozoic orogenic belts represent laterally accreted island arc regimes around pre-existing continental nuclei. Archaean crust is thus an incidental component. Kröner (1981; 1983) has proposed a model compatible with the concept of horizontal plate tectonics but differing from the Wilson cycle in that anhydrous subcrustal lithosphere is partially subducted.

Structural, tectonostratigraphic, geochemical, geochronologic, palaeomagnetic and seismic evidence has been compiled by many in support for one or any of these models, from extensive localities all over the world. In this chapter I endeavour to identify the major periods of crustal formation with respect to T_{DM} model ages of the Olary Block, South Australia. In light of these results, and following compilation with the data of McCulloch (1987), it is hoped that Proterozoic crustal formation events may be distinguished from recycling of Archaean crust during the Proterozoic.

6.2 Application of Olary Data

Current thinking suggests growth of the Earths crust began about 3.9 Ga ago (Tarney and Jones, 1994), but questions regarding episodic or continuous growth, rates and mechanisms and whether the crust has grown at all are issues that have been the subject of intense debate over the last two decades.

Initial models for the Earth's continental crustal growth suggested a three-stage process, namely:

- creation of basaltic oceanic crust at mid-ocean ridges

• hydrous melting of that crust and/or of the mantle wedge at subduction zones to form andesitic island arcs

• lateral accretion of island arcs with re-melting to form a granitic upper crust and a depleted granulite facies lower crust (Taylor and McLennan, 1985; Fyfe, 1973).

Inherent in such a model are assumptions that subduction (and plate tectonics) have been important processes throughout Earth history, and thus island arcs have been a persistent feature. Such models also require the constant availability of thermal energy to remobilise island-arc crust, and that the lower continental crust must to some extent be a compositional complement of the upper crust. Another consequence is that progressive depletion of the upper mantle has resulted from continuous extraction of continental crust (Tarney and Jones, 1994).

With these factors in mind, estimates of the rate of growth of the Earth's continental crust with time, based on age data, isotope systematics, and a little prejudice as to tectonic models, have been made, resulting in a number of possible scenarios (schematically illustrated in fig. 6.2.1).

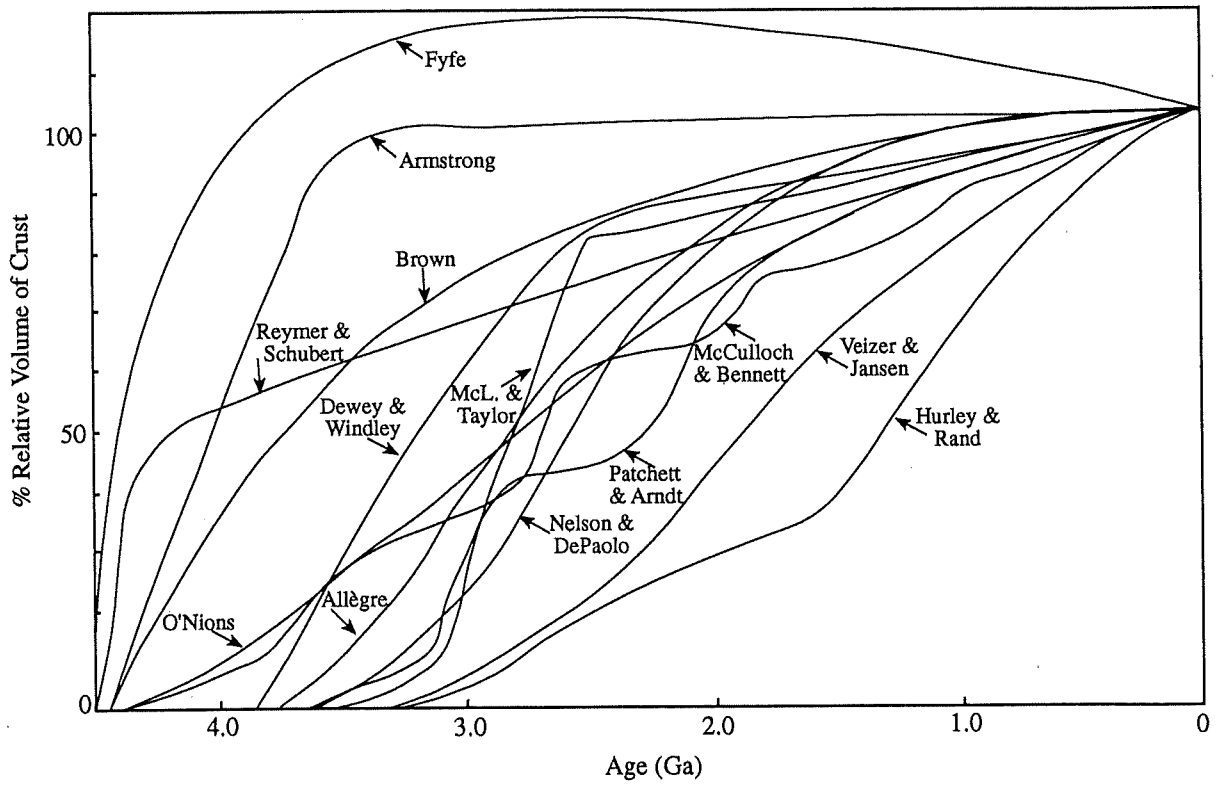

Figure 6.2.1 - Estimates of the rate of growth of the Earth's continental crust with time (present day = 100%). Note the significant differences between the models (after Tarney and Jones, 1994).

Some models require much of the present continental volume to have been attained very early (eg., at ~4 Ga - Armstrong, 1981; 1991), with steady state recycling of crust back to the

mantle. Others require progressive growth of the continents since the early Archaean (O'Nions and McKenzie, 1988), some episodically (Patchett and Arndt, 1986).

Regardless of the exact rates detailed for models outlined above, it is clear that large volumes of continental crust were formed during the Palaeoproterozoic. Two stages of crustal production exist for the Olary Block, one at ~2600 Ma recorded in the T_{DM} values of the Bimbowrie Granite and metasedimentary sequence, and the second around ~2130 Ma as observed in the Basso Granodiorite T_{DM} values. This is consistent with conclusions made by McCulloch (1987); he identifies peaks in crustal production for the Australian continent at ~3600 Ma, ~2600 Ma, ~2200 Ma and ~1800 Ma (fig. 6.2.2), and suggests that at these times, periods of significantly higher than average crustal production took place.

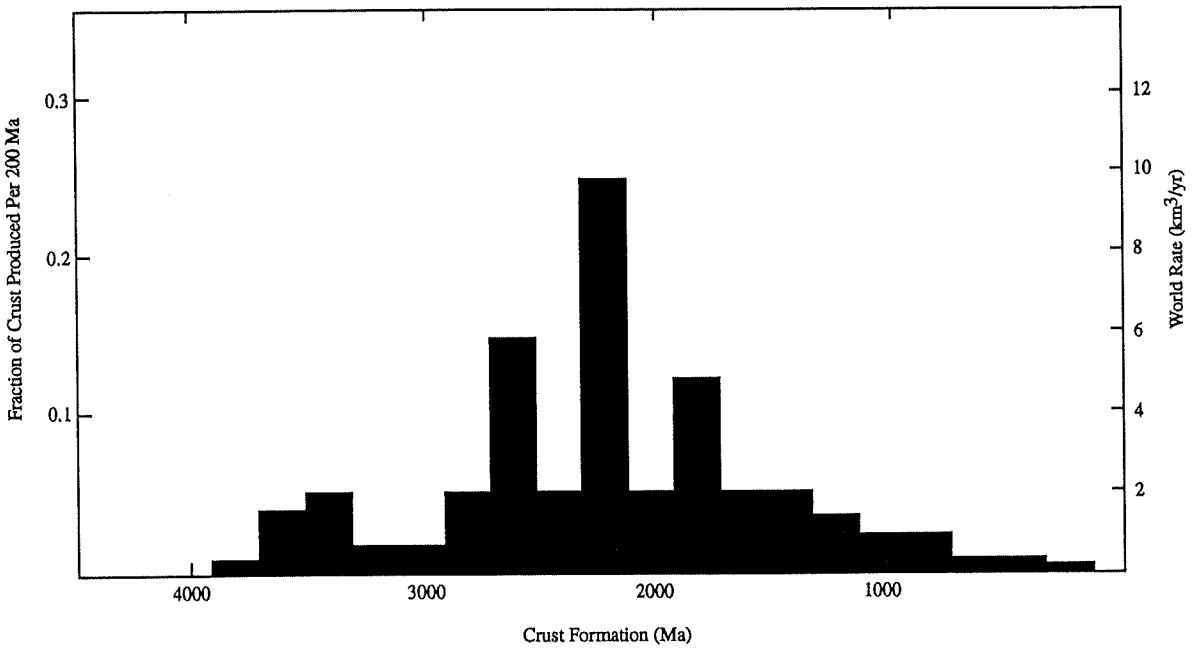

Figure 6.2.2 - Crustal formation ages, based on T_{Nd} model ages for the Australian continent. Four main periods of high crustal production are apparent at ~3600 Ma, ~2600 Ma, ~2200 Ma and ~1800 Ma (after McCulloch, 1987)

From the studies of McCulloch (1987) it may be said that the Palaeoproterozoic is the single most important period of crustal production (assuming no recycling of continental crust into the mantle through geologic time). Data obtained for the Olary Block is consistent with this proposal. The numerical rates are not as significant as the realisation that the crust was growing rapidly during this period.

An alternative to this is discussed by Gurnis and Davies (1986), who suggest that the observed peaks of crustal growth reflect a variation in the rate of recycling of continental crust into the mantle, rather than discrete growth episodes.

The steady state model of Armstrong (1981) illustrates this point (fig. 6.2.1); and is reinforced in the schematic diagram of no recycling versus recycling (fig. 6.2.3). Massive

recycling of continental crust such that constant continental masses are retained is an unlikely scenario, as production rates of ~10km^3/yr for a period of 1000 Ma are required (McCulloch, 1987). By contrast, the no recycling model requires only short periods <200 Ma of high crustal production. Thus the possibility of variations in rates of crustal recycling being the explanation for peaks at ~2200 and ~2600 is unlikely. Instead, the initial viewpoint that crustal growth occurred by injection of new material at ~2200 and ~2600 seems more plausible. Recycling of *minor* volumes of continental crust into the Earth's mantle is however, likely, and has probably been a continuous process (in one form or another) throughout Earth history.

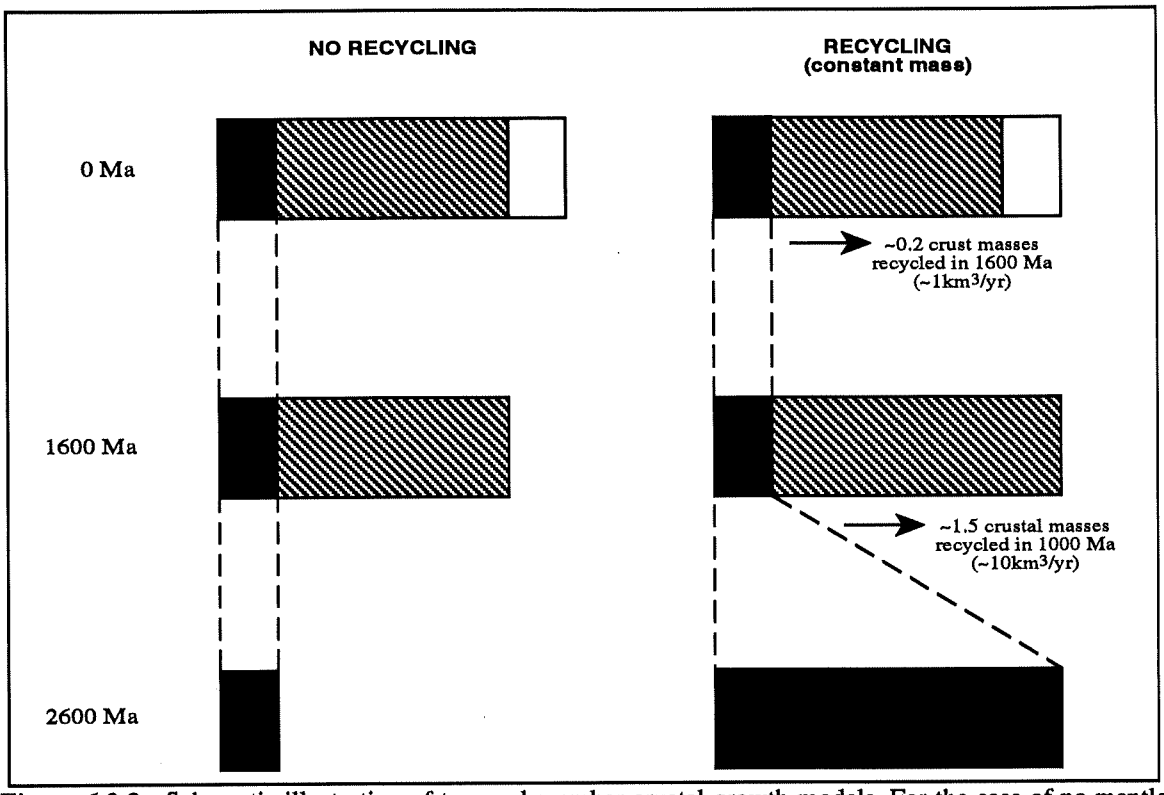

Figure 6.2.3 - Schematic illustration of two end-member crustal growth models. For the case of no mantle recycling of continental crust, the age distribution pattern directly indicates the rate of growth of continental crust. In this sketch, growth periods may be accounted for by limited periods (~200 Ma) of more rapid crustal growth. The alternate model of a near-steady state constant continental mass with crustal recycling (eg., Armstrong, 1981) requires extremely rapid recycling of crust from ~1600 to ~2600 Ma

6.3 Models for Proterozoic Crustal Growth

The role of plate tectonics in the Proterozoic crustal growth debate has been the focus of much discussion over the last few decades. Mueller and Wooden (1988) suggest that extensive crustal recycling has occurred throughout the history of the Earth, dominated by plate-tectonic (or plate-tectonic like) processes. The available geological evidence however, may not be easily reconciled with contemporary style tectonics of the Proterozoic. The flaw in such an argument lies in the notable lack of subduction related components (eg., andesites, ophiolite complexes and blueschist terrains), the occurrence of bimodal volcanic suites (Etheridge *et al.*, 1987) and a lack of paired metamorphic belts (Kröner, 1984).

An alternative model for Proterozoic crustal growth proposed by Etheridge *et al.* (1987) and similarly by Kröner (1977), incorporates lithospheric underplating and subsequent delamination of the underplate. In this scenario, relatively mafic material is underplated onto pre-existing Archaean crust. At a later stage, this material is partially melted to produce widespread felsic magmatism, and associated mafic magmas through higher degrees of partial melting of the mafic underplate; or may possibly be derived directly from the thermal perturbation responsible for the felsic magmatism.

This model satisfies both the isotopic and geochemical requirements of the protolith having an extended prehistory as well as a relatively uniform chemical composition, as observed in northern Australia (McCulloch, 1987). However, this model too, has a number of unsatisfactory aspects. First a lack of evidence exists for the essential process of underplating onto Archaean crust. Second, large volumes of Archaean crust are required to be buried beneath younger basin cover and only Proterozoic terrains should be exposed today (McCulloch, 1987). Furthermore, the Sm-Nd isotopic data requires a large time gap between initial underplating and magmatism, hence a difficulty exists in that two separate mantle convection events are required at subsequent times to induce the tectonism (Etheridge *et al.*, 1987). This is difficult to infer, mechanically and rheologically as well as thermally.

If it is assumed that underplating occurred onto pre-existing basaltic Archaean crust or alternatively highly attenuated Archaean felsic crust, these difficulties may be resolved.

Other models have been suggested, for example the 'Hot Spot' model of Fyfe (1978), yet fail to explain adequately the geological observations.

Although the isotopic data presented here does not characterise the tectonic environment, it is consistent with McCulloch's (1987) interpretations involving nonuniformitarianistic tectonics and orogeny. Thus in conclusion, it may be said that the Proterozoic is a complicated period in Earth's history where tectonic processes may have acted in quite a different manner to the plate tectonic regime of the Phanerozoic.

CHAPTER 7 - CONCLUSIONS

The Willyama Inlier forms a series of semi-isolated partly exposed blocks which are unconformably overlain by Adelaidean sediments. The oldest, mixed clastic and sedimentary sequences are referred to as the Willyama Supergroup and are suggested in the Olary Block portion to represent a rift margin, with the sequences deposited in a predominantly shallow marine environment interspersed with non-marine playa lakes, deepening upwards (ie., shelf or intracratonic basin).

Five broad lithological suites have been proposed for the Olary Block by Clarke *et al.* (1986), these include, the Composite Gneiss, Quartzofeldspathic, Calcsilicate, Bimba and Carbonaceous Pelite Suites.

The field area revealed three granitoid suites, previously un-defined and an older metasedimentary sequence. The metasediments consisted of a series of finely laminated to thickly bedded, medium to fine grained pelitic and psammitic schists, with thin calcsilicate bands and albitised layers. The pelitic schists commonly contained garnet, while the more psammitic, quartzofeldspathic sequences contained retrograded andalusite porphyroblasts, now represented by coarse muscovite. The calcsilicate bands of epidote, actinolite and diopside were found in the more psammitic rocks. The geochemistry of the metasediments mirrored patterns seen in the S-type Bimbowrie Granites, reinforcing the genetic link suggested earlier.

The Antro Tonalite, of only minimal extent, is composed of essentially plag-qtz-cpx and K-fld. It is extensively recrystallised and poorly exposed. Based on its geochemistry, this granite is classified as I-type and exhibits high Fe_2O_3, Na_2O, CaO and TiO_2 levels and low LREE and K_2O.

The Basso Granodiorite is medium grained, equigranular and composed of qtz-plag-K-fld and significant biotite. It is regionally extensive and exhibits a strong foliation, delineated by the planar arrangement of micaceous aggregates. The Basso Granodiorite intrudes the host metasediments and at a later date, both lithologies are intruded by the Bimbowrie Granite. It has distinctive A-type geochemical affinities, the genesis of which is the subject of considerable controversy. The geochemical signatures documented by White and Chappell (1983) for A-type granites are reproduced in this granitoids geochemistry. They have high SiO_2, Zr, Nb, Y and LREE and low CaO, Al, Mg, V, Ba and Sr. The Bimbowrie Granite is medium to coarse grained, relatively leucocratic, pink to buff in colour and composed of qtz-mu-bt-K-fld (microcline) and plag. The diagnostic feature of this granite, is the presence of very coarse grained, feldspar phenocrysts.

The field relations imply that this granite is largely the product of variable segregation of migmatite leucosomes, exhibiting a complete range of contact phenomena ranging from sharply intrusive (with the Basso Granodiorite) to gradational into migmatites. Thus it is considered that

they are largely the products of partial anatexis and melt segregation from adjacent and underlying migmatitic rocks, formed during a high grade metamorphic event. This granite has strong S-type characteristics, supporting the notion that it is derived by *in situ* anatexis of local sediments, with only minimal melt migration. The genetic S-type classification implies a sedimentary precursor. High Al_2O_3, CaO, K_2O, P_2O_5, Rb, Sr, Pb, Zn and low Na_2O, Nb, Zr, Ga and Y are indicative of this granite.

Throughout the Olary Block, the Willyama Supergroup has been extensively deformed and metamorphosed. The Olarian and Delamerian Orogeny with collectively five deformational events can be seen in the basement sequences. Four metamorphic zones, increasing in grade to the south are present in the Olary Block. It is suggested that amphibolite facies metamorphism during the first deformational event gave rise to sillimanite, andalusite, kyanite and garnet at estimated temperature and pressure conditions of 650-720°C and 2-4 kb.

An integral part of geochemistry is the ability to compare and contrast data with that obtained from terrains further abroad, offering insights into large scale tectonic and magmatic processes. Positive correlation was met when the Bimbowrie Granite and the metasediments from which they were sourced, were compared with Archaean sediments from the Gawler Craton. This initially implies a possible source region for the Olary metasedimentary sequences, however without detailed isotopic studies, this cannot be verified.

Multi-element variation diagrams also display excellent correlations between the Palaeoproterozoic Basso Granodiorite and the contemporaneous Hiltaba Suite of the Gawler Craton. Similar major element characteristics and distinctive elevated levels of Zr, Nb, Ga and Y highlights this correlation.

Isochron ages obtained for the Bimbowrie and Basso Granitoid Suites were inconclusive. The Basso Granodiorite with an established U-Pb zircon age of 1703 ± 6 Ma produced a Rb-Sr isochron age of 1638 ± 6 Ma and with the metasediment, an age of 1642 ± 5 Ma, reflecting a metamorphic event at this stage which reset the Rb-Sr system of both lithologies. An isochron age for the Bimbowrie Granite was 1809 ± 20 Ma, as the crystallisation of this granite is believed to have occurred after metamorphism, this age is not a true reflection, simply a factor of a disturbed isotopic system.

Sm-Nd isotope systematics provides a means of determining the age of the continental crust, where age refers to the amount of time the crustal rock material has been isolated from the convecting mantle (Sm-Nd model age). Investigations into the Olary Block, revealed a clustering of model ages. The Bimbowrie Granite has DM model ages of 2.6 - 2.67 Ga, recording the age of extraction from the mantle. One sample did however produce an age of 3.28 Ga, reflecting the granites source. That is, it may be sampling metasediment derived from older crust, present either as a basal sequence upon which the current stratigraphy is deposited or alternatively it may be sourcing a metasedimentary pile with a greater crustal residence time than the exposed metasediments. DM model age for the metasediment of 2.55 Ga further

supports the notion that the Bimbowrie Granite formed as a result of *in situ* melting of the metasedimentary sequence.

2.12 - 2.13 Ga T_{DM} model ages were determined for the Basso Granodiorite. One sample did however have a T_{DM} similar to the S-type granites of 2.61 Ga; this clearly indicates crustal contamination of this sample during emplacement, whereas the other samples reflect true mantle separation ages.

Regardless of the exact rates of crustal growth, it is clear that large volumes of continental crust were formed during the Palaeo- Mesoproterozoic. Identification of crustal production peaks for the Australian continent at ~3600 Ma, ~2600 Ma, ~2200 Ma and ~1800 Ma by McCulloch (1987), are reinforced by the data obtained herein. Two peaks were established, one at ~2600 Ma for the Bimbowrie Granite and the other at ~2200 for the Basso Granodiorite. Controversy still remains over whether these periods are discrete growth episodes or simply reflect a variation in the rate of recycling of continental crust into the mantle.

ACKNOWLEDGMENTS

In a year of highs and lows, there has been tremendous support in all stages of production of this thesis, without which none of this would have been possible.

Thanks must first go to my supervisor, John Foden, for his valuable time, patience and critical evaluation of data and interpretations. Fieldwork was made possible by the generosity of North Exploration (previously Geopeko), in particular Leigh Schmidt and Colin Rothnie. Thankyou for the opportunity to undertake this project, and for provision of a vehicle, aerial photographs, general field support and for advice in the initial stages of the project.

The technical staff of the department, I owe many thanks to, particularly David Bruce for his patience and time when it came to isotope preparation and running the very temperamental mass spec! Thanks also to John Stanley, Rick Barrett and Geoff Trevelyan.

Thanks to Mike Sandiford and once again John Foden for a fantastic honours trip to the Eyre Peninsula. It was a most memorable occasion and I'll guarantee diopside will never be forgotten.

To Martin Hand for odd bits of advice, some useful, some impossible to comprehend, and Jon Teasdale for draft reading and culling - I thankyou.

The 1994 honours crew has been unforgettable. Over the year we have become a team, with high spirits and enthusiasm shed from all. I extend best wishes to all of you for the future, and hope you achieve all that you set out to do. A special thanks must go to Wal for advice, help and general discussion of what we really should be doing. And also to Matt and Mandy for high spirits and support on the job front. To a very special friend who unfortunately hasn't been a great part of the honours year, yet made the years of undergraduate study most memorable, I extend my thankyous - thanks Kez.

A very special thanks must go to Bruce Schaefer; his support, advice and countless hours put into proof reading has enabled me to achieve everything I had set out to do. To my mum and dad, brother - Justin, and sister - Tonya, thanks for the support (both financially and personally) and putting up with me during the final stages of this year!

REFERENCES

Armstrong, R.L., 1981. Radiogenic isotopes: The case for crustal recycling on a near-steady-state no-continental-growth Earth. *Philos. Trans. R. Soc. London, Ser. A,* **301**, p. 443-472.

Armstrong, R.L., 1991. The persistent myth of continental growth. *Aust. Jl. Earth Sc.* **38**, p.613-630.

Ashley, P.M., 1984. Sodic granitoids and felsic gneisses associated with Uranium-Thorium mineralisation, Crockers Well, S.A. *Mineralium Deposita* **19**, p. 7-18.

Ashley, P.M., Cook, N.D.J., Lottermoser, B.G. and Plimer, I.R. 1994. Notes on geology and field guide to excursion stops in the Olary Block. *South Australia. Department of Mines and Energy. Geological Survey. Report Book,* **94/8**.

Berry, R.F., Flint, R.B. and Grady, A.E., 1978. Deformational history of the Outalpa area and its application to the Olary Province, South Australia. *Royal Society of South Australia. Transactions*, **102**, p. 43-54.

Blissett, A.H., 1975. Willyama, Mount Painter and Denison Inliers- sundry mineralisation in South Australia. *In*: Knight, C.L. (Ed.) Economic geology of Australia and Papua New Guinea, 1, Metals. *AUSIMM Monograph Series,* **5**, p. 498-505.

Brown, G.C., Thorpe, R.S, and Webb, P.C., 1984. The geochemical characteristics of granitoids in contrasting arcs and comments on magma sources. *J. Geol. Soc. London,* **141**, p. 413-426.

Burke, K., Dewey, J.F. and Kidd, W.S.F., 1976. Precambrian palaeomagnetic results compatible with contemporary operation of the Wilson Cycle. *Tectonophysics*, **33**, p.287-299.

Campana, B. and King, D., 1958. Regional geology and mineral resources of the Olary Province.*South Australia. Geological Survey. Bulletin,* **34**.

Chappell, B.W. and White, A.J.R., 1974. Two contrasting granite types. *Pacif. Geol.*, **8**, p. 173-174.

Chappell, B.W. and White, A.J.R., 1992. I- and S-type granites in the Lachlan Fold Belt. *Trans. Royal Soc. Edinburgh.* **83**, p. 1-26.

Clarke, G.L., Burg, J.P. and Wilson, C.J.L., 1986. Stratigraphic and structural constraints on the Proterozoic tectonic history of the Olary Block, South Australia. *Precambrian Research*, **34**, p. 107-137.

Clarke, G.L., Guirard, M., Powell, R. and Burg, J.P., 1987. Metamorphism in the Olary Block, South Australia: compression with cooling in a Proterozoic fold belt. *Jl. Met. Geol.* **5**, p. 291-306.

Collins, W.J., Beams, S.D., White, A.J.R. and Chappell, B.W., 1982. Nature and origin of A-type granites with particular reference to south-eastern Australia.*Contrib. Mineral. Petrol.*, **80**, p. 189-200.

Cook, N.D.J. and Ashley, P.M., 1992. Meta-evaporite sequence, exhalative chemical sediments and associated rocks in the Proterozoic Willyama Supergroup, South Australia: implications for metallogenesis. *Precambrian Research,* **56**, p. 211-226.

DePaolo, D.J., 1981. Trace element and isotopic effects of combined wallrock assimilation and fractional crystallisation. *EPSL.* **53**, p. 189-202.

DePaolo, D.J., Linn, A.M. and Schubert, G., 1991. The continental crustal age distribution: Methods of determining mantle separation ages from Sm-Nd isotopic data and application to the Southwestern United States. *Jl. Geophys. Res.* **96 B2**, p. 2071-2088.

DePaolo, D.J. and Wasserburg, G.J. 1976., Inferences about magma sources and mantle structure from variations of $^{143}Nd/^{144}Nd$. *Geophys. Res. Lett.* **3**, p. 743-746.

Drexel, J.F., Preiss, W.V. and Parker, A.J., 1993. The geology of South Australia. Vol. 1, The Precambrian. *South Australia. Geological Survey. Bulletin*, **54**.

Etheridge, M.A., Rutland, R.W.R. and Wyborn, L.A.I., 1987. Orogenesis and tectonic process in the early to middle Proterozoic of northern Australia. *In*: Proterozoic Lithospheric Evolution, *Am. Geophys. Union Geodyn. Ser.*, **17**, p.131-147.

Flint, D.J., 1981. Petrographic descriptions of the Willyama Complex rocks and Umberatana Group metasediments, southern Outalpa Inlier, Olary Province. *South Australia. Department of Mines and Energy. Report Book,* **81/2.**

Flint, R.B. and Flint, D.J., 1975. Preliminary geological investigations on the Curnamona 1:250000 sheet. *South Australia. Department of Mines. Report Book,* **75/124.**

Flint, D.J. and Parker, A.J., 1993. Willyama Inliers. p. 82-93. *In:* Drexel, J.F., Preiss, W.V. and Parker, A.J., 1993. The geology of South Australia. Vol. 1, The Precambrian. *South Australia. Geological Survey. Bulletin,* **54.**

Flint, D.J. and Webb, A.W., 1980. Geochronological investigations of the Willyama Complex, South Australia. *Sth. Aust. Dept. of Mines and Energy. Report Book,* **79/136.**

Forbes, B.G. and Pitt, G.M., 1980. Geology of the Olary region. *Sth .Aust. Dept. of Mines and Energy. Report Book,* **80/151.**

Fyfe, W.S., 1973. The ganulite facies, partial melting and the Archaean crust. *Phil. Trans. Roy. Soc. Lon.* **A273**, p. 457-462.

Fyfe, W.S., 1978. The evolution of the Earth's crust: modern plate tectonics to ancient hot spot tectonics? *Chemical Geology,* **23**, p. 89-114.

Garcia, D., Fonteilles, M. and Moutte, J., 1994. Sedimentary Fractionations between Al, Ti, and Zr and the Genesis of Strongly Peraluminous Granites. *Jnl of Geology,* **102**, p. 411-422.

Glen, R.A., Laing, W.P., Parker, A.J. and Rutland, R.W.R., 1977. Tectonic relationships between the Proterozoic Gawler and Willyama Orogenic Domains, Australia. *Geological Society of Australia. Journal,* **24**, p. 125-150.

Goldstein, S.L., 1988. Decoupled evolution of Nd and Sr isotopes in the continental crust and the mantle. *Nature* **336**, p. 733-738.

Grady, A.E., Flint, D.J. and Wiltshire, R., 1984. The Willyama Complex and related rocks, Olary District, South Australia. Field excursion guide, June 1984, Geol. Soc. Aust. (unpublished).

Gurnis, M. and Davies, G.F., 1986. Apparent episodic crustal growth arising from a smoothly evolving mantle. *Geology.* **14**, p. 396-399.

Hine, R., Williams, I.S., Chappell, B.W. and White, A.J.R., 1978. Contrasts between I- and S-type granitoids of the Kosciusko Batholith. *Geol. Soc. of Aust. Journal*, **25, pt. 4**, p. 219-234.

Hoffman, P.F., 1980. A Wilson cycle of early Proterozoic age in the northwest of the Canadian Shield. *In:* The Continental Crust and its Mineral deposits. D.W. Strangway (Ed.) *Geol. Assoc. Can.* **Spec. Paper 20**, p.523-549.

Katz, M.B., 1985. The tectonics of Precambrian craton-mobile belts: progressive deformation of polygonal miniplates. *Precambrian Research*, **27**, p. 307-319.

Kolbe, P. and Taylor, S.R., 1966. Geochemical investigation of the granitic rocks of the Snowy mountains Area, N.S.W. *J. Geol. Soc. Aust.*, **13**, p. 1-25.

Kröner, A., 1977. Precambrian mobile belts of southern and eastern Africa - ancient sutures or sites of ensialic mobility? A case for crustal evolution towards plate tectonics. *Tectonophysics* **40**, p. 101-135.

Kröner, A., 1981. Precambrian plate tectonics, In: Kroner, A. (Ed.) *Precambrian Plate Tectonics*, Amsterdam, Elsevier, p. 57-90.

Kröner, A., 1983. Proterozoic mobile belts compatible with the plate tectonics concent. *In* : Proterozoic Geology: selected papers from an international Proterozoic symposium. (Ed.) Medaris, G.M., Byers, C.W., Mikelson, D.M. and Shanks, W.G. *Geol. Soc. Am. Mem.*, **161**, p. 59-74.

Kröner, A., 1984. Evolution, growth and stabilisation of the Precambrian lithosphere. *In:* Structure and Evolution of the Continental Lithosphere. H.N. Pollack and U.R. Murthy (Ed.), Physics of the Earth, **15**, p. 69-106.

LeFort, P., 1975. Himalyas: the collided range. Present knowledge of the continental arc. *Amer. Jl. Sc.* **275A**, p. 1-44.

Loiselle, M.C. and Wones, D.R., 1979. Characteristics and origin of anorogenic granites. *Geol. Soc. Am. Abst. Prog*, **11**, p. 468.

Mawson, D., 1912. Geological investigations in the Broken Hill area. *Roy. Soc. S.A., Memoirs.* **2**, p. 211-319.

McCulloch, M.T. and Wasserburg, G.J., 1978. Sm-Nd and Rb-Sr chronology of continental crust formation. *Science*, **200**, p. 1003-1011.

McCulloch, M.T. and Compston, W., 1981. Sm-Nd age of Kambalda and Kanowna greenstones and heterogeneities in the Archaean mantle. *Nature*. **294**, p. 322-327.

McCulloch, M.T., 1987. Sm-Nd isotopic constraints on the evolution of Pre-Cambrian crust in the Australian continent, *In*: Proterozoic Lithospheric Evolution, *Am. Geophys. Union Geodyn. Ser.*, **17**, p. 115-130.

Mueller, P.A. and Wooden, J.L., 1988. Evidence for Archaean subduction and crustal recycling, Wyoming province. *Geology* **16**, p. 871-874.

Nelson, B.K. and DePaolo, D.J., 1985. Rapid production of continental crust 1.7-1.9 b.y. ago: Nd isotopic evidence from the basement of the North American mid-continent. *Geol. Soc. Amer. Bull.* **96**, p. 746-754.

O'Nions, R.K. and McKenzie, D., 1988. Melting continent generation. *EPSL.* **90**, p. 449-456.

Page, R.W. and Laing, W.P., 1992. Felsic metavolcanic rocks related to the Broken Hill Pb-Zn-Ag orebody, Australia: geology, depositional age, and timing of high-grade metamorphism. *Economic Geology*, **87**, p. 2138-2168.

Parker, A.J., 1972. A petrological and structural study of portion of the Olary Province, west of Wiperaminga Hill, South Australia. *University of Adelaide. B.Sc. (Hons) thesis* (unpublished).

Parker, A.J. (compiler), 1986. Geological excursions of the Adelaide Geosyncline, Gawler Craton and Broken Hill regions. Excursion guide for the eighth Australian Geological Convention. *S.A. Dept Mines and Energy, Rpt Bk.* **86/51**.

Patchett , P.J. and Arndt, N.T., 1986. Nd isotopes and tectonics of 1.9-1.7 Ga crustal genesis. *EPSL.* **78**, p. 329-338.

Pearce, J.A. and Cann J.R., 1973. Tectonic setting of basic volcanic rocks investigated using trace element analysis. *Earth Planet. Sci. Lett.*, **19**, p. 290-300.

Pearce, J.A., Harris, N.B.W. and Tindle, A.G., 1984. Trace element discrimination diagrams for the tectonic interpretation of granitic rocks. *Jl. of Petrology,* **25 part 4**, p. 956-983.

Phillips, G.N., 1980. Water activity changes across an amphibolite-granulite facies transition, Broken Hill, Australia. *Contrib. Min. Pet.* **75**, p. 377-386.

Pitt, G.M., 1977. Willyama Complex Excursion: 27 March to 7 April, 1977. *South Australia. Department of Mines and Energy. Report* **77/56** (unpublished).

Pitt, G.M., 1978.The mineral potential of the Willyama Complex, South Australia. *S.A. Dept Mines and Energy. Rpt. Bk.* **78/2.**

Rutland, R.W.R., 1976. Orogenic evolution of Australia. *Earth-Science Reviews*, **12**, p. 161-196.

Stevens, B.P.J. and Stroud, W.J. (Eds), 1983. Rocks of the Broken Hill Block: their classification, nature, stratigraphic, distribution and origin. *New South Wales. Geological Survey. Records*, **21**, p. 407-442.

Streckisen, A.L. (chairman), 1973. Plutonic rocks. Classification and nomenclature recommended by the I.U.G.S. Subcommission on the systematics of Igneous Rocks. *Geotimes*, **18**, p. 26-30.

Talbot, J.L., 1967. Subdivision and structure of the Precambrian (Willyama Complex and Adelaide System), Weekeroo, South Australia. *Royal Society of South Australia. Transactions*, **91**, p. 45-58.

Tarney, J. and Jones, C.E., 1994. Trace element geochemistry of orogenic igneous rocks and crustal growth models. *Jnl. Geol. Soc., London*, **151**, p. 855-868.

Taylor, S.R. and McLennan, S.M., 1985. The continental crust: Its composition and evolution. Blackwell. Oxford, 312pp.

Thomson, B.P., 1969a. Precambrian crystalline basement. In: Parkin, L.W. (Ed.), *Handbook of South Australian geology*. Geological Survey of South Australia, p. 21-48.

Thomson, B.P., 1969b. Precambrian basement cover: the Adelaide System. In: Parkin, L.W. (Ed.), *Handbook of South Australian geology*. Geological Survey of South Australia, p. 49-83.

Turekian, K.K. and Wedepohl, K.H., 1961. Distribution of the elements in some major units of the Earth's crust. *Bull. Geol. Soc. Amer.*, **72**, p. 175-192.

Turner, S.P., Foden, J.D. and Morrison, R.S., 1992a. Derivation of some A-type magmas by fractionation of basaltic magma: An example from the Padthaway Ridge, South Australia. *Lithos.* **28**, p.151-179.

Turner, S.P., Foden, J.D., Sandiford, M. and Bruce, D. 1992. Sm-Nd isotopic evidence for the provenance of sediments from the Adelaide Fold Belt and southeastern Australia with implications for episodic crustal addition. *Geochim. et Cosmo. Acta.* **57**, p. 1837-1856.

Whalen, J.B., Currie, K.L. and Chappell, B.W., 1987. A-type granites: geochemical characteristics, discrimination and petrogenesis. *Contrib. Min. Petr.* **95**, p. 407-419.

White, A.J.R. and Chappell, B.W., 1983. Granitoid types and their distribution in the Lachlan Fold Belt, southeastern Australia. *Geol. Soc. Am. Mem.*, **159**, p. 21-34.

Windley, B.F., 1981. Precambrian rocks in the light of the plate tectonic concept. *In:* Precambrian Plate Tectonics. (Ed.) A. Kröner. p. 1-20.

Wyborn, L.A.I., Page, R.W. and Parker, A.J., 1987. Geochemical and geochronological signatures in Australian Proterozoic igneous rocks. *From*: Pharaoh, T.C., Beckinsale, R.D. & Rickard, D. (eds) 1987, *Geochemistry and Mineralisation of Proterozoic Volcanic Suites,* Geological Society Special Publication **No. 33**, p. 377-394.

Zingg, A., 1980. Regional metamorphism in the Ivrea zone (southern Alps, north Italy): field and microscopic investigations. *Schw. Min. Petrog. Mitte.* **60**, p. 153-179.

APPENDIX A

FORMAL DEFINITIONS OF STRATIGRAPHIC UNITS

APPENDIX A - FORMAL DEFINITIONS OF STRATIGRAPHIC UNITS

Name of unit : ***Bimbowrie Granite***

Derivation of Name : Bimbowrie homestead, 35 km north-west of Olary, South Australia; (OLARY 1:250 000 sheet).

Distribution : N-S trending outcrop near Antro Woolshed, batholiths and isolated outcrops near Tommie Wattie Bore and Tietz Dam; associated with migmatisation around Brady Mine and intrusive into the Basso Granodiorite at Doughboy Well Mine, Basso Mine and Boundary Deposit.

Type Locality : Outcrop south of Antro-Bimbowrie track, 7.5 km west of Bimbowrie homestead. AMG - 413291 E, 6455287 N.

Petrography : Beige megacrystic quartz-rich granite, containing coarse grained elongate feldspar phenocrysts in a med-coarse grained qtz-fld-bt-mu matrix. Phenocrysts comprise up to 30% of the rock. Fine-medium grained samples with a few phenocrysts exist in a few localities (ie., type locality).

Relationship : Formation appears to be due to migmatisation of the metasediments and is clearly intrusive into the Basso Granodiorite (as below).

Remarks : A weak fabric trending ~042 prevails in these large, essentially homogeneous bodies as defined by the orientation of feldspar phenocrysts. Minor Basso Granodiorite and significant metasedimentary xenoliths exist at the contacts with the appropriate lithological sequences.

Name of Unit : ***Basso Granodiorite***

Derivation of Name : Basso Mine, 5 km south - southeast of Bimbowrie homestead, Olary, South Australia; (OLARY 1:250 000 sheet).

Distribution : Located near Basso Mine, Tommie Wattie Bore, Ameroo Hill, Boundary Deposit and Doughboy Well Mine, it is intruded by the Bimbowrie granitoid, and at these localities displays obvious contact margins. This group includes the rock informally referred to as Ameroo Hill granite by previous workers.

Type Locality : Basso Mine, Outalpa Station, 5 km south - southeast of Bimbowrie homestead. AMG - 421517 E, 6449801 N.

Petrography : Medium grained, light grey - buff, bt rich granitoid exhibiting a strong foliation delineated by the planar arrangement of micaceous aggregates. Composed of qtz-plag-bt-K-fld ± mu ± magnetite ± apatite.

Relationship : Intimately associated yet intruded by the Bimbowrie granite, this granite exhibits a strong foliation.

Remarks : Despite the discontinuous and spatially variable distribution of these granitoids, they appear in outcrop to be the same; exhibiting a distinctive weathering pattern - delineated by the biotite coagulations.

Name of Unit : ***Antro Tonalite***

Derivation of Name : Antro woolshed, 11 km west of Bimbowrie homestead, Olary, South Australia; (OLARY 1:250 000 sheet).

Distribution : Exists as a poorly exposed and highly weathered outcrop, 1-2 km northeast of Antro woolshed.

Type Locality : Outcrop 1-2 km northeast of Antro woolshed, north of Antro-Bimbowrie track. AMG - 412992 E, 6456048 N.

Petrography : Fine grained, medium grey, quartz poor tonalite, consisting of Na-plag-px-qtz-K-fld-hb ± chlorite ± epidote ± sphene ± mu ± apatite; + significant numbers of opaques (magnetite). It appears to be relatively mafic and extensively recrystallised.

Relationship : Its poor exposure and highly weathered nature, makes it difficult to distinguish an intrusive or otherwise relationship with the host rocks, a sequence of phyllitic metasediments.

Remarks : Due to its extensive recrystallisation, it seems likely that this body was emplaced prior to deformational events.

APPENDIX B

THIN SECTION DESCRIPTIONS

ANTRO TONALITE

Sample Number - ***A1027-001***

Sample Description - In outcrop, this rock is poorly exposed, highly weathered and extensively recrystallised (as is evident in thin section). It is a fine to medium grained feldspathic granitoid, medium grey in colour with abundant opaques.

Thin Section Description - No strong fabric is seen in thin section, however it appears to have deformed brittley, as observed in plagioclase grains which have been drawn apart and filled with secondary chlorite. It appears to be extensively recrystallised, with smaller quart grains, over-riding the original much larger plagioclase and quartz grains. Opaques are frequently euhedral (cubic-rhomboidal) suggesting this mineral to be magnetite. Euhedral to subhedral apatite exists as an accessory mineral, it has poor cleavage, high to moderate relief, low birefringence and is pink to colourless with weak pleochroism. Pale green chlorite appears as an alteration product of pyroxene (ie., it is a secondary mineral), it is pleochroic has one cleavage, low to moderate relief and low birefringence. Sphene, another accessory mineral, is pale-dark brown, pleochroic, isotropic, has extremely high relief and forms euhedral crystals commonly diamond shaped. Pyroxene exists as the clinopyroxene form, is weakly pleochroic, from pale green to pale pink/brown. It has moderate to high relief and poor cleavage.

Mineral	**Percentage**
Plagioclase	55%
Quartz	20%
Opaques	15%
Clinopyroxene	10%
K-feldspar	<5%
Sphene	minor
Apatite	minor
Muscovite	minor
Chlorite	minor

ANTRO TONALITE

Sample Number - ***A1027-002***

Sample Description - In outcrop, this rock is poorly exposed, highly weathered and extensively recrystallised (as is evident in thin section). It is a fine to medium grained feldspathic granitoid, medium grey in colour with abundant opaques.

Thin Section Description - As for A1027-001. However this section does not contain any sphene, yet has the presence of biotite. Biotite, appears straw-yellow to brown in colour, is strongly pleochroic, has parallel extinction, a high birefringence and moderate to high relief. Fractures running through the thin section, contain secondary chlorite.

Mineral	**Percentage**
Plagioclase	50%
Opaques	20%
Quartz	15%
Clinopyroxene	5%
K-feldspar	<5%
Biotite	<5%
Apatite	minor
Muscovite	minor
Chlorite	minor

BIMBOWRIE GRANITE

Sample Number - ***A1027-005***

Sample Description - Appears in outcrop as large relatively homogeneous plutons, exhibiting a weak fabric (~042). In hand specimen, the rock has very coarse grained elongate K-feldspar phenocrysts in a predominantly quartz matrix, with plagioclase, muscovite and biotite. The matrix is medium to coarse grained and pink-buff in colour.

Thin Section Description - Quart with strong undulose extinction is the most common mineral. Multiply twinned, prismatic plagioclase, colourless under plane light, exhibits low relief, is anisotropic and non pleochroic. Microcline, another member of the feldspar group is very much like plagioclase yet has cross hatched twinning. Muscovite with distinctive birefringence colours (high), is colourless, non pleochroic, has low relief and one perfect cleavage. The biotite seen in thin section is typically red-brown in colour, and invariably contains zircon crystals with circular outlines and black pleochroic haloes. It too is pleochroic, has relatively high birefringence and moderate to high relief.

Under thin section no fabric can be identified. It is relatively homogeneous and doesn't appear to have been deformed to any degree.

Mineral	**Percentage**
Quartz	40%
Microcline	25%
Plagioclase	20%
Muscovite	10%
Biotite	5%

BIMBOWRIE GRANITE

Sample Number - ***A1027-009***

Sample Description - This sample is similar to A1027-005. It is pink to buff in colour, and has the diagnostic large, elongate K-feldspar phenocrysts typical of the Bimbowrie Granite. In the field the outcrop was essentially homogeneous and no obvious fabric identified.

Thin Section Description - Quartz with strong undulose extinction is the most common mineral. Microcline, a member of the feldspar group with distinctive cross hatched twinning is colourless, anisotropic, has low birefringence and is non pleochroic, much like, the multiply twinned plagioclase. Biotite and muscovite are as they appear in sample A1027-005 however muscovite is in lesser quantities and biotite in greater.

Once again, under thin section no fabric can be identified. It is relatively homogeneous and doesn't appear to have been deformed to any degree.

Mineral	**Percentage**
Quartz	40%
Microcline	30%
Plagioclase	20%
Biotite	10%
Muscovite	<5%

MINERAL	Bimbowrie Granite	Basso Granodiorite	Antro Tonalite	Metasediment	Calc-Silicate
Quartz	40%	50%	25%	45%	20%
Plagioclase	30%	25%	55%		10%
K-feldspar	(microcline) 20%	(microcline) 10%	<5%	10%	
Biotite	5%	20%		25%	
Muscovite	10%	minor	minor	20%	5%
Apatite		minor	minor		
Epidote					15%
Sphene			minor		minor
Pyroxene			(cpx) 15%	minor	(diopside) 25%
Garnet				minor	
Amphibole					(actinolite)10%
Chlorite			minor		5%
Opaque	minor	minor	20%	minor	minor

PLATE 4

A Beryl crystal, commonly associated with pegmatite veins.

B Randomly oriented relic ?andalusite porphyroblasts as they appear in the field.

C Original sedimentary layering is enhanced by metamorphism, with variation in initial bulk composition defining the growth of porphyroblasts.

D Deformed pegmatite vein cross-cutting metasediments.

E Brittle deformation of a pegmatite vein, cross-cutting the Bimbowrie Granite.

F Ameroo Hill Granite, part of the Basso Granodiorite (sample number 1027-105).

G Bimbowrie Granite displaying a fabric defined by the orientation of feldspar phenocrysts.

H Tommie Wattie Bore, Outalpa Station.

A

B

C

D

E

F

G

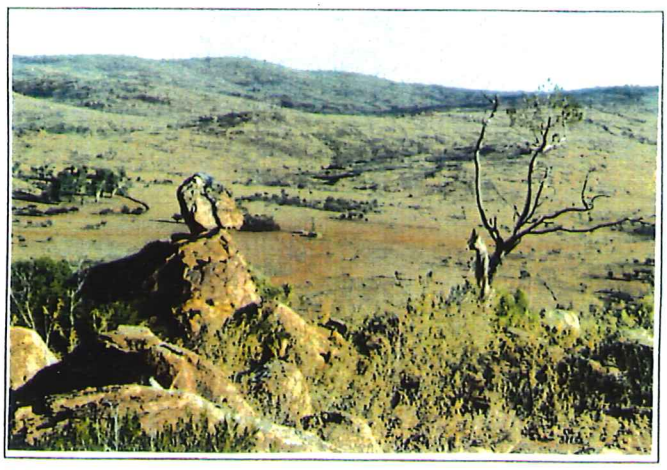

H

APPENDIX C

ANALYTICAL TECHNIQUES

APPENDIX C - ANALYTICAL TECHNIQUES

Sample Selection and Preparation

Considerable care was taken when selecting rock samples for analysis within the laboratory at a later date. The basis for field selection lay solely on the apparent 'freshness' of the rock, as it appeared in outcrop. Once returning from the field, a diamond saw was used to remove all weathering from the rock, in order to obtain the most accurate result when analysed. A small portion of the rock (~4 x 4 cm) was then crushed in the jaw crusher and subsequently milled in a tungsten carbide mill for the purpose of isotopic and XRF analysis.

X-ray Fluorescent (XRF) Analysis

Both major and trace elements were required for geochemical comparison. Trace element analysis involved the production of pellets, made from ~5 g of rock powder mixed with ~1 ml of PVA solution encased by boric acid.

For major element analysis, an initial 3-4 g of rock powder was dried in an oven at 110°C for several hours in order to drive off excess water. Subsequently, samples were ignited at 960°C overnight within the muffle furnace, in order to drive off any volatiles present. One gram the ignited sample was mixed with 4 g of flux (a mixture of lithium tetraborate and lithium metaborate) and fused within a Pt/5% Au crucible. After heating for ~10 minutes (until fusion was complete) the melt was poured into a Pt/Au mould and cooled to room temperature using air 'jets'.

Analysis was undertaken on the Phillips PW 1480 XRF spectrometer for both major and trace elements.

Isotope Analysis

Approximately 200 mg of milled sample was weighed out and added to a HF/HNO_3 (hydrofluoric acid / nitric acid) solution used for digestion in a teflon vessel emplaced within a steel autoclave. Teflon bombs were used so as to decompose samples and ensure that all the refractory minerals such as zircon and monazite were completely dissolved. These vessels were then placed in an oven at 180°C and over a period of 5 days additional HF was added for complete dissolution. Approximately 2 drops of a Sm-Nd (^{150}Nd - ^{147}Sm) spike solution for determination of element concentrations was added to $^1/_3$ of the dissolved solution.

Rubidium, strontium and the REE's were separated by standard cation exchange columns using HCl as an elutriant. Neodymium and samarium were further separated using cation resin columns of teflon and EDEHP with once again HCl as the elutriant. Neodymium and samarium were loaded on tantalum side filaments opposing a rhenium filament. Strontium

was loaded on single tantalum filaments prepared with phosphoric acid. Measurements were made on the Finnigan Mat 261 solid source mass spectrometer.

APPENDIX D

WHOLE ROCK ANALYSIS DATA-
MAJOR AND TRACE ELEMENTS

LITHOLOGY	Bimbowrie	Bimbowrie	Bimbowrie	Bimbowrie	Bimbowrie	Bimbowrie	Bimbowrie	Bimbowrie	Bimbowrie	Bimbowrie	Bimbowrie	Bimbowrie	Bimbowrie	Bimbowrie
REGION	Antro	TWB	Brady	Brady	Brady	Domenic	TWB	TWB	Boundary	TWB	TWB	Antro	Antro	Antro
Northing (AMG)	6455260	6446818					6447846	6447999	6450799	6448907	6455282	6455265	6455287	
Easting (AMG)	413229	420871					421648	421225	421540	420784	413298	413330	413291	
ELEMENT	A1027-005	A1027-009	A1027-012	A1027-013	A1027-014	A1027-015	A1027-030	A1027-034	A1027-035	A1027-037	A1027-038	A1027-040	A1027-042	A1027-044
Major (Wt. %)														
SiO2	73.23	72.64	71.66	72.62	72.76	75.34	72.45	72.54	72.45	71.57	73.18	72.23	72.03	73.43
Al2O3	14.84	14.68	15.10	14.69	14.80	14.02	14.73	14.92	14.80	15.04	14.60	14.90	14.80	14.76
Fe2O3	1.46	1.98	2.01	1.65	1.60	0.98	1.78	2.13	2.03	2.43	1.44	1.59	1.99	0.92
MnO	0.01	0.02	0.01	0.01	0.01	0.01	0.03	0.01	0.01	0.02	0.01	0.02	0.02	0.02
MgO	0.36	0.42	0.54	0.44	0.44	0.27	0.42	0.55	0.56	0.59	0.38	0.46	0.45	0.39
CaO	0.52	0.50	0.57	0.50	0.35	0.35	0.51	0.46	0.78	0.47	0.50	0.60	0.46	0.43
Na2O	3.84	3.51	3.55	3.57	3.55	3.96	3.45	3.42	4.32	3.51	3.57	4.35	3.71	4.19
K2O	4.73	4.90	5.17	5.33	5.36	4.18	5.14	4.88	3.90	5.19	5.03	5.01	5.00	4.73
TiO2	0.16	0.23	0.38	0.26	0.26	0.11	0.23	0.30	0.32	0.35	0.20	0.23	0.23	0.20
P2O5	0.23	0.23	0.16	0.20	0.19	0.19	0.29	0.19	0.18	0.16	0.24	0.17	0.22	0.22
SO3	0.00	0.00	0.00	0.00	0.00	0.00	0.00	0.00	0.00	0.00	0.00	0.00	0.00	0.00
LOI	0.70	0.83	0.81	0.64	0.71	0.68	0.87	0.93	0.84	0.86	0.76	0.47	0.84	0.65
Total	100.07	99.93	99.95	99.92	100.03	100.08	99.91	100.34	100.19	100.18	99.89	100.02	99.74	99.94
AI Index	1.20	1.22	1.21	1.17	1.21	1.20	1.21	1.27	1.16	1.23	1.19	1.09	1.20	1.15
Trace (ppm)														
Rb	409.92	444.31	397.86	410.04	401.55	339.19	442.48	337.66	260.53	309.86	439.51	406.71	405.63	629.26
Ba	188.00	212.00	25.00	265.00	205.00	270.00	186.00	180.00	177.00	128.00	233.00	299.00	253.00	279.00
Th	31.60	40.90	88.90	54.70	56.20	19.60	41.90	58.00	64.00	66.00	36.30	46.60	45.40	39.30
U	13.00	16.90	17.20	15.40	18.30	6.50	11.10	11.10	9.30	8.50	9.50	21.60	12.10	6.20
Nb	24.30	24.20	32.50	24.70	25.90	18.90	26.20	22.00	19.60	17.60	20.40	19.30	22.80	26.50
K	39266.03	40677.28	42918.68	44246.92	44495.97	34700.21	42669.64	40511.25	32375.80	43084.71	41756.48	41590.45	41507.43	39266.03
La	36.00	19.00	85.00	29.00	38.00	48.00	42.00	48.00	52.00	17.00	64.00	68.00	43.00	47.00
Ce	72.00	76.00	188.00	62.00	90.00	112.00	114.00	110.00	127.00	36.00	122.00	116.00	87.00	87.00
Pb	22.20	26.10	25.50	26.90	22.60	21.70	30.30	27.20	26.20	42.20	28.80	33.10	29.20	24.30
Sr	64.48	35.07	33.68	27.64	26.61	26.46	33.43	65.41	50.53	41.36	35.40	56.26	47.91	47.29
P	1003.77	1003.77	698.27	872.84	829.20	829.20	1265.62	829.20	785.56	698.27	1047.41	741.92	960.13	960.13
Nd	38.00	21.60	107.00	51.90	43.00	57.00	60.00	62.00	64.00	19.00	65.00	59.00	45.00	46.00
Zr	109.00	158.00	220.90	151.40	151.10	71.20	149.40	202.40	228.80	233.20	133.50	139.90	154.10	131.70
Sm		5.44		11.34										
Ti	959.20	1378.85	2278.10	1558.70	1558.70	659.45	1378.85	1798.50	1918.40	2098.25	1199.00	1378.85	1378.85	1199.00
Y	22.20	28.60	21.60	30.40	27.40	12.60	26.70	33.20	48.80	34.50	35.70	26.20	24.60	28.20
Sc	3.00	3.90	9.50	3.80	3.00	4.90	5.20	3.60	2.40	1.60	3.30	3.50	3.10	2.80
Cr	4.00	7.00	1.00	1.00	2.00	3.00	14.00	5.00	9.00	11.00	6.00	46.00	1.00	3.00
V	12.90	18.70	2.30	6.30	15.40	22.20	18.20	14.30	12.80	7.50	14.20	18.90	18.90	15.50
Co	59.00	95.20	44.70	57.90	57.00	39.90	82.10	62.90	65.60	78.70	69.30	74.30	84.30	93.50
Ga	22.60	23.60	21.20	21.20	20.60	19.00	22.10	22.90	20.40	21.20	20.20	20.70	22.00	20.90
Cu	3.00	6.00	1.00	1.00	3.00	8.00	7.00	2.00	6.00	8.00	7.00	5.00	7.00	2.00
Zn	22.00	47.00	36.00	41.00	18.00	19.00	45.00	43.00	32.00	42.00	32.00	53.00	33.00	21.00
Ni	0.00	0.00	0.00	0.00	0.00	0.00	3.00	3.00	3.00	3.00	1.00	10.00	0.00	0.00
Normalised Data														
Rb	645.54	699.70	626.55	645.73	632.36	534.16	696.83	531.75	410.28	487.97	692.14	640.48	638.78	990.97
Ba	26.90	30.33	3.58	37.92	29.33	38.63	26.61	25.75	25.33	18.31	33.34	42.78	36.20	39.92
Th	371.76	481.18	1045.88	643.53	661.18	230.59	492.94	682.35	752.94	776.47	427.06	548.24	534.12	462.35
U	619.05	804.76	819.05	733.33	871.43	309.52	528.57	528.57	442.86	404.76	452.38	1028.57	576.19	295.24
Nb	34.08	33.94	45.58	34.64	36.33	26.51	36.75	30.86	27.49	24.68	28.61	27.07	31.98	37.17
K	157.06	162.71	171.67	176.99	177.98	138.80	170.68	162.05	129.50	172.34	167.03	166.36	166.03	157.06
La	52.40	27.66	123.73	42.21	55.31	69.87	61.14	69.87	75.69	24.75	93.16	98.98	62.59	68.41
Ce	40.56	42.82	105.92	34.93	50.70	63.10	64.23	61.97	71.55	20.28	68.73	65.35	49.01	49.01
Pb	120.00	141.08	137.84	145.41	122.16	117.30	163.78	147.03	141.62	228.11	155.68	178.92	157.84	131.35
Sr	3.06	1.66	1.60	1.31	1.26	1.25	1.58	3.10	2.39	1.96	1.68	2.67	2.27	2.24
P	10.57	10.57	7.35	9.19	8.73	8.73	13.32	8.73	8.27	7.35	11.03	7.81	10.11	10.11
Nd	28.06	15.95	79.03	38.33	31.76	42.10	44.31	45.79	47.27	14.03	48.01	43.57	33.23	33.97
Zr	9.73	14.11	19.72	13.52	13.49	6.36	13.34	18.07	20.43	20.82	11.92	12.49	13.76	11.76
Sm		12.26												
Ti	0.74	1.06	1.75	1.20	1.20	0.51	1.06	1.38	1.48	1.61	0.92	1.06	1.06	0.92
Y	4.88	6.29	4.75	6.68	6.02	2.77	5.87	7.30	10.73	7.58	7.85	5.76	5.41	6.20

LITHOLOGY	Bimbowrie	Bimbowrie	Bimbowrie	Bimbowrie	Bimbowrie	Bimbowrie	Bimbowrie	Bimbowrie	Bimbowrie	Bimbowrie	Bimbowrie	Bimbowrie	Bimbowrie	Bimbowrie
REGION	Antro	Antro	TWB	TWB	TWB	Basso	Basso	Antro	TWB	TWB	Boundary	~Ameroo	Boundary	Basso
Northing (AMG)				6448783								6445326	6450811	6449973
Easting (AMG)				423241								423828	420300	420576
ELEMENT	A1027-046	A1027-047	A1027-049	A1027-050	A1027-052	A1027-054	A1027-055	A1027-058	A1027-065	A1027-069	A1027-085	A1027-090	A1027-093	A1027-094
Major (Wt. %)														
SiO2	72.87	73.59	73.04	73.00	73.55	72.22	71.22	74.03	72.82	73.14	72.43	72.28	72.02	71.86
Al2O3	14.92	14.84	14.47	14.51	14.84	14.95	15.00	14.24	15.28	15.26	15.02	14.70	14.78	14.92
Fe2O3	1.13	1.54	1.86	1.72	0.83	1.74	2.29	1.49	1.20	1.46	1.70	0.75	2.09	2.12
MnO	0.01	0.01	0.03	0.01	0.01	0.01	0.01	0.01	0.01	0.01	0.01	0.03	0.01	0.01
MgO	0.39	0.35	0.45	0.44	0.38	0.45	0.62	0.45	0.27	0.60	0.49	0.46	0.57	0.57
CaO	0.41	0.23	0.59	0.53	0.58	0.50	0.56	0.36	0.56	0.51	0.58	0.50	0.52	0.44
Na2O	4.15	3.80	3.73	3.61	4.93	3.68	4.70	3.46	4.09	5.68	4.44	3.69	3.85	3.58
K2O	5.12	4.50	4.72	5.07	4.12	5.26	4.14	4.77	4.47	1.84	4.31	6.51	5.06	5.16
TiO2	0.22	0.16	0.25	0.25	0.13	0.25	0.38	0.19	0.14	0.32	0.27	0.21	0.31	0.30
P2O5	0.14	0.25	0.20	0.22	0.28	0.18	0.13	0.19	0.36	0.16	0.19	0.21	0.15	0.16
SO3	0.00	0.00	0.00	0.00	0.00	0.00	0.00	0.00	0.00	0.00	0.00	0.00	0.00	0.00
LOI	0.69	0.98	0.77	0.76	0.51	0.75	0.76	0.81	0.82	0.82	0.68	0.44	0.63	0.82
Total	100.04	100.24	100.09	100.12	100.16	99.99	99.81	100.00	100.03	99.80	100.13	99.76	100.00	99.93
Al Index	1.14	1.29	1.17	1.17	1.09	1.18	1.13	1.24	1.21	1.24	1.15	1.05	1.16	1.22
Trace (ppm)														
Rb	375.05	497.77	379.17	394.48	273.24	369.12	263.89	345.78	285.94	101.10	295.70	299.00	297.70	377.40
Ba	329.00	131.00	209.00	255.00	181.00	279.00	367.00	205.00	117.00	206.00	324.00	658.00	356.00	270.00
Th	45.70	27.00	46.00	47.00	26.20	46.10	73.40	37.00	22.20	58.40	54.60	40.80	64.10	55.40
U	15.30	15.80	15.50	17.40	5.10	6.80	10.50	5.50	9.60	5.70	10.50	3.00	8.60	11.90
Nb	17.70	30.10	22.20	19.70	21.40	17.70	18.00	19.00	27.80	15.40	19.40	25.70	18.00	19.40
K	42503.61	37356.69	39183.01	42088.54	34202.12	43665.82	34368.15	39598.09	37107.64	15274.73	35779.41	54042.68	42005.52	42835.67
La	52.00	33.00	54.00	67.00	16.00	21.00	68.00	33.00	16.00	81.00	56.00	29.00	55.00	39.00
Ce	99.00	65.00	109.00	130.00	41.00	85.00	296.00	72.00	33.00	150.00	125.00	73.00	154.00	108.00
Pb	25.70	24.50	27.80	29.00	12.80	31.80	28.90	19.00	20.30	10.80	25.80	15.50	33.60	29.80
Sr	43.95	52.80	33.27	41.35	33.11	37.93	47.54	34.05	20.78	66.40	44.10	75.00	45.20	37.30
P	610.99	1091.05	872.84	960.13	1221.98	785.56	567.35	829.20	1571.12	698.27	829.20	916.48	654.63	698.27
Nd	37.08	32.00	44.90	68.00	22.00	30.00	76.00	35.00	23.00	84.00	62.00	40.00	69.00	44.00
Zr	141.50	89.10	168.60	165.70	96.20	167.30	256.80	104.00	81.70	200.60	200.90	121.90	221.50	186.80
Sm	7.61		9.59											
Tl	1318.90	959.20	1498.75	1498.75	779.35	1498.75	2278.10	1139.05	839.30	1918.40	1618.65	1258.95	1858.45	1798.50
Y	24.40	15.90	33.10	37.80	14.20	26.20	85.50	18.50	16.30	21.10	42.40	20.80	36.30	25.30
Sc	4.20	4.10	4.50	4.00	2.90	2.90	5.50	2.30	3.10	3.90	3.70	4.40	3.30	5.40
Cr	4.00	22.00	3.00	8.00	81.00	7.00	8.00	61.00	10.00	7.00	1.00	2.00	4.00	6.00
V	19.40	12.40	17.70	18.70	10.40	18.30	29.90	14.90	9.90	25.60	19.00	16.60	22.90	25.00
Co	54.90	56.30	65.50	60.20	74.10	76.00	44.90	73.50	52.70	64.10	67.50	73.80	71.60	87.60
Ga	18.40	24.20	21.80	20.00	18.10	20.40	19.50	20.80	21.20	18.80	20.30	17.40	18.50	21.80
Cu	3.00	6.00	5.00	6.00	4.00	4.00	8.00	57.00	6.00	6.00	5.00	9.00	9.00	12.00
Zn	12.00	17.00	46.00	41.00	8.00	40.00	38.00	13.00	9.00	19.00	27.00	13.00	31.00	40.00
Ni	3.00	4.00	0.00	2.00	18.00	1.00	4.00	13.00	4.00	4.00	0.00	1.00	0.00	0.00
Normalised Data														
Rb	590.64	783.88	597.12	621.23	430.30	581.29	415.58	544.53	450.29	159.21	465.67	470.87	468.82	594.33
Ba	47.07	18.74	29.90	36.49	25.90	39.92	52.51	29.33	16.74	29.47	46.36	94.15	50.94	38.63
Th	537.65	317.65	541.18	552.94	308.24	542.35	863.53	435.29	261.18	687.06	642.35	480.00	754.12	651.76
U	728.57	752.38	738.10	828.57	242.86	323.81	500.00	261.90	457.14	271.43	500.00	142.86	409.52	566.67
Nb	24.82	42.22	31.14	27.63	30.01	24.82	25.25	26.65	38.99	21.60	27.21	36.04	25.25	27.21
K	170.01	149.43	156.73	168.35	136.81	174.66	137.47	158.39	148.43	61.10	143.12	216.17	168.02	171.34
La	75.69	48.03	78.60	97.53	23.29	30.57	98.98	48.03	23.29	117.90	81.51	42.21	80.06	56.77
Ce	55.77	36.62	61.41	73.24	23.10	47.89	166.76	40.56	18.59	84.51	70.42	41.13	86.76	60.85
Pb	138.92	132.43	150.27	156.76	69.19	171.89	156.22	102.70	109.73	58.38	139.46	83.78	181.62	161.08
Sr	2.08	2.50	1.58	1.96	1.57	1.80	2.25	1.61	0.98	3.15	2.09	3.55	2.14	1.77
P	6.43	11.48	9.19	10.11	12.86	8.27	5.97	8.73	16.54	7.35	8.73	9.65	6.89	7.35
Nd	27.39	23.63	33.16	50.22	16.25	22.16	56.13	25.85	16.99	62.04	45.79	29.54	50.96	32.50
Zr	12.63	7.96	15.05	14.79	8.59	14.94	22.93	9.29	7.29	17.91	17.94	10.88	19.78	16.68
Sm	17.15		21.60											
Tl	1.01	0.74	1.15	1.15	0.60	1.15	1.75	0.88	0.65	1.48	1.25	0.97	1.43	1.38
Y	5.36	3.49	7.27	8.31	3.12	5.76	18.79	4.07	3.58	4.64	9.32	4.57	7.98	5.56

LITHOLOGY	Bimbowrie	Bimbowrie	Bimbowrie	Bimbowrie	Bimbowrie	Bimbowrie	Bimbowrie	Bimbowrie	Bimbowrie	Bimbowrie	Basso	Basso	Basso	Basso
REGION	TWB	~Ameroo	~Ameroo	Brady	Brady	Doughboy	Doughboy	Domenic	Ameroo	Boolcoomata	Basso Mine	Doughboy	Boundary	Boundary
Northing (AMG)	6446109	6445253	6445347	6443966	6442228	6450399	6450003		Proterozic		6449801	6450953	6450840	
Easting (AMG)	421494	423222	423867	428692	431446	416912	416619	North Exp.	North Exp.	North Exp.	421517	416497	420934	
ELEMENT	A1027-096	A1027-103	A1027-104	A1027-106	A1027-109	A1027-112	A1027-113	ZA000016 A105	ZA000017 A121	ZA001211 A383	A1027-017	A1027-026	A1027-079	A1027-087
Major (Wt. %)														
SiO2	74.16	73.29	72.07	73.41	72.93	71.33	71.49	75.00	70.80	71.40	78.14	77.29	76.96	77.37
Al2O3	14.69	14.46	13.75	14.20	14.74	14.90	14.95	13.80	14.60	14.30	11.77	11.67	11.51	11.94
Fe2O3	0.97	1.48	2.65	1.36	1.49	2.41	2.31	1.22	2.18	1.48	1.43	3.51	2.14	2.15
MnO	0.01	0.01	0.02	0.01	0.01	0.01	0.02	0.01	0.01	0.00	0.01	0.00	0.01	0.01
MgO	0.25	0.32	0.60	0.42	0.43	0.72	0.61	0.23	0.42	0.34	1.15	0.41	1.72	0.92
CaO	0.39	0.31	0.43	0.33	0.46	0.52	0.62	0.28	0.38	0.55	0.11	0.06	0.08	0.11
Na2O	3.92	3.57	3.87	4.03	3.65	3.60	3.43	3.88	4.26	4.12	6.04	6.59	5.26	6.60
K2O	4.35	5.07	5.15	4.97	5.02	4.45	4.97	4.12	5.55	4.64	0.91	0.24	1.74	0.46
TiO2	0.11	0.15	0.52	0.16	0.21	0.33	0.32	0.12	0.32	0.18	0.19	0.18	0.18	0.18
P2O5	0.24	0.14	0.19	0.16	0.23	0.22	0.19	0.20	0.21	0.16	0.01	0.01	0.01	0.01
SO3	0.00	0.00	0.00	0.00	0.00	0.00	0.00				0.01	0.01	0.00	0.00
LOI	0.80	0.78	0.43	0.51	0.79	1.30	0.95	0.74	0.46	0.79	0.23	0.16	0.29	0.26
Total	99.89	99.57	99.67	99.56	99.98	99.79	99.86				99.97	100.11	99.88	99.99
Al Index	1.24	1.21	1.08	1.13	1.20	1.28	1.23	1.22	1.07	1.12	1.06	1.04	1.08	1.03
Trace (ppm)														
Rb	376.10	285.00	398.40	334.80	371.40	266.80	358.80	320.00	270.00	175.00	126.43	32.27	171.00	36.00
Ba	117.00	201.00	203.00	167.00	222.00	362.00	341.00	155.00	320.00	480.00	321.00	329.00	39.00	25.00
Th	17.50	27.50	97.30	31.60	37.40	58.90	67.20	9.50	32.00	20.00	37.40	41.80	39.30	44.40
U	5.60	3.90	13.20	4.70	12.50	7.20	6.60	4.00	5.50	7.50	11.20	15.20	10.70	3.90
Nb	19.00	22.10	28.30	20.40	26.10	24.00	24.60	20.00	15.00	10.00	83.10	80.30	93.10	86.70
K	36111.46	42088.54	42752.65	41258.39	41673.46	36941.61	41258.39	34202.12	46073.25	38518.90	7554.35	1992.36	14444.59	3818.68
La	15.00	22.00	30.00	21.00	26.00	53.00	104.00	24.00	52.00	19.00	72.00	68.00	26.00	57.00
Ce	32.00	46.00	131.00	56.00	64.00	110.00	236.00	40.00	88.00	0.00	153.00	162.00	66.00	132.00
Pb	31.00	13.90	28.90	8.10	36.90	19.70	24.70	50.00	50.00	4.00	5.70	9.20	6.70	5.40
Sr	78.80	24.10	32.30	22.10	28.10	69.00	60.40	25.00	45.00	50.00	18.52	22.50	12.30	13.40
P	1047.41	610.99	829.20	698.27	1003.77	960.13	829.20	872.84	916.48	698.27	43.64	43.64	43.64	43.64
Nd	20.00	24.00	41.00	27.00	35.00	64.00	116.00	22.00	50.00	25.00	90.07	36.99	71.00	101.00
Zr	60.30	89.10	322.70	132.40	119.30	198.70	179.70	70.00	200.00	120.00	337.60	379.80	432.20	523.70
Sm								4.00	8.50	4.00	21.29	10.19		
Tl	659.45	899.25	3117.40	959.20	1258.95	1978.35	1918.40	719.40	1918.40	1079.10	1139.05	1079.10	1079.10	1079.10
Y	13.70	35.50	41.70	63.80	32.60	52.50	57.20	8.00	20.00	20.00	115.40	90.10	196.60	251.90
Sc	1.40	4.20	7.40	4.60	6.30	5.50	4.20	<10	<10	0.00	4.80	3.40	4.60	4.40
Cr	2.00	1.00	0.00	0.00	0.00	9.00	2.00	<50	<50	0.00	2.00	2.00	4.00	1.00
V	7.50	8.00	31.80	8.70	10.90	26.00	23.30	<20	<20	0.00	22.60	25.10	19.40	3.70
Co	55.80	110.10	92.20	81.80	85.80	64.30	48.70	<10	<10	45.00	46.10	44.00	40.40	86.80
Ga	20.10	20.70	18.00	16.10	17.30	20.50	19.90	22.00	22.00	18.00	28.50	27.60	27.30	31.60
Cu	4.00	7.00	26.00	4.00	3.00	4.00	7.00	<50	<50	7.00	0.00	5.00	0.00	6.00
Zn	25.00	12.00	45.00	13.00	26.00	17.00	30.00	<20	<20	0.00	5.00	9.00	12.00	2.00
Ni	0.00	0.00	0.00	0.00	0.00	1.00	0.00	<10	<10	20.00	1.00	0.00	12.00	0.00
Normalised Data														
Rb	592.28	448.82	627.40	527.24	584.88	420.16	565.04	503.94	425.20	275.59	199.11	50.81	269.29	56.69
Ba	16.74	28.76	29.05	23.89	31.76	51.80	48.79	22.18	45.79	68.68	45.93	47.07	5.58	3.58
Th	205.88	323.53	1144.71	371.76	440.00	692.94	790.59	111.76	376.47	235.29	440.00	491.76	462.35	522.35
U	266.67	185.71	628.57	223.81	595.24	342.86	314.29	190.48	261.90	357.14	533.33	723.81	509.52	185.71
Nb	26.65	31.00	39.69	28.61	36.61	33.66	34.50	28.05	21.04	14.03	116.55	112.62	130.58	121.60
K	144.45	168.35	171.01	165.03	166.69	147.77	165.03	136.81	184.29	154.08	30.22	7.97	57.78	15.27
La	21.83	32.02	43.67	30.57	37.85	77.15	151.38	34.93	75.69	27.66	104.80	98.98	37.85	82.97
Ce	18.03	25.92	73.80	31.55	36.06	61.97	132.96	22.54	49.58	0.00	86.20	91.27	37.18	74.37
Pb	167.57	75.14	156.22	43.78	199.46	106.49	133.51	270.27	270.27	21.62	30.81	49.73	36.22	29.19
Sr	3.73	1.14	1.53	1.05	1.33	3.27	2.86	1.18	2.13	2.37	0.88	1.07	0.58	0.64
P	11.03	6.43	8.73	7.35	10.57	10.11	8.73	9.19	9.65	7.35	0.46	0.46	0.46	0.46
Nd	14.77	17.73	30.28	19.94	25.85	47.27	85.67	16.25	36.93	18.46	66.52	27.32	52.44	74.59
Zr	5.38	7.96	28.81	11.82	10.65	17.74	16.04	6.25	17.86	10.71	30.14	33.91	38.59	46.76
Sm								9.01	19.14	9.01	47.95	22.95		
Tl	0.51	0.69	2.40	0.74	0.97	1.52	1.48	0.55	1.48	0.83	0.88	0.83	0.83	0.83
Y	3.01	7.80	9.16	14.02	7.16	11.54	12.57	1.76	4.40	4.40	25.36	19.80	43.21	55.36

LITHOLOGY	Basso	Basso	Ameroo	Antro	Antro	Antro	Antro	Antro	Antro	Poodla	Poodla	Metased.	Metased.
REGION	Boundary	Boundary	Ameroo	Antro	Antro	Antro	Antro	Ameroo	Doughboy	Koolka Hut	Poodla Dam	Antro	Boundary
Northing (AMG)			6445328		6456048							6452000	
Easting (AMG)		North Exp.	425140		412992	North Exp.	North Exp.	North Exp.	North Exp.	North Exp.	North Exp.	413669	
ELEMENT	A1027-091	ZA001206	A1027-105	A1027-059	A1027-117	ZA000018	ZA000020	ZA001201	ZA001202	ZA001203	ZA001205	A1027-073	A1027-092
Major (Wt. %)						A127c	A140	A294	A297	A361	A414		
SiO2	77.12	76.00	77.34	59.11	64.72	63.20	64.70	65.60	53.80	62.70	64.10	62.27	74.53
Al2O3	11.83	11.10	11.65	13.52	14.25	13.80	12.50	13.10	12.00	13.90	14.20	19.14	13.25
Fe2O3	2.25	2.30	3.33	14.68	9.89	10.50	11.40	8.60	13.90	7.20	7.25	3.60	2.85
MnO	0.00	0.00	0.01	0.04	0.02	0.02	0.02	0.10	0.07	0.05	0.02	0.03	0.02
MgO	1.14	1.35	0.06	0.89	0.53	0.70	0.49	0.70	3.62	1.43	1.90	3.45	1.22
CaO	0.08	0.08	0.46	3.03	1.06	1.54	1.29	3.14	5.85	1.83	0.61	0.85	0.77
Na2O	6.23	5.90	5.96	7.23	8.18	8.20	7.25	6.70	6.65	3.82	4.32	8.15	3.24
K2O	0.77	0.92	0.52	0.24	0.13	0.13	0.14	0.55	0.33	5.30	4.72	0.86	2.71
TiO2	0.18	0.31	0.19	1.14	0.99	1.01	0.83	0.85	2.38	1.07	0.95	0.66	0.29
P2O5	0.01	0.02	0.00	0.36	0.32	0.31	0.21	0.22	0.35	0.30	0.28	0.12	0.05
SO3	0.00		0.00	0.00	0.00							0.00	0.00
LOI	0.25	0.45	0.20	0.09	0.18	0.37	0.10	0.28	0.52	1.02	0.93	1.41	1.14
Total	99.85		99.71	100.33	100.24							100.52	100.06
Al Index	1.05	1.02	1.04	0.77	0.92	0.84	0.87	0.76	0.55	0.91	1.07	1.21	1.37
Trace (ppm)													
Rb	57.20	110.00	8.13	6.42	1.90	4.00	4.50	15.00	4.50	175.00	175.00	76.40	230.00
Ba	42.00	70.00	148.00	170.00	32.00	65.00	35.00	220.00	100.00	2150.00	1650.00	191.00	491.00
Th	43.00	40.00	38.50	7.30	7.80	7.50	6.00	8.50	9.50	16.00	16.00	19.20	25.80
U	7.20	7.50	5.50	4.20	3.20	4.00	1.50	3.50	6.00	6.00	4.50	3.20	8.20
Nb	86.90	75.00	65.20	17.80	19.90	20.00	20.00	25.00	25.00	30.00	30.00	14.70	14.70
K	6392.14	7637.37	4316.77	1992.36	1079.19	1079.19	1162.21	4565.82	2739.49	43997.88	39183.01	7139.28	22497.03
La	67.00	40.00	163.00	26.00	41.00	60.00	32.00	25.00	45.00	50.00	35.00	43.00	41.00
Ce	155.00	115.00	421.00	56.00	101.00	110.00	56.00	75.00	130.00	115.00	90.00	76.00	78.00
Pb	8.30	4.00	7.00	3.40	4.60	50.00	50.00	7.00	9.00	7.00	7.00	7.90	7.90
Sr	14.80	20.00	25.05	61.15	18.40	20.00	15.00	65.00	50.00	130.00	50.00	109.70	90.00
P	43.64	87.28	0.00	1571.12	1396.55	1352.91	916.48	960.13	1527.47	1309.26	1221.98	523.71	218.21
Nd	102.00	135.00	171.62	33.00	54.00	55.00	34.00	40.00	70.00	55.00	50.00	30.00	40.00
Zr	468.30	630.00	358.40	204.40	252.00	350.00	400.00	280.00	300.00	360.00	310.00	155.40	150.50
Sm		25.00	36.92			10.00	6.50	8.50	9.50	4.00	5.50		
Tl	1079.10	1858.45	1139.05	6834.29	5935.04	6054.94	4975.84	5095.74	14268.09	6414.64	5695.24	3956.70	1738.55
Y	178.50	140.00	187.00	77.70	103.90	80.00	55.00	70.00	45.00	45.00	45.00	20.40	44.50
Sc	5.00	5.00	1.20	30.00	26.50	20.00	20.00	25.00	30.00	15.00	10.00	14.80	6.70
Cr	5.00	0.00	2.00	16.00	0.00	<50	<50	0.00	0.00	30.00	30.00	91.00	29.00
V	3.00	20.00	0.30	10.50	24.80	30.00	<20	0.00	330.00	50.00	70.00	119.80	26.30
Co	53.90	50.00	84.60	64.50	56.50	10.00	20.00	55.00	50.00	55.00	50.00	48.40	49.50
Ga	29.20	35.00	27.10	28.20	27.20	22.00	20.00	30.00	25.00	25.00	25.00	21.20	14.50
Cu	1.00	0.00	11.00	133.00	57.00	100.00	150.00	18.00	110.00	50.00	17.00	1.00	13.00
Zn	8.00	60.00	8.00	14.00	6.00	<20	<20	80.00	110.00	110.00	120.00	14.00	22.00
Ni	3.00	30.00	0.00	8.00	4.00	20.00	<10	25.00	35.00	30.00	25.00	30.00	9.00
Normalised Data													
Rb	90.08	173.23	12.80	10.11	2.99	6.30	7.09	23.62	7.09	275.59	275.59	120.31	362.20
Ba	6.01	10.02	21.18	24.32	4.58	9.30	5.01	31.48	14.31	307.63	236.09	27.33	70.25
Th	505.88	470.59	452.94	85.88	91.76	88.24	70.59	100.00	111.76	188.24	188.24	225.88	303.53
U	342.86	357.14	261.90	200.00	152.38	190.48	71.43	166.67	285.71	285.71	214.29	152.38	390.48
Nb	121.88	105.19	91.44	24.96	27.91	28.05	28.05	35.06	35.06	42.08	42.08	20.62	20.62
K	25.57	30.55	17.27	7.97	4.32	4.32	4.65	18.26	10.96	175.99	156.73	28.56	89.99
La	97.53	58.22	237.26	37.85	59.68	87.34	46.58	36.39	65.50	72.78	50.95	62.59	59.68
Ce	87.32	64.79	237.18	31.55	56.90	61.97	31.55	42.25	73.24	64.79	50.70	42.82	43.94
Pb	44.86	21.62	37.84	18.38	24.86	270.27	270.27	37.84	48.65	37.84	37.84	42.70	42.70
Sr	0.70	0.95	1.19	2.90	0.87	0.95	0.71	3.08	2.37	6.16	2.37	5.20	4.27
P	0.46	0.92	0.00	16.54	14.70	14.24	9.65	10.11	16.08	13.78	12.86	5.51	2.30
Nd	75.33	99.70	126.75	24.37	39.88	40.62	25.11	29.54	51.70	40.62	36.93	22.16	29.54
Zr	41.81	56.25	32.00	18.25	22.50	31.25	35.71	25.00	26.79	32.14	27.68	13.88	13.44
Sm		56.31	83.14			22.52	14.64	19.14	21.40	9.01	12.39		
Tl	0.83	1.43	0.88	5.26	4.57	4.66	3.83	3.92	10.98	4.93	4.38	3.04	1.34
Y	39.23	30.77	41.10	17.08	22.84	17.58	12.09	15.38	9.89	9.89	9.89	4.48	9.78

LITHOLOGY	Metased.	Marginal	Marginal	Pegmatite	Migmatite	Migmatite
REGION	TWB	Basso	Doughboy	Brady	Pennynellie	Pennynellie
Northing (AMG)	6447200	6449389	6449982	6441933	6441555	6441555
Easting (AMG)	422650	420949	416569	431954	429524	429524
ELEMENT	A1027-102	A1027-095	A1027-115	A1027-108	A1027-110	A1027-111
Major (Wt. %)						
SiO2	59.72	75.11	74.35	74.08	68.09	49.98
Al2O3	20.36	13.44	13.18	14.48	16.82	14.57
Fe2O3	3.73	1.75	3.02	0.99	2.82	19.01
MnO	0.03	0.01	0.01	0.01	0.02	0.06
MgO	1.83	0.73	0.68	0.27	1.43	1.09
CaO	0.24	0.32	0.26	0.36	0.80	4.85
Na2O	5.82	6.94	6.83	3.99	6.68	4.70
K2O	6.38	0.68	0.84	4.89	2.16	1.83
TiO2	0.69	0.39	0.45	0.12	0.36	3.32
P2O5	0.08	0.11	0.10	0.23	0.18	0.37
SO3	0.00	0.00	0.00	0.00	0.00	0.00
LOI	0.97	0.37	0.21	0.57	0.66	0.00
Total	99.86	99.84	99.92	99.99	100.04	99.66
AI Index	1.20	1.06	1.04	1.16	1.14	0.79
Trace (ppm)						
Rb	499.24	64.90	44.60	264.70	232.30	160.90
Ba	686.00	79.00	76.00	239.00	92.00	108.00
Th	22.60	29.20	32.80	8.50	19.90	3.70
U	19.80	3.40	10.30	2.90	4.30	9.10
Nb	17.80	42.20	46.80	14.50	26.40	16.70
K	52963.48	5645.01	6973.25	40594.27	17931.21	15191.72
La	51.00	55.00	74.00	8.00	37.00	24.00
Ce	102.00	113.00	156.00	16.00	73.00	66.00
Pb	14.60	2.90	3.40	11.00	7.30	3.90
Sr	65.05	57.10	45.30	23.70	54.80	40.10
P	349.14	480.06	436.42	1003.77	785.56	1614.76
Nd	33.35	65.00	88.00	11.00	35.00	29.00
Zr	158.40	364.50	393.90	59.40	175.60	208.80
Sm	6.05					
Tl	4136.55	2338.05	2697.75	719.40	2158.20	19903.38
Y	37.00	93.20	125.00	29.60	25.10	46.10
Sc	14.60	9.70	10.10	2.40	11.20	46.90
Cr	87.00	6.00	10.00	10.00	51.00	96.00
V	85.80	16.40	12.90	8.90	43.50	469.70
Co	30.10	81.50	89.60	94.20	62.90	37.00
Ga	25.90	20.80	21.90	16.20	20.80	20.60
Cu	8.00	0.00	8.00	0.00	4.00	0.00
Zn	18.00	7.00	5.00	13.00	25.00	37.00
Ni	24.00	0.00	0.00	0.00	16.00	28.00
Normalised Data						
Rb	786.20	102.20	70.24	416.85	365.83	253.39
Ba	98.15	11.30	10.87	34.20	13.16	15.45
Th	265.88	343.53	385.88	100.00	234.12	43.53
U	942.86	161.90	490.48	138.10	204.76	433.33
Nb	24.96	59.19	65.64	20.34	37.03	23.42
K	211.85	22.58	27.89	162.38	71.72	60.77
La	74.24	80.06	107.71	11.64	53.86	34.93
Ce	57.46	63.66	87.89	9.01	41.13	37.18
Pb	78.92	15.68	18.38	59.46	39.46	21.08
Sr	3.08	2.71	2.15	1.12	2.60	1.90
P	3.68	5.05	4.59	10.57	8.27	17.00
Nd	24.63	48.01	64.99	8.12	25.85	21.42
Zr	14.14	32.54	35.17	5.30	15.68	18.64
Sm	13.63					
Tl	3.18	1.80	2.08	0.55	1.66	15.31
Y	8.13	20.48	27.47	6.51	5.52	10.13

LITHOLOGY	I-Type	I-Type	I-Type	I-Type	I-Type	I-Type	I-Type	I-Type	I-Type	I-Type	I-Type	S-Type	S-Type	S-Type	S-Type	S-Type	S-Type	S-Type	S-Type	S-Type	S-Type	S-Type
REGION	LFB	LFB	LFB	LFB	LFB	LFB	LFB	LFB	LFB	LFB	LFB	LFB	LFB	LFB	LFB	LFB	LFB	LFB	LFB	LFB	LFB	LFB
Age	Phanerozoic	Phanerozoic	Phanerozoic	Phanerozoic	Phanerozoic	Phanerozoic	Phanerozoic	Phanerozoic	Phanerozoic	Phanerozoic	Phanerozoic	Phanerozoic	Phanerozoic	Phanerozoic	Phanerozoic	Phanerozoic	Phanerozoic	Phanerozoic	Phanerozoic	Phanerozoic	Phanerozoic	Phanerozoic
Source	C & W 1992	C & W 1992	C & W 1992	C & W 1992	C & W 1992	C & W 1992	C & W 1992	C & W 1992	C & W 1992	C & W 1992	C & W 1992	C & W 1992	C & W 1992	C & W 1992	C & W 1992	C & W 1992	C & W 1992	C & W 1992	C & W 1992	C & W 1992	C & W 1992	C & W 1992
ELEMENT	MG42	MG20	AB6	KB139	KB22	BP16	CV87	BB21	VB230	TB12	AVERAGE	VB221	CC1	ER62	KB32	KB102	BB11	BB2	CV115	VB140	TB83	AVERAGE 704
Major (Wt. %)																						
SiO2	60.13	74.91	67.39	55.50	62.29	62.26	63.73	76.56	76.73	75.71	69.50	67.87	72.00	65.04	67.68	73.81	70.89	73.48	73.65	72.48	73.37	70.91
Al2O3	16.42	13.37	14.48	18.63	16.46	15.42	15.14	12.60	12.44	12.31	14.21	14.80	13.72	14.82	14.70	13.22	13.92	13.41	13.08	14.50	15.09	14.00
Fe2O3	2.04	0.38	1.58	2.03	1.85	2.24	0.87	0.43	0.37	0.40	1.01	0.38	0.59	0.91	0.68	0.62	0.72	0.44	0.16	0.29	0.03	0.52
MnO	0.11	0.07	0.09	0.12	0.10	0.10	0.07	0.02	0.04	0.02	0.07	0.06	0.06	0.06	0.07	0.04	0.06	0.04	0.05	0.03	0.03	0.06
MgO	3.27	0.24	1.72	4.81	2.85	3.35	2.40	0.21	0.22	0.02	1.38	2.01	1.76	3.27	2.22	0.60	1.00	0.71	0.61	0.47	0.02	1.24
CaO	5.91	1.10	4.32	8.10	6.05	5.94	3.74	0.97	0.45	0.64	3.07	1.05	0.95	3.98	2.26	1.68	2.31	1.70	1.20	0.66	0.29	1.88
Na2O	3.94	4.21	2.63	2.22	2.60	3.02	2.65	3.52	3.46	3.42	3.16	1.38	1.49	1.73	1.92	2.97	2.56	2.63	2.58	2.80	4.62	2.51
K2O	1.41	3.50	2.99	0.95	2.01	2.14	4.08	4.16	4.78	4.38	3.48	4.37	3.73	2.91	3.60	4.05	3.96	4.63	4.60	5.20	4.09	4.09
TiO2	0.99	0.15	0.53	0.70	0.54	0.54	0.88	0.19	0.08	0.07	0.41	0.73	0.54	0.73	0.64	0.30	0.35	0.22	0.36	0.25	0.01	0.44
P2O5	0.28	0.06	0.11	0.10	0.11	0.17	0.24	0.03	0.02	0.01	0.11	0.19	0.13	0.12	0.15	0.09	0.09	0.08	0.17	0.33	0.29	0.15
SO3	3.73	1.16	3.02	4.98	3.41	3.57	3.77	0.43	0.47	0.40	3.12	4.30	3.48	4.65	4.03	1.65	2.26	1.47	2.27	1.33	0.65	3.06
LOI	0.18	0.13	0.15	0.14	0.16	0.23	0.31	0.14	0.10	0.19		0.21	0.21	0.20	0.19	0.15	0.18	0.13	0.19	0.13	0.18	
Total	99.90	100.06	100.17	100.18	99.93	100.30	99.42	99.99	99.90	99.59		99.73	100.21	99.82	99.99	99.90	100.13	99.93	100.07	99.82	99.64	
Al Index	0.88	1.05	0.94	0.96	0.94	0.85	0.97	1.05	1.06	1.07	0.98	1.66	1.67	1.12	1.32	1.07	1.10	1.08	1.15	1.27	1.20	1.17
Trace (ppm)																						
Rb	36.50	90.00	135.00	38.50	89.00	72.00	215.00	214.00	367.00	765.00	164.00	186.00	153.00	142.00	183.00	187.00	178.00	236.00	244.00	419.00	1400.00	245.00
Ba	325.00	580.00	415.00	215.00	355.00	555.00	1150.00	545.00	56.00	6.00	519.00	610.00	765.00	475.00	475.00	495.00	625.00	350.00	755.00	220.00	2.00	440.00
Th	5.80	9.00	16.80	4.40	9.20	11.20	26.00	19.80	32.50	86.00	20.00	26.50	21.50	19.40	19.20	18.60	18.00	19.20	15.60	14.20	11.80	19.00
U	1.80	3.40	3.00	0.80	1.40	2.20	5.80	3.60	15.20	26.00	5.00	2.60	3.80	1.20	4.00	3.60	4.20	6.40	5.80	10.80	3.40	5.00
Nb	14.00	12.00	9.00	4.50	6.50	5.50	20.50	16.50	27.00	32.50	11.00	18.00	9.00	11.00	13.00	7.50	10.50	10.00	11.50	20.00	39.50	13.00
K	11705.10	29055.20	24821.44	7886.41	16685.99	17765.18	33870.06	34534.18	39681.10	36360.51	28889.17	36277.49	30964.54	24157.32	29885.35	33621.02	32873.89	38435.88	38186.84	43167.73	33953.08	33953.08
La	20.00	19.00	26.00	13.00	23.00	28.00	39.00	33.00	15.00	42.00	31.00	37.00	31.00	43.00	32.00	24.00	31.00	23.00	24.00	20.00	2.00	27.00
Ce	50.00	44.00	62.00	30.00	47.00	63.00	85.00	66.00	38.00	111.00	66.00	82.00	68.00	88.00	69.00	58.00	70.00	49.00	58.00	45.00	7.00	61.00
Pb	6.00	15.00	15.00	6.00	9.00	14.00	22.00	17.00	42.00	60.00	19.00	35.00	35.00	20.00	27.00	29.00	33.00	37.00	25.00	36.00	4.00	27.00
Sr	487.00	123.00	148.00	256.00	254.00	578.00	301.00	99.00	24.00	6.50	235.00	126.00	127.00	160.00	139.00	89.00	198.00	97.00	79.00	65.00	8.00	112.00
F	1221.98	261.85	480.06	436.42	480.06	741.92	1047.41	130.93	87.28	43.64	480.06	829.20	567.35	523.71	654.63	392.78	392.78	349.14	741.92	1440.19	1265.62	654.63
Nd																						
Zr	168.00	102.00	145.00	68.00	112.00	115.00	297.00	115.00	79.00	157.00	150.00	245.00	201.00	168.00	187.00	139.00	136.00	100.00	183.00	99.00	22.00	157.00
Sm																						
Ti	5935.04	899.25	3177.35	4196.50	3237.30	3237.30	5275.59	1139.05	479.60	419.65	2457.95	4376.35	3237.30	4376.35	3836.80	1798.50	2098.25	1318.90	2158.20	1498.75	59.95	2637.80
Y	23.00	25.00	32.00	18.00	21.00	19.00	27.00	26.00	72.00	180.00	31.00	24.00	39.00	15.00	27.00	40.00	40.00	33.00	35.00	14.00	13.00	32.00
Sc	19.00	4.00	20.00	32.00	23.00	24.00	15.00	5.00		4.00	13.00	13.00	12.00	20.00	15.00	7.00	12.00	7.00	7.00	4.00	2.00	11.00
Cr	33.00	3.00	9.00	37.00	25.00	70.00	71.00	1.00	1.00	1.00	20.00	54.00	56.00	118.00	61.00	8.00	13.00	10.00	13.00	10.00	1.00	30.00
V	113.00	6.00	101.00	169.00	131.00	142.00	115.00	7.00	3.00	1.00	57.00	71.00	64.00	123.00	87.00	29.00	42.00	25.00	25.00	15.00	1.00	49.00
Co	20.00	3.00	13.00	26.00	17.00	21.00	14.00	1.00	1.00	1.00	10.00	17.00	15.00	21.00	17.00	7.00	8.00	6.00	8.00	4.00	1.00	10.00
Ga	17.40	15.00	15.80	17.40	17.40	15.80	18.60	12.00	14.00	30.00	16.00	20.40	15.00	18.20	18.20	39.00	47.00	28.00	67.00	77.00	63.00	18.00
Cu	23.00	2.00	3.00	8.00	13.00	38.00	39.00	1.00	1.00	1.00	9.00	16.00	11.00	23.00	17.00	5.00	6.00	3.00	8.00	11.00	1.00	9.00
Zn	68.00	37.00	55.00	76.00	62.00	74.00	72.00	17.00	14.00	55.00	48.00	95.00	71.00	83.00	82.00	39.00	47.00	28.00	67.00	77.00	63.00	59.00
Ni	26.00	1.00	4.00	15.00	7.00	18.00	35.00	1.00	1.00	1.00	8.00	24.00	24.00	32.00	20.00	5.00	6.00	4.00	7.00	4.00	1.00	11.00
Normalised Data																						
Rb	57.48	141.73	212.60	60.63	140.16	113.39	338.58	337.01	577.95	1204.72	258.27	292.91	240.94	223.62	288.19	294.49	280.31	371.65	384.25	659.84	2204.72	385.83
Ba	46.50	82.99	59.38	30.76	50.79	79.41	164.54	77.98	8.01	0.86	74.26	87.28	109.46	67.96	67.96	70.83	89.43	50.08	108.03	31.48	0.29	62.96
Th	68.24	105.88	197.65	51.76	108.24	131.76	305.88	232.94	382.35	1011.76	235.29	311.76	252.94	228.24	225.88	218.82	211.76	225.88	183.53	167.06	138.82	223.53
U	85.71	161.90	142.86	38.10	66.67	104.76	276.19	171.43	723.81	1238.10	238.10	123.81	180.95	57.14	190.48	171.43	200.00	304.76	276.19	514.29	161.90	238.10
Nb	19.64	16.83	12.62	6.31	9.12	7.71	28.75	23.14	37.87	45.58	15.43	25.25	12.62	15.43	18.23	10.52	14.73	14.03	16.13	28.05	55.40	18.23
K	46.82	116.22	99.29	31.55	66.74	71.06	135.48	138.14	158.72	145.44	115.56	145.11	123.86	96.63	119.54	134.48	131.50	153.74	152.75	172.67	135.81	135.81
La	29.11	27.66	37.85	18.92	33.48	40.76	56.77	48.03	21.83	61.14	45.12	53.86	45.12	62.59	46.58	34.93	45.12	33.48	34.93	29.11	2.91	39.30
Ce	28.17	24.79	34.93	16.90	26.48	35.49	47.89	37.18	21.41	62.54	37.18	46.20	38.31	49.58	38.87	32.68	39.44	27.61	32.68	25.35	3.94	34.37
Pb	32.43	81.08	81.08	32.43	48.65	75.68	118.92	91.89	227.03	324.32	102.70	189.19	189.19	108.11	145.95	156.76	178.38	200.00	135.14	194.59	21.62	145.95
Sr	23.08	5.83	7.01	12.13	12.04	27.39	14.27	4.69	1.14	0.31	11.14	5.97	6.02	7.58	6.59	4.22	9.38	4.60	3.74	3.08	0.38	5.31
F	12.86	2.76	5.05	4.59	5.05	7.81	11.03	1.38	0.92	0.46	5.05	8.73	5.97	5.51	6.89	4.13	4.13	3.68	7.81	15.16	13.32	6.89
Nd	0.00	0.00	0.00	0.00	0.00	0.00	0.00	0.00	0.00	0.00	0.00	0.00	0.00	0.00	0.00	0.00	0.00	0.00	0.00	0.00	0.00	
Zr	15.00	9.11	12.95	6.07	10.00	10.27	26.52	10.27	7.05	14.02	13.39	21.88	17.95	15.00	16.70	12.41	12.14	8.93	16.34	8.84	1.96	14.02
Sm	0.00	0.00	0.00	0.00	0.00	0.00	0.00	0.00	0.00	0.00	0.00	0.00	0.00	0.00	0.00	0.00	0.00	0.00	0.00	0.00	0.00	
Ti	4.57	0.69	2.44	3.23	2.49	2.49	4.06	0.88	0.37	0.32	1.89	3.37	2.49	3.37	2.95	1.38	1.61	1.01	1.66	1.15	0.05	2.03
Y	5.05	5.49	7.03	3.96	4.62	4.18	5.93	5.71	15.82	39.56	6.81	5.27	8.57	3.30	5.93	8.79	8.79	7.25	7.69	3.08	2.86	7.03

LITHOLOGY	I-type	S-type	A-type	Leucogneiss	Augen Gneiss	Rhyolite	Paragneiss	Alkali Gr.	Donning.	Leucogranite	Granite	S1 Granite	Granite	qtz-fld Gr.	Granite	Granite	Felsic Gr.	Granite	Granite	Granite
REGION	Rathjen Gn.	K.L Granite	Mannum Gr.	Cape Carnot	Cape Carnot	Devils Play.	W Eyre Pen.	Don. Pen	Tumby H's		Cape Don.	B'broke	Cape Don.	Cape Don.	Hiltaba	Kokatha	Olympic D.	Minnipa	Buckleboo	Cultana
Age	Delamerian	Delamerian	Delamerian	Archaean	Archaean	Archaean	Archaean	Palaeo-Prot.	Palaeo-Prot.	Palaeo-Prot.	Palaeo-Prot.	Palaeo-Prot.	Palaeo-Prot.	Palaeo-Prot.	Meso-Prot.	Meso-Prot.	Meso-Prot.	Meso-Prot.	Meso-Prot.	Meso-Prot.
Source	Turner et al.	Turner et al.	Turner et al.	Turner et al.	Turner et al.	Turner et al.	Turner et al.	Turner et al.	Schaefer	Schaefer	Schaefer	Schaefer	Schaefer	Schaefer	Flint, 1993	Flint, 1993	Flint, 1993	Flint, 1993	Flint, 1993	Flint, 1993
ELEMENT																				
Major (Wt. %)																				
SiO2	73.97	71.50	72.24	76.75	70.08	73.15	73.24	77.01	71.14	73.88	76.23	76.49	78.18	78.73	76.49	75.56	71.57	74.57	76.60	77.60
Al2O3	12.45	13.31	13.77	12.87	14.97	12.45	14.30	11.88	12.96	14.39	11.94	13.12	11.93	11.61	11.80	12.45	13.41	13.25	12.40	10.70
Fe2O3	2.81	3.71	2.13	1.77	3.59	4.25	2.45	1.04	4.60	0.87	1.54	0.26	0.60	0.47	1.21	0.94	1.26	0.66	0.44	1.29
MnO	0.03	0.06	0.07	0.02	0.04	0.06	0.02	0.03	0.06	0.03	0.02	0.00	0.01	0.00	0.03	0.03	0.04	0.07	0.02	0.02
MgO	0.81	1.67	0.55	0.40	2.08	1.53	0.69	0.18	0.60	0.19	0.26	0.11	0.11	0.08	0.13	0.16	0.54	0.22	0.15	0.29
CaO	1.66	1.84	0.87	2.02	1.32	0.83	1.16	0.74	1.45	0.48	1.17	1.20	0.69	0.59	0.46	0.64	0.78	0.82	0.57	0.11
Na2O	3.55	2.59	4.01	3.75	2.79	3.69	3.24	3.03	2.65	3.82	2.16	2.31	2.69	2.62	3.20	3.02	2.91	3.12	3.15	2.32
K2O	3.17	3.48	5.66	2.31	5.50	1.66	4.62	5.20	4.92	4.84	5.51	5.80	5.40	5.41	5.44	5.29	6.06	5.64	5.22	6.65
TiO2	0.44	0.46	0.38	0.25	0.64	0.33	0.27	0.07	0.46	0.05	0.21	0.06	0.08	0.07	0.16	0.19	0.29	0.26	0.16	0.21
P2O5	0.10	0.07	0.08	0.03	0.09	0.05	0.09	0.00	0.12	0.25	0.02	0.01	0.00	0.00	0.03	0.03	0.07	0.04	0.02	0.04
SO3															0.54	0.81	1.16	0.72	0.74	
LOI	0.25	0.54	0.36	0.33	0.15	2.31	0.27	0.22	0.35	0.56	0.39	0.28	0.22	0.17	0.61	0.62				0.78
Total	99.24	99.23	100.12	100.5	101.25	100.31	100.35	99.4	99.32	99.36	99.45	99.64	99.91	99.75						
Al Index	1.01	1.17	0.96	1.04	1.16	1.33	1.15	0.99	1.05	1.16	1.03	1.07	1.04	1.03	0.98	1.05	1.05	1.04	1.05	0.95
Trace (ppm)																				
Rb	137.20	152.20	189.80	43.00	126.00	45.90	177.10	413.00	118.40	393.63	288.18	256.49	321.97	350.66	324.00	291.00	253.00	244.00		550.00
Ba	697.00	596.00	641.00	503.00	664.00	503.00	415.00	6.00		66.00	324.00	667.00	17.00	9.00	221.00	416.00	691.00	308.00		380.00
Th	25.00		27.00	11.00	52.00	11.00	32.00	36.00	15.20	4.60	59.50	13.10	16.40	17.00	41.00	43.00	58.00	45.00		120.00
U	4.60		9.40	0.20	2.30	1.80	14.40	13.30	2.40	8.70	7.10	3.90	4.10	4.30	9.00	9.00	49.00	7.00		22.00
Nb	12.80	13.00	49.00	6.00	7.00	12.00	12.00	6.00	17.00	17.20	8.50	3.70	4.50	5.30	22.00		30.00			38.00
K	26315.71	28889.17	46986.41	19176.43	45658.17	13780.47	38352.87	43167.73	40843.31	40179.19	45741.19	48148.62	44828.03	44911.04	45160.08	43914.86	50307.01	46820.38	43333.76	55204.88
La	48.00	27.00	80.00	39.00	88.00	28.00	28.00	39.00		3.00	123.00	12.00	68.00	6.00						
Ce	102.00	67.00	155.00	70.00	215.00	59.00	61.00	74.00		3.00	232.00	27.00	94.00	5.00	152.00		169.00			60.00
Pb	5.00		12.00	14.90	40.00	4.50	31.00	48.60	29.40	26.60	38.30	41.70	44.10	42.60						
Sr	110.30	151.90	133.30	135.00	140.00	48.20	59.60	12.00	132.70	27.77	63.17	129.40	13.68	10.48	34.00	63.00	73.00	86.00		30.00
F	436.42	305.49	349.14	130.93	392.78	218.21	392.78	0.00	523.71	1091.05	87.28	43.64	0.00	0.00	130.93	130.93	305.49	174.57	87.28	174.57
Nd	56.89	17.43	59.89	17.12	40.24	26.46	29.37	33.80		3.00	92.00	15.00	32.00	6.00						
Zr	260.00	175.00	334.00	171.00	275.00	300.00	135.00	118.00	264.60	30.10	167.30	157.20	111.40	65.00	197.00	244.00	258.00	236.00		200.00
Sm	10.99	3.64	10.53	2.64	6.78	6.09	5.46	5.74												
Ti	2637.80	2757.70	2278.10	1498.75	3836.80	1978.35	1618.65	419.65	2757.70	299.75	1258.95	359.70	479.60	419.65	959.20	1139.05	1738.55	1558.70	959.20	1258.95
Y	41.00	53.00	62.00	10.00	16.00	45.00	12.00	52.00	42.30	12.40	28.90	7.40	18.30	9.50	31.00		53.00			40.00
Sc	8.70	12.00	5.50	4.00	6.00	7.00	5.00	1.00		1.40	4.50	2.20	1.30	0.70						
Cr	17.00	68.00	5.00	398.00	434.00	146.00	240.00	1.00	9.00	2.00	2.00	3.00	2.00	2.00			2.00			<5
V	40.00	67.00	21.00	17.00	60.00	10.00	27.00	1.00		3.70	7.10	9.10	3.70	4.20						
Co										55.20	96.90	54.30	59.90	53.00						45.00
Ga	16.00		21.00	13.00	19.00	15.00	17.60	16.00	23.10	19.00	15.00	15.70	16.00	15.40						
Cu									7.00	7.00	11.00	0.00	4.00	0.00						
Zn									84.00	29.00	26.00	6.00	14.00	10.00						
Ni	7.00	25.00	1.00	11.00	21.00	7.00	12.00	11.00	2.00	0.00	0.00	1.00	0.00	0.00		<5	3.00			<5
Normalised Data																				
Rb	216.06	239.69	298.90	67.72	198.43	72.28	278.90	650.39	186.46	619.89	453.83	403.92	507.04	552.22	510.24	458.27	398.43	384.25		866.14
Ba	99.73	85.28	91.72	71.97	95.01	71.97	59.38	0.86		9.44	46.36	95.44	2.43	1.29	31.62	59.52	98.87	44.07		54.37
Th	294.12		317.65	129.41	611.76	129.41	376.47	423.53	178.82	54.12	700.00	154.12	192.94	200.00	482.35	505.88	682.35	529.41		1411.76
U	219.05		447.62	9.52	109.52	85.71	685.71	633.33	114.29	414.29	338.10	185.71	195.24	204.76	428.57	428.57	2333.33	333.33		1047.62
Nb	17.95	18.23	68.72	8.42	9.82	16.83	16.83	8.42	23.84	24.12	11.92	5.19	6.31	7.43	30.86		42.08			53.30
K	105.26	115.56	187.95	76.71	182.63	55.12	153.41	172.67	163.37	160.72	182.96	192.59	179.31	179.64	180.64	175.66	201.23	187.28	173.34	220.82
La	69.87	39.30	116.45	56.77	128.09	40.76	40.76	56.77		4.37	179.04	17.47	98.98	8.73						
Ce	57.46	37.75	87.32	39.44	121.13	33.24	34.37	41.69		1.69	130.70	15.21	52.96	2.82	85.63		95.21			33.80
Pb	27.03		64.86	80.54	216.22	24.32	167.57	262.70	158.92	143.78	207.03	225.41	238.38	230.27						
Sr	5.23	7.20	6.32	6.40	6.64	2.28	2.82	0.57	6.29	1.32	2.99	6.13	0.65	0.50	1.61	2.99	3.46	4.08		1.42
F	4.59	3.22	3.68	1.38	4.13	2.30	4.13	0.00	5.51	11.48	0.92	0.46	0.00	0.00	1.38	1.38	3.22	1.84	0.92	1.84
Nd	42.02	12.87	44.23	12.64	29.72	19.54	21.69	24.96		2.22	67.95	11.08	23.63	4.43						
Zr	23.21	15.63	29.82	15.27	24.55	26.79	12.05	10.54	23.63	2.69	14.94	14.04	9.95	5.80	17.59	21.79	23.04	21.07		17.86
Sm	24.75	8.20	23.72	5.95	15.27	13.72	12.30	12.93		0.00	0.00	0.00	0.00	0.00						
Ti	2.03	2.12	1.75	1.15	2.95	1.52	1.25	0.32	2.12	0.23	0.97	0.28	0.37	0.32	0.74	0.88	1.34	1.20	0.74	0.97
Y	9.01	11.65	13.63	2.20	3.52	9.89	2.64	11.43	9.30	2.73	6.35	1.63	4.02	2.09	6.81		11.65			8.79

APPENDIX E

ISOTOPE SYSTEMATICS

APPENDIX E - ISOTOPE SYSTEMATICS

Neodymium and Samarium are light rare earth elements (LREE) that occur in many rock forming silicate, phosphate and carbonate minerals. The ^{147}Sm isotope is radioactive and decays by alpha emission to a stable isotope of ^{143}Nd, with a half-life of 1.06×10^{11} y.

The growth of radiogenic ^{143}Nd and ^{87}Sr together provide new insight into the genesis of igneous rocks. The concentrations of both of these elements in igneous rocks increase with incresing degree of differentiation but their Sm/Nd ratios decrease.

The abundance of radiogenic ^{143}Nd, and hence the $^{143}Nd/^{144}Nd$ ratio, of the Earth has increased with time because of the decay of ^{147}Sm to ^{143}Nd. The time dependent increase of the $^{143}Nd/^{144}Nd$ ratio of the Earth can be described by a model based on the age and Sm/Nd ratio of the Earth and on its primordial $^{143}Nd/^{144}Nd$ ratio (McCulloch and Wasserburg, 1978). Analysis of stony meteorites provides the primordial $^{143}Nd/^{144}Nd$ ratio and the age of the Earth.

The isotopic evolution of Nd in the Earth is described in terms of a model called CHUR, which stands for "chrondritic uniform reservoir" (DePaolo and Wasserburg, 1976a) This model assumes that terrestrial Nd has evolved in a uniform reservoir whose Sm/Nd ratio is equal to that of chrondritic meteorites. The present value of the $^{143}Nd/^{144}Nd$ ratio of this reservoir is 0.512638 relative to $^{146}Nd/^{144}Nd$ ratio of 0.7219. The present $^{147}Sm/^{144}Nd$ ratio of CHUR is 0.1967. This information permits the calculation of the $^{143}Nd/^{144}Nd$ ratio of CHUR at any time (t) in the past.

Partial melting of CHUR gives rise to magmas having lower Sm/Nd ratios than CHUR. Igneous rocks that form from this magma therefore have lower present day $^{143}Nd/^{144}Nd$ ratios than CHUR. The residual solids that remain behind after withdrawal of the magma have correspondingly higher Sm/Nd ratios than the chrondritic reservoir. Consequently, these 'depleted' regions of the reservoir have higher $^{143}Nd/^{144}Nd$ ratios than CHUR at the present time. This serves as a reference for the isotopic evolution of Nd in rocks that formed from magma generated within the reservoir in the past. Comparison of the initial $^{143}Nd/^{144}Nd$ ratios of igneous and metamorphic rocks in the crust with the corresponding $^{143}Nd/^{144}Nd$ ratios of CHUR at the time of crystallisation of the rocks is required. This is what we want to know, whether the initial $^{143}Nd/^{144}Nd$ ratios of different kinds of rocks are higher or lower than those of CHUR at the appropriate times.

DePaolo and Wasserburg (1976) introduced an epsilon parameter so as to allow simple comparisons of the differences in isotope ratios. Thus ε^{t}_{CHUR} expresses the difference between the initial $^{143}Nd/^{144}Nd$ ratio of a suite of rocks and the corresponding value of this ratio in CHUR at the time of crystallisation of the rocks.

A positive ε value indicates that the rocks were derived from residual solids in the reservoir after magma had been withdrawn at an earlier time (ie., Nd was derived from a

depleted source and thus has a higher Sm/Nd ratio than CHUR). The more lithophile elements that are preferentially partioned into the liquid phase during partial melting are depleted within this reservoir.

A negative ε value indicates that the rocks were derived from sources that had a lower Sm/Nd ratio than the chondritic reservoir (ie., an enriched source). Hence it seems such rocks were derived from, or assimilated, old crustal rocks whose Sm/Nd had been lowered originally when they separated from CHUR. Therefore, magmas formed by partial melting in the mantle have lower Sm/Nd ratios than CHUR whereas the residual solids have higher Sm/Nd ratios.

In addition to this CHUR enables the calculation of when the Nd in a crustal rock separated from the chondritic reservoir. Model dates are determined by establishing when the $^{143}Nd/^{144}Nd$ ratio of the rock equalled the $^{143}Nd/^{144}Nd$ of CHUR. In general the Sm/Nd ratio of crustal rocks is not changed by metamorphism or even by erosion and redeposition. Thus the model dates may be regarded as estimates of Nd crustal residence time.

APPENDIX F

ISOTOPE DATA

Isotope Data for the Olary Block

Sample no.	9	13	46	49	17	26	105	102
Rock type	Bimbowrie	Bimbowrie	Bimbowrie	Bimbowrie	Basso	Basso	Ameroo	Metasediment
Nd ppm	21.595	51.900	37.080	44.903	90.066	36.988	171.616	33.350
Sm ppm	5.443	11.343	7.614	9.589	21.291	10.192	36.916	6.050
143/144 Nd	0.511738	0.511638	0.511536	0.511613	0.512090	0.512265	0.511912	0.511323
2 sigma	0.000050	0.000058	0.000015	0.000014	0.000015	0.000043	0.000067	0.000021
Sm/Nd	0.2521	0.2186	0.2053	0.2135	0.2364	0.2755	0.2151	0.1814
147Sm/144Nd	0.1525	0.1322	0.1242	0.1292	0.1430	0.1667	0.1301	0.1097
143/144Nd ch	0.512638	0.512638	0.512638	0.512638	0.512638	0.512638	0.512638	0.512638
143/144Nd dep	0.513108	0.513108	0.513108	0.513108	0.513108	0.513108	0.513108	0.513108
T mod:chur	3.08	2.35	2.31	2.30	1.55	1.89	1.66	2.29
T mod:dep	**3.28**	**2.67**	**2.60**	**2.62**	**2.13**	**2.61**	**2.12**	**2.55**
eps Nd (0)	-17.56	-19.51	-21.50	-19.99	-10.69	-7.28	-14.16	-25.64
age (T)	1.55	1.55	1.55	1.55	1.7	1.7	1.7	1.65
143/144(T)	0.510184	0.510291	0.510270	0.510297	0.510491	0.510402	0.510457	0.510133
143/144ch T	0.510634	0.510634	0.510634	0.510634	0.510439	0.510439	0.510439	0.510504
eps Nd chT	**-8.80**	**-6.71**	**-7.12**	**-6.60**	**1.03**	**-0.73**	**0.36**	**-7.27**
Sr87/86	1.574065	1.783022	1.224500	1.495513	1.186490	0.814368	0.735311	1.264030
2 sigma	0.000045	0.000059	0.000045	0.000055	0.000059	0.000055	0.000059	0.000061
Sr ppm	35.07171	27.63597	43.9518	33.2671	18.51906	22.50189	25.05311	65.4996
Rb ppm	444.3104	410.0377	375.0544	379.169	126.4333	32.26629	8.12846	499.2401
Rb/Sr	12.6686	14.8371	8.5333	11.3977	6.8272	1.4339	0.3244	7.6220
frac 87	1.314099491	1.339048957	1.27236143	1.304720382	1.267823071	1.223391669	1.213952263	1.277081312
at wtSr	87.56111777	87.54896364	87.58251615	87.56580702	87.58492782	87.60948357	87.61493192	87.58002621
87Rb/86Sr	39.76009538	47.44329866	25.93724524	35.51797662	20.67801745	4.192036068	0.941249375	23.2526669
87Rb/86Sr	39.76009538	47.44329866	25.93724524	35.51797662	20.67801745	4.192036068	0.941249375	23.2526669
87/86(T)	0.689244	0.727219	0.647292	0.705096	0.681249	0.711941	0.712313	0.712787
Sr T dep	**1.528**	**1.586**	**1.404**	**1.556**	**1.631**	**1.864**	**2.487**	**1.682**
Sr T chur	**1.527**	**1.586**	**1.402**	**1.555**	**1.629**	**1.858**	**2.480**	**1.680**

APPENDIX G

ISOCHRON PLOTS

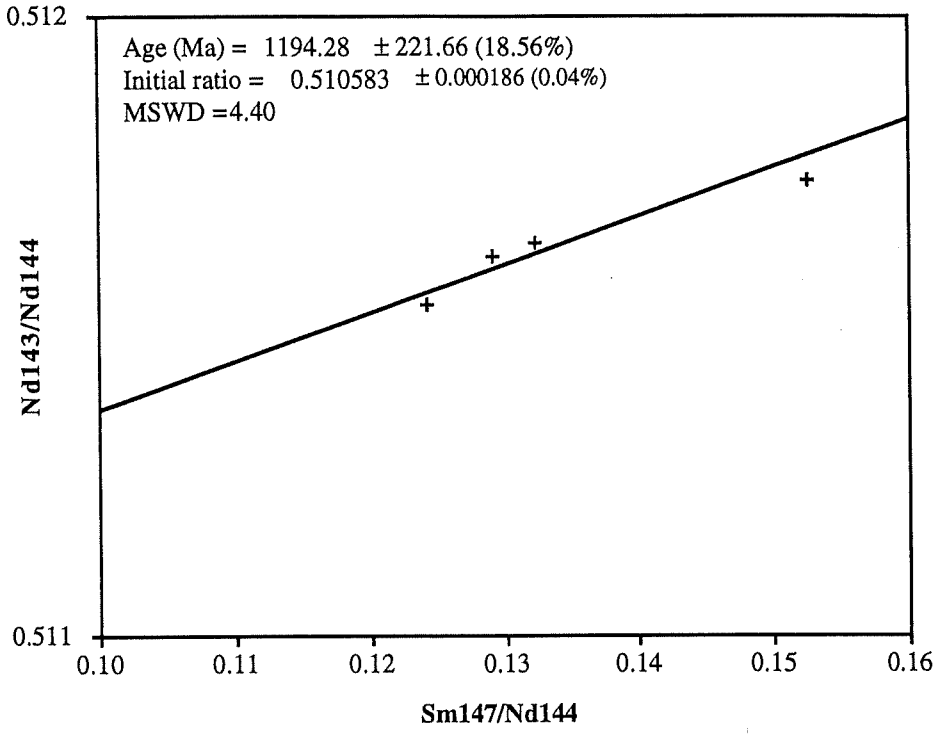

Sm-Nd Isochron for the Bimbowrie Granite

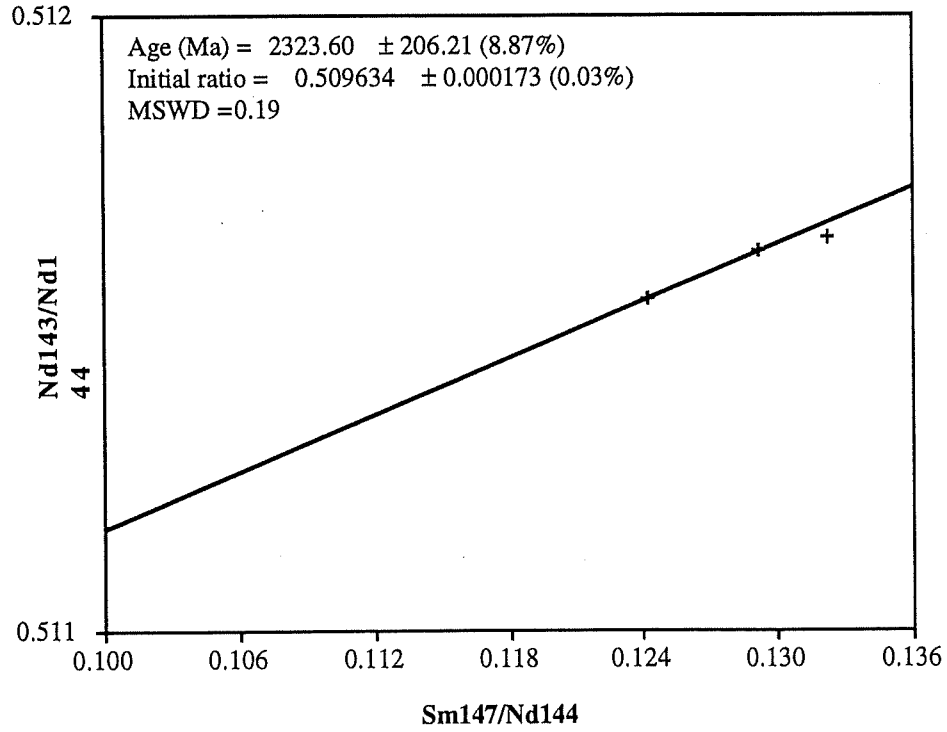

Sm-Nd isochron for the Bimbowrie Granite minus sample 1027-009

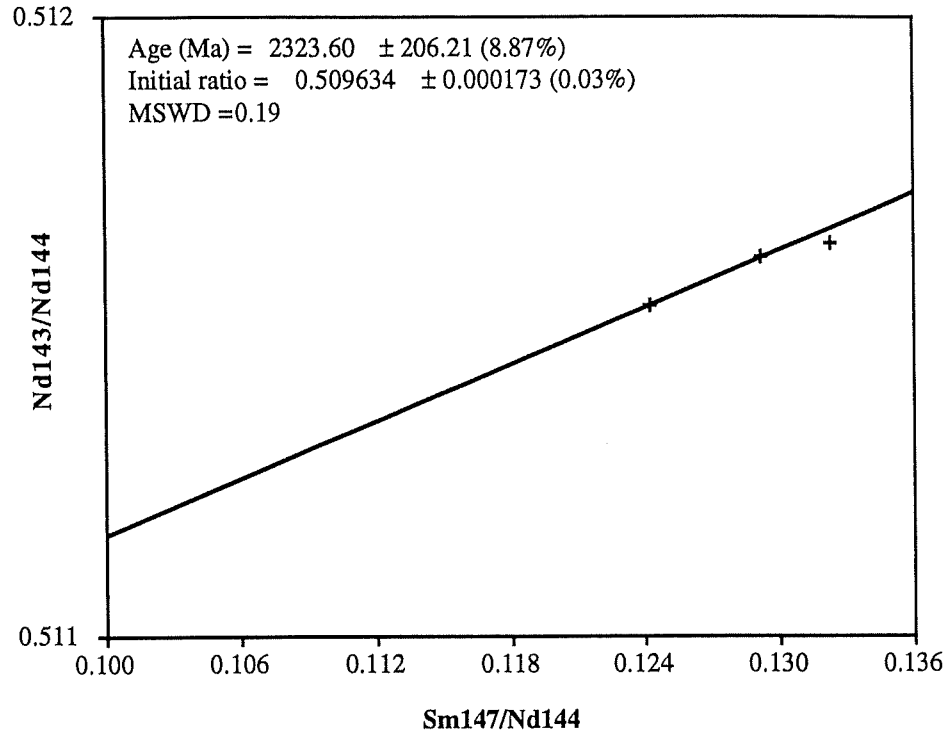

Sm-Nd isochron for the Basso Granodiorite

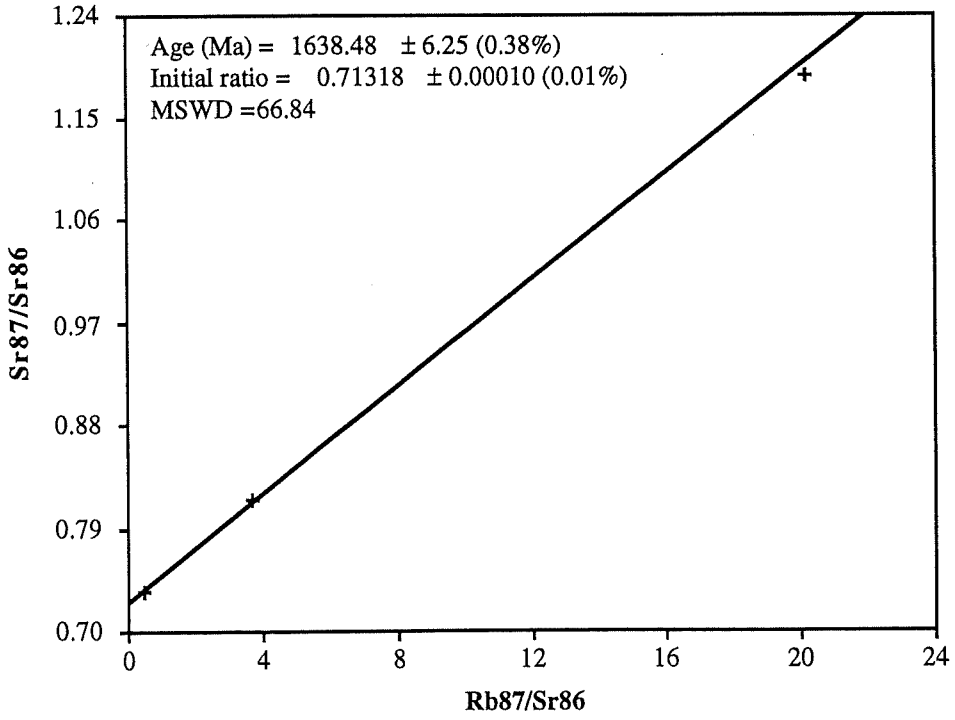

Rb-Sr isochron for the Basso Granodiorite

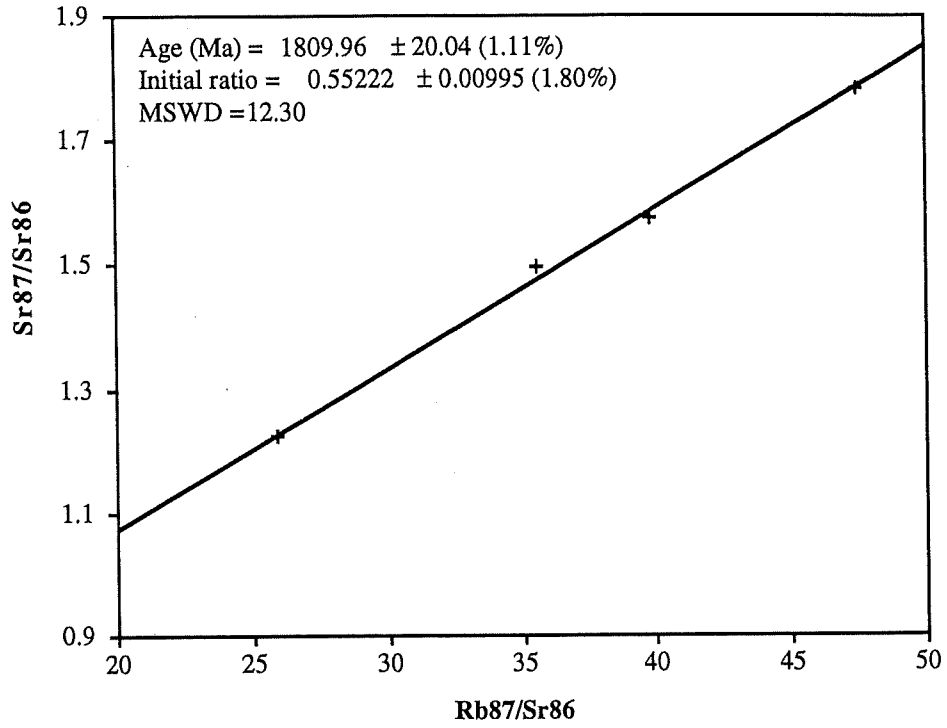

Rb-Sr isochron for the Bimbowrie Granite

APPENDIX H

GEOLOGICAL MAP OF THE ANTRO AREA, BIMBOWRIE STATION and TWB - BASSO MINE AREA OLARY, SOUTH AUSTRALIA

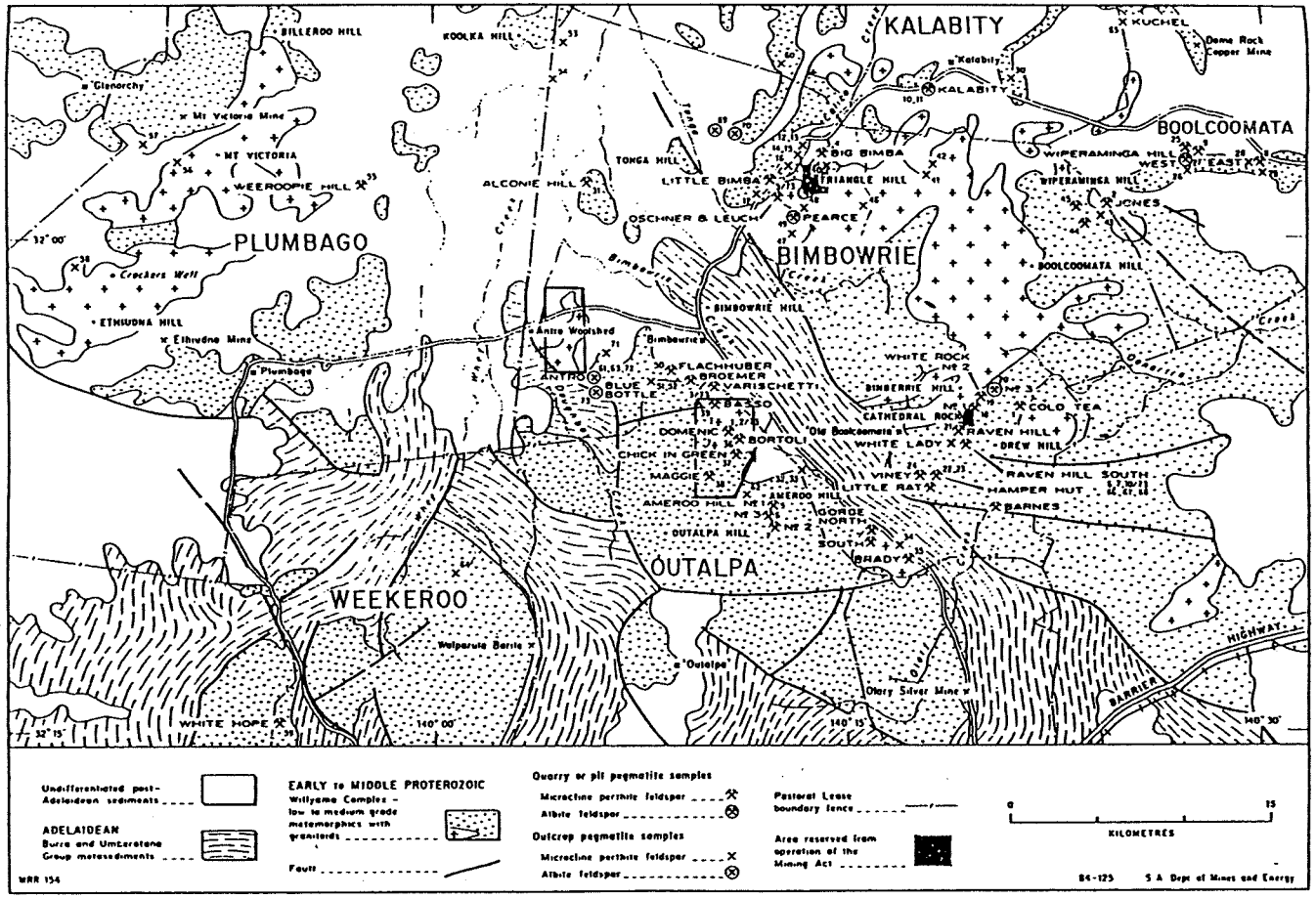

Regional Geological Map of the Olary Region. Boxes indicate map area.